

การสังเคราะห์ ฤทธิ์ต้านแบคทีเรียและการสร้างแบบจำลองเชิงโมเลกุลของสารกลุ่มไดคูมารอล



นางสาวกนกพร เพชรนภาพรรณ

จุฬาลงกรณ์มหาวิทยาลัย

CHULALONGKORN UNIVERSITY

วิทยานิพนธ์นี้เป็นส่วนหนึ่งของการศึกษาตามหลักสูตรปริญญาวิทยาศาสตรมหาบัณฑิต

สาขาวิชาเคมี ภาควิชาเคมี

คณะวิทยาศาสตร์ จุฬาลงกรณ์มหาวิทยาลัย

ปีการศึกษา 2556

ลิขสิทธิ์ของจุฬาลงกรณ์มหาวิทยาลัย

บทคัดย่อและแฟ้มข้อมูลฉบับเต็มของวิทยานิพนธ์ตั้งแต่ปีการศึกษา 2554 ที่ให้บริการในคลังปัญญาจุฬาฯ (CUIR)

เป็นแฟ้มข้อมูลของนิสิตเจ้าของวิทยานิพนธ์ ที่ส่งผ่านทางบัณฑิตวิทยาลัย

The abstract and full text of theses from the academic year 2011 in Chulalongkorn University Intellectual Repository (CUIR) are the thesis authors' files submitted through the University Graduate School.

SYNTHESIS, ANTIBACTERIAL ACTIVITY AND MOLECULAR MODELING OF
DICOUMAROLS

Miss Kanokporn Petnapapun



จุฬาลงกรณ์มหาวิทยาลัย

CHULALONGKORN UNIVERSITY

A Thesis Submitted in Partial Fulfillment of the Requirements
for the Degree of Master of Science Program in Chemistry

Department of Chemistry

Faculty of Science

Chulalongkorn University

Academic Year 2013

Copyright of Chulalongkorn University

Thesis Title	SYNTHESIS, ANTIBACTERIAL ACTIVITY AND MOLECULAR MODELING OF DICOUMAROLS
By	Miss Kanokporn Petnapapun
Field of Study	Chemistry
Thesis Advisor	Assistant Professor Warinthorn Chavasiri, Ph.D.
Thesis Co-Advisor	Associate Professor Pornthep Sompornpisut, Ph.D.

Accepted by the Faculty of Science, Chulalongkorn University in Partial Fulfillment of the Requirements for the Master's Degree

.....Dean of the Faculty of Science
(Professor Supot Hannongbua, Dr.rer.nat.)

THESIS COMMITTEE

.....Chairman
(Assistant Professor Preecha Lertpratchya, Ph.D.)

.....Thesis Advisor
(Assistant Professor Warinthorn Chavasiri, Ph.D.)

.....Thesis Co-Advisor
(Associate Professor Pornthep Sompornpisut, Ph.D.)

.....Examiner
(Assistant Professor Sumrit Wacharasindhu, Ph.D.)

.....External Examiner
(Nadtanet Nunthaboot, Ph.D.)

กนกพร เพชรนภาพรรณ : การสังเคราะห์ ฤทธิ์ต้านแบคทีเรียและการสร้างแบบจำลองเชิงโมเลกุลของสารกลุ่มไดคูมารอล. (SYNTHESIS, ANTIBACTERIAL ACTIVITY AND MOLECULAR MODELING OF DICOUMAROLS) อ.ที่ปรึกษาวิทยานิพนธ์หลัก: ผศ. ดร.วรินทร์ ขวศิริ, อ.ที่ปรึกษาวิทยานิพนธ์ร่วม: รศ. ดร.พรเทพ สมพรพิสุทธิ์, , 87 หน้า.

ได้สังเคราะห์สารในกลุ่มไดคูมารอลและอนุพันธ์ยีสืบสารจากปฏิกิริยาคอนเดนเซชันระหว่าง 4-ไฮดรอกซีคูมารินกับแอโรมาติกอัลดีไฮด์ที่สนใจ นำสารเหล่านี้มาศึกษาฤทธิ์ต้านเชื้อแบคทีเรียแกรมบวก ได้แก่ Staphylococcus aureus กับ Bacillus subtilis และแบคทีเรียแกรมลบ ได้แก่ Escherichia coli กับ Klebsiella sp. พบว่า สารเหล่านี้แสดงฤทธิ์ต้านแบคทีเรียแกรมบวกอย่างจำเพาะ อย่างไรก็ตามอนุพันธ์ของไดคูมารอลส่วนใหญ่ที่มีหมู่แทนที่ที่เกาะกะในตำแหน่งเมทิลลีนจะมีฤทธิ์ต้านแบคทีเรียน้อยลง ผลของฤทธิ์ทางชีวภาพดังกล่าวข้างต้นถูกอธิบายด้วยตำแหน่งการเข้าจับเชิงโมเลกุลที่ลดลงระหว่างอนุพันธ์ไดคูมารอลกับแบบจำลองโอมโบลีของ S. aureus flavoprotein การศึกษาชีวสามมิติแสดงให้เห็นลักษณะเด่นทางโครงสร้างแผนภาพคอนทัวร์ของคอมฟ้าและคอมเซียสนับสนุนแนวคิดในเรื่องฤทธิ์ทางชีวภาพที่ลดลงเนื่องจากแรงผลักของหมู่ที่เกาะกะที่ตำแหน่งพารา นอกจากนี้อนุพันธ์ไดคูมารอลมีสมบัติทางยาสอดคล้องกับกฎของลิปินส์กี ผลการศึกษานี้ทำให้เข้าใจพื้นฐานของโมเลกุลกับฤทธิ์ต้านแบคทีเรียของสารอนุพันธ์ไดคูมารอลมากขึ้น



จุฬาลงกรณ์มหาวิทยาลัย
CHULALONGKORN UNIVERSITY

ภาควิชา เคมี

สาขาวิชา เคมี

ปีการศึกษา 2556

ลายมือชื่อนิสิต

ลายมือชื่อ อ.ที่ปรึกษาวิทยานิพนธ์หลัก

ลายมือชื่อ อ.ที่ปรึกษาวิทยานิพนธ์ร่วม

5471903123 : MAJOR CHEMISTRY

KEYWORDS: DICOUMAROL / ANTIBACTERIAL ACTIVITY / MOLECULAR DOCKING / QSAR

KANOKPORN PETNAPAPUN: SYNTHESIS, ANTIBACTERIAL ACTIVITY AND MOLECULAR MODELING OF DICOUMAROLS. ADVISOR: ASST. PROF. WARINTHORN CHAVASIRI, Ph.D., CO-ADVISOR: ASSOC. PROF. PORNTHEP SOMPORNPIST, Ph.D., 87 pp.

Dicoumarol and its nineteen derivatives containing the substituted benzene ring at the methylenebis position were synthesized from the condensation reaction between 4-hydroxycoumarin with interesting aromatic aldehydes. These well-characterized compounds were evaluated for their antibacterial activity against gram-positive bacteria: *Staphylococcus aureus* and *Bacillus subtilis* and gram-negative bacteria: *Escherichia coli* and *Klebsiella sp.* The synthesized dicoumarols exhibited antibacterial activity selectively against gram-positive bacteria. Most derivatives with the substitution of steric bulky group on the methylenebis position appear to decrease in the efficacy of antibacterial effect. This finding is roughly described by the poorer docked poses of the derivatives to a homology model of *S. aureus* flavoprotein. 3D-QSAR study highlighted structural features around the substituted benzene ring of dicoumarols as the antibacterial activity. CoMFA and CoMSIA contour maps support the idea that steric repulsion at the para position could diminish the antibacterial activity. Furthermore, drug-likeness properties of the synthesized compounds were fallen in criterions for Lipinski rule. The results of this study provide a better understanding of the molecular basis for the antibacterial activity of dicoumarols.

Department: Chemistry

Student's Signature

Field of Study: Chemistry

Advisor's Signature

Academic Year: 2013

Co-Advisor's Signature

CHULALONGKORN UNIVERSITY

ACKNOWLEDGEMENTS

Firstly, the author wishes to express her sincere gratitude to Assistant Professor Dr. Warinthorn Chavasiri, her major advisor and Assistant Professor Dr. Pornthep Sompornpisut, her co advisor, for her kindly helpful suggestions, valuable assistance and encouraging throughout the entire period of this research. Sincere thanks are also extended to Assistant Professor Dr. Preecha Lertpratchya, Assistant Professor Dr. Sumrit Wacharasindhu and Dr. Nadtanet Nunthaboot, her thesis committee, for their comments and suggestions. Gratitude is also expressed to the staff of the Natural Products Research Unit, Department of Chemistry, Chulalongkorn University for their helpful discussion. Beside, the author greatly appreciated Dr. Somsak Pianwanit for guiding QSAR method.

This work is supported by the National Research University Project of CHE (HR1155A), the 90th Anniversary of Chulalongkorn University Fund, Ratchadaphiseksomphot Endowment Fund and H.M. and the King's 72nd Birthday Scholarship, Chulalongkorn University. National Electronics and Computer Technology Center (NECTEC), Computational Chemistry Unit Cell (CCUC) and The Thai Government Stimulus Package 2 (TKK2555) are gratefully acknowledged for supporting computational facilities.

Moreover, the author would like to express her sincere gratitude to her parents and family members for their love, understanding, encouragement and advice throughout the entire study.

CONTENTS

	Page
THAI ABSTRACT	v
ENGLISH ABSTRACT	vi
ACKNOWLEDGEMENTS	vi
CONTENTS	vii
LIST OF TABLES	ix
LIST OF FIGURES	x
LIST OF ABRIVIATIONS	xiv
CHAPTER I INTRODUCTION.....	1
1.1 Synthesis of Dicoumarols.....	1
1.2 Biological and Pharmacological Properties of Coumarin Derivatives.....	4
1.2.1 4-Hydroxycoumarin	4
1.2.2 Dicoumarols.....	7
1.3. Computational Study.....	14
3. Aims of Research.....	18
CHAPTER II MATERIALS AND METHODS	19
2.1 Chemicals.....	19
2.2 Instruments and Equipment.....	19
2.3 Hardware	19
2.4 Software.....	19
2.5 Synthesis of Dicoumarols.....	19
2.6 Antibacterial Susceptibility Testing	24
2.7 Molecular Modeling	25
2.7.1 Comparative Modeling of a Protein Target from <i>S. aureus</i>	25
2.7.2 Molecular Docking Study of Dicoumarols for Antibacterial Activity.....	27
2.7.3 Physicochemical Properties of the Synthesized Compounds.....	27
2.7.4 Quantitative Antibacterial Structure Activity Relationship (QSAR) Study .	27
CHAPTER III RESULTS AND DISCUSSION.....	29

	Page
3.1 Synthesis of Dicoumarols.....	29
3.2 Antibacterial Susceptibility Testing	34
3.3 Structure Antibacterial Activity against <i>S. aureus</i> Relationship Analysis of Dicoumarol Derivatives.....	42
3.3.1 Effect of <i>Mono</i> -substitution on Antibacterial Activity.....	43
3.3.2 Effect of <i>di</i> -substitution on the antibacterial activity.....	43
3.4 Structure-Activity Relationship Analysis of Dicoumarol Derivatives against <i>B. subtilis</i> 44	
3.5 Exploring Putative Target and Binding Site of Dicoumarols.....	44
3.6 Physicochemical properties of the synthesized compounds.....	53
3.7 Analysis of 3D-QSAR: CoMFA and CoMSIA Analysis	56
CHAPTER IV CONCLUSION.....	61
4.1 Propose for the Future Work	62
REFERENCES	63
APPENDICES.....	66
VITA.....	87

LIST OF TABLES

	Page
Table 2. 1 The structures of synthesized dicoumarol and derivatives.	21
Table 3. 1 Physical property and % yield of synthesized dicoumarols.....	30
Table 3. 2 The ¹ H NMR spectral assignments of synthesized dicoumarols.....	32
Table 3.3 Antibacterial activities of synthesized dicoumarol and its derivatives.....	35
Table 3. 4 Binding energy of dicoumarols.....	51
Table 3. 5 Physicochemical properties of dicoumarols	54
Table 3. 6 Statistical results of CoMFA and CoMSIA models	57
Table 3. 7 Experimental and predicted activities of test set compounds	58

LIST OF FIGURES

	Page
Figure 1.1 A Azor in complex with dicoumarol B NQO1 of human in complex with dicoumarol C NQO1 of rat in complex with duroquinone	15
Figure 1.2 The possible arrangements of dicoumarols : A pose A B pose B.....	16
Figure 1. 3 structure of the hNQO1	17
Figure 1. 4 dicoumarol/hNQO1 interactions.....	17
Figure 2. 1 NCBI BLAST search.....	26
Figure 3. 1 Labeling of dicoumarol core structure	29
Figure 3. 2 The ¹ H NMR spectrum of compound 1	31
Figure 3. 3 positive control (A) penicillin G (B) chloramphenicol.....	36
Figure 3. 4 no inhibition zone for (A) E.coli (B) Klebsiella sp.....	37
Figure 3. 5 Inhibition tests of sample on B. subtilis for 24 h., incubated at 37oC.....	38
Figure 3. 6 Inhibition tests of samples on Klebsiella sp. for 24 h, incubated at 37oC.....	39
Figure 3. 7 Inhibition tests of sample on E. coli for 24 h, incubated at 37oC	40
Figure 3. 8 Inhibition tests of sample on S. aureus for 24 h, incubated at 37oC.....	41
Figure 3. 9 Amino acid sequence alignment of azoreductase from S. aureus, B. subtilis, E. coli and Klebsiella sp.	45
Figure 3. 10 Amino acid sequence alignment of azoreductase from E.coli (2Z9C) and from S. aureus (A9635). Exactly conserved residues are in dark blue, and similar residues are in medium and light blue. The sequence identity is of 34%.	45
Figure 3. 11 Comparative model of S. aureus azoreductase in complex with FMN and dicoumarol.	46
Figure 3. 12 Docked orientations and interactions of dicoumarol in the enzyme binding sites. (A) and (B) represented the ligand poses A and poses B, respectively. The surrounding conserved residues, FMN and dicoumarol molecules are in stick representation.	48
Figure 3. 13 (A) and (B) are schematic 2D diagrams of protein-ligand binding pose A and B, respectively. Spoked arcs represent residues making hydrophobic	

contacts with the ligand whereas dashed lines represent hydrogen bonds between the atoms involved. The 2D representation was created using the program LigPlot.. 49

Figure 3.14 Docked orientations and interactions of dicoumarol derivatives in the enzyme binding site. (B) and (C) are the docking poses A and B of compound derivatives in comparison with the pose A of dicoumarol (A) in the pocket (surface representation). (D) and (E) are schematic 2D diagrams of protein-ligand binding pose A and B, respectively. 52

Figure 3.15 Docked orientations and interactions of compound 1 that formed hydrogen bond 55

Figure 3. 16 Docked orientations and interactions of compound 12 that formed hydrogen bond 56

Figure 3. 17 Plots between the experimental and predicted biological activities of training (filled square) and test set (filled circle): (A) CoMFA plot and (B) CoMSIA plot 58

Figure 3. 18 The stdev*coeff. contour maps. (A) and (B) represent CoMFA steric and electrostatic, respectively. (C) to (F) represent CoMSIA steric, electrostatic, hydrophobic, hydrogen bond donor and hydrogen bond acceptor, respectively. Steric field is represented by green and yellow contour maps. Electrostatic field is represented by blue and red contour maps. Hydrophobic field is represented by orange and white contour maps. Hydrogen bond donor field is represented by cyan and purple contour maps. Hydrogen bond acceptor field is represented by magenta and red contour maps. All the contours represented the default 80% and 20% level contributions for favorable and unfavorable regions, respectively. 60

Figure 4. 1 The structures of synthesized compound (A) dicoumarol (B) derivatives of 61

Figure A. 1 The ¹H NMR spectrum of 3,3'-methylene-bis-4-hydroxy-2H-chromen-2-one (1) 67

Figure A. 2 The ¹H NMR spectrum of 3,3'-(2,4-dichlorophenylmethylene)bis-(4-hydroxy-2H-chromen-2-one) (2) 68

Figure A. 3 The ¹ H NMR spectrum of 3,3'-(3,4-dichlorophenylmethylene)bis-(4-hydroxy-2H-chromen-2-one) (3)	69
Figure A. 4 The ¹ H NMR spectrum of 3,3'-(2-chlorophenylmethylene)bis-(4-hydroxy-2H-chromen-2-one) (4)	70
Figure A. 5 The ¹ H NMR spectrum of 3,3'-(3-chlorophenylmethylene)bis-(4-hydroxy-2H-chromen-2-one) (5)	71
Figure A. 6 The ¹ H NMR spectrum of 3,3'-(4-chlorophenylmethylene)bis-(4-hydroxy-2H-chromen-2-one) (6)	72
Figure A. 7 The ¹ H NMR spectrum of 3,3'-(4-bromophenylmethylene)bis-(4-hydroxy-2H-chromen-2-one) (7)	73
Figure A. 8 The ¹ H NMR spectrum of 3,3'-(phenylmethylene)bis-(4-hydroxy-2H-chromen-2-one) (8)	74
Figure A. 9 The ¹ H NMR spectrum of 3,3'-(4-methylphenylmethylene)bis-(4-hydroxy-2H-chromen-2-one) (9)	75
Figure A. 10 The ¹ H NMR spectrum of 3,3'-(4-tertbutylphenylmethylene)bis-(4-hydroxy-2H-chromen-2-one) (10)	76
Figure A. 11 The ¹ H NMR spectrum of 3,3'-(4-hydroxyphenylmethylene)bis-(4-hydroxy-2H-chromen-2-one) (11)	77
Figure A. 12 The ¹ H NMR spectrum of 3,3'-(3-nitrophenylmethylene)bis-(4-hydroxy-2H-chromen-2-one) (12)	78
Figure A. 13 The ¹ H NMR spectrum of 3,3'-(3-hydroxyphenylmethylene)bis-(4-hydroxy-2H-chromen-2-one) (13)	79
Figure A. 14 The ¹ H NMR spectrum of 3,3'-(4-hydroxy-3-methoxyphenylmethylene)bis-(4-hydroxy-2H-chromen-2-one) (14)	80
Figure A. 15 The ¹ H NMR spectrum of 3,3'-(4-hydroxy-3,5-dimethoxyphenylmethylene)bis-(4-hydroxy-2H-chromen-2-one) (15)	81
Figure A. 16 The ¹ H NMR spectrum of 3,3'-(3,4,5-trimethoxyphenylmethylene)bis-(4-hydroxy-2H-chromen-2-one) (16)	82
Figure A. 17 The ¹ H NMR spectrum of 3,3'-(3,4-dimethoxyphenylmethylene)bis-(4-hydroxy-2H-chromen-2-one) (17)	83

Figure A. 18 The ^1H NMR spectrum of 3,3'-(4-methoxyphenylmethylene)bis-(4-hydroxy-2H-chromen-2-one) (18)	84
Figure A. 19 The ^1H NMR spectrum of 3,3'-(2-methoxyphenylmethylene)bis-(4-hydroxy-2H-chromen-2-one) (19)	85
Figure A. 20 The ^1H NMR spectrum of 3,3'-(2,4-dimethoxyphenylmethylene)bis-(4-hydroxy-2H-chromen-2-one) (20)	86



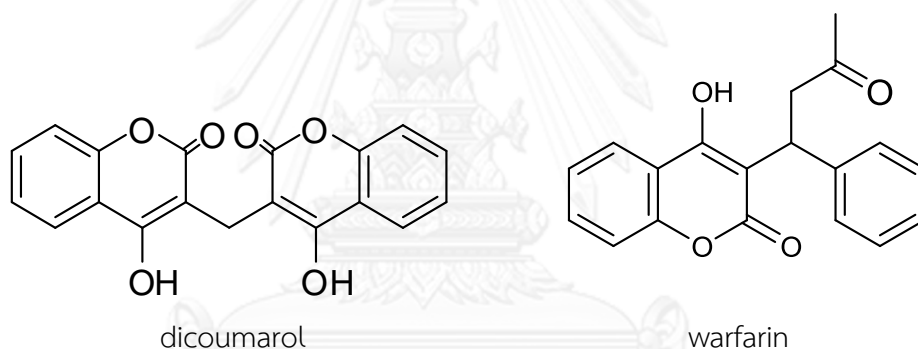
LIST OF ABRVIATIONS

br	broad
°C	degree Celsius
d	doublet (NMR)
NMR	nuclear magnetic resonance
ppm	part per million
s	singlet (NMR)
J	coupling constant
m	multiplet (NMR)
mL	milliliter (s)
t	triplet (NMR)
δ	chemical shift
μL	microliter (s)
μg	microgram (s)

CHAPTER I

INTRODUCTION

Dicoumarol (3,3'-methylene-bis-4-hydroxycoumarin) is a naturally coumarin-based compound which has long been used as an oral anticoagulant drug. It was first isolated from Tonka bean (*Dipteryx odorata* Aubl.) and sweet clover (*Melilotus alba* Medik and *Melilotus officinalis* Pall.)¹. It is now known to be present in many other plants. Moreover, synthetic derivatives based on 4-hydroxycoumarins are interesting. For example, warfarin (3-(α -acetyl benzyl)-4-hydroxycoumarin) is commonly used as an anticoagulant for the prevention and treatment of excessive blood-clotting disorder.² Many dicoumarols and coumarin derivatives have also shown a variety of pharmaceutical activities such as anti-inflammatory, antibacterial, antiviral, anticancer, anti-HIV and antiproliferative activities³. Dicoumarols have received much attention for medical and pharmaceutical applications.

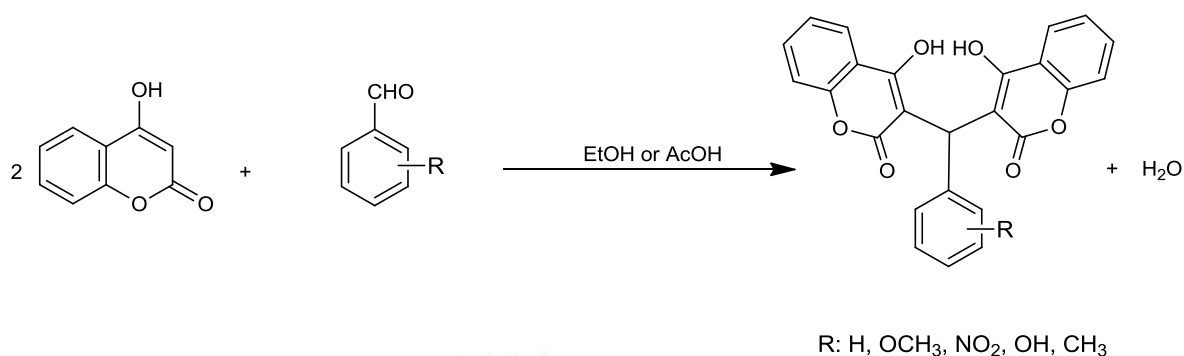


Literature Reviews

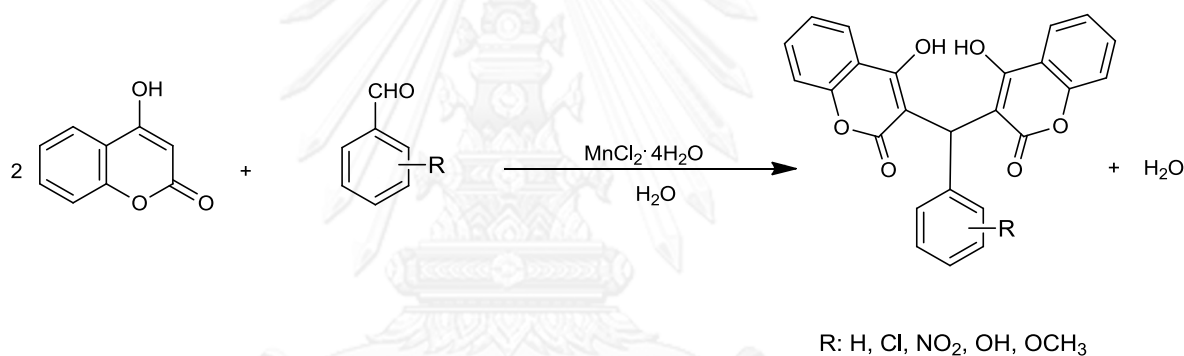
1.1 Synthesis of Dicoumarols

Dicoumarol is 4-hydroxycoumarin derivatives which are a small group in part of natural coumarins. This compound has recently drawn much attention because of many biological and pharmacological properties. The synthesis of 4-hydroxycoumarin derivatives and their biological properties have been reported.⁴ This thesis summarizes the synthesis of dicoumarols reported during the last five years.

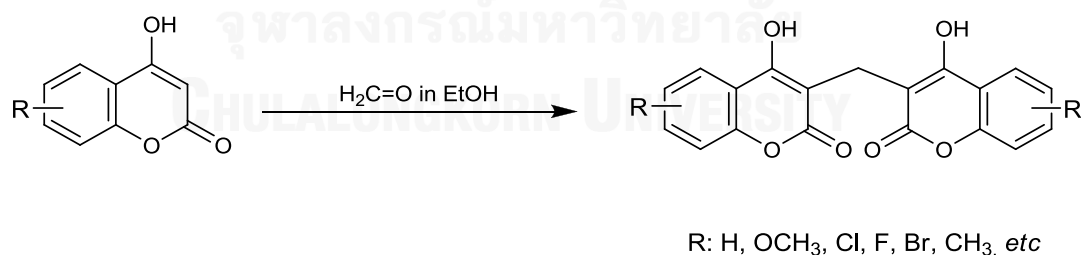
Hamdi *et al.* synthesized dicoumarols by condensation different substituted aromatic aldehydes with 4-hydroxycoumarin in hot EtOH or glacial acetic acid for 5 h with yields of 65-78%.³



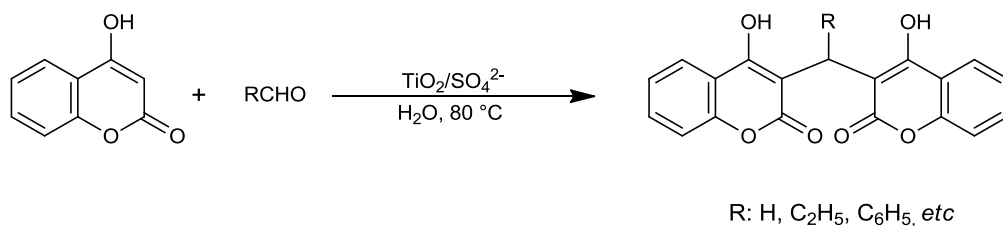
Sangshetti and coworkers reported water mediated efficient one-pot synthesis of different substituted aromatic aldehydes with 4-hydroxycoumarin in water to prepare dicoumarols using MnCl₂·4H₂O as catalyst for an improved and rapid one-pot synthesis. The reaction was completed in 20-40 min with high yield.



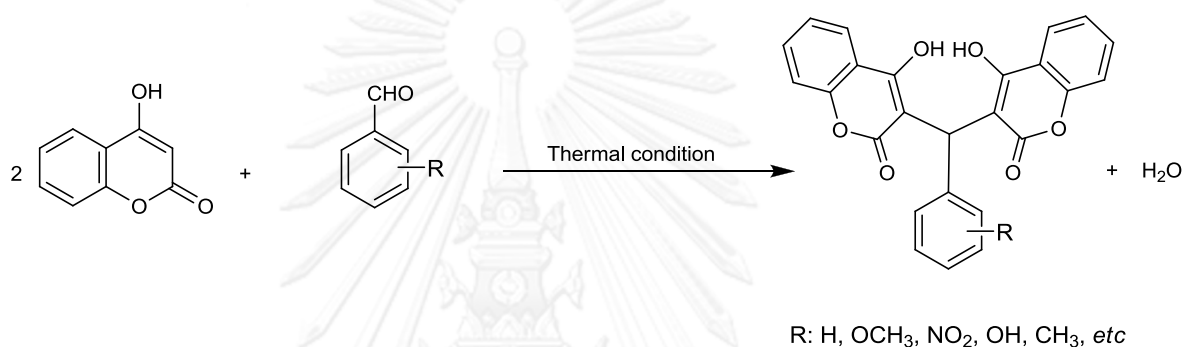
Karen and his teams prepared dicoumarols by condensation 4-hydroxycoumarin with formaldehyde in EtOH for 24 h.⁵



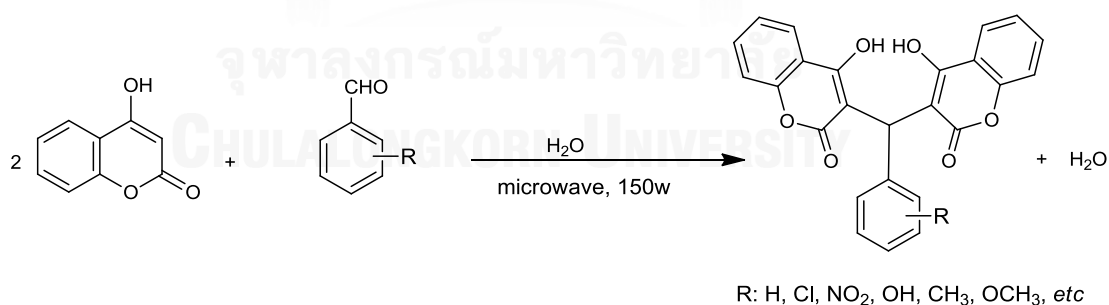
Karmakar *et al.* synthesized dicoumarols by condensation of 4-hydroxycoumarin with different aldehydes in water over TiO₂/SO₄²⁻ (15%) catalyst. The catalyst could reuse several times without significant change in activity. These reactions were completed within 10–30 min.⁶



Shaterian reported one-pot synthesis of dicoumarols under thermal solvent-free conditions. The reaction was completed in 50-130 °C within 3-90 min under catalyst-free and solvent-free conditions. This method is friendly environmental reaction with high yield.⁷

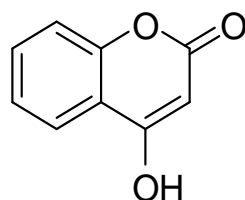


Xia and coworkers developed catalyst-free synthesis of dicoumarols by the reaction of different substituted aromatic aldehydes with 4-hydroxycoumarin in aqueous media under microwave irradiation. The reaction was completed in short reaction time of 8-10 min with high yields of 76-94%.



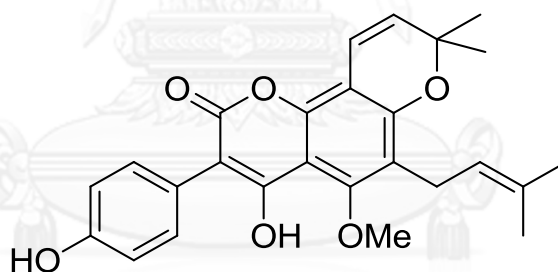
1.2 Biological and Pharmacological Properties of Coumarin Derivatives

1.2.1 4-Hydroxycoumarin

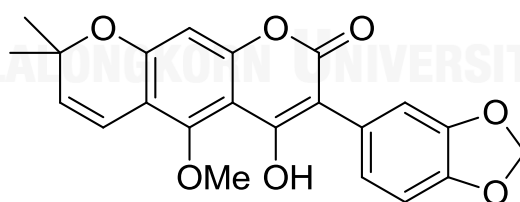


4-hydroxycoumarin

4-Hydroxycoumarin is a small group in part of coumarins substituted in pyrone ring. Some compounds containing the substituent at 3-position displayed high biological activity particularly anticoagulant and antibiotic drugs. 3-Substituted 4-hydroxycoumarins were isolated from many parts of plants. 3-Aryl-4-hydroxycoumarins have been isolated from Leguminosae in genera *Derris* and *Millettia*. They have been assigned by trivial names which they were found. For example, scandenin from the roots of *D. scandens* Benth,⁸ robustin from the roots of *D. robusta* Alfred.⁹



scandenin

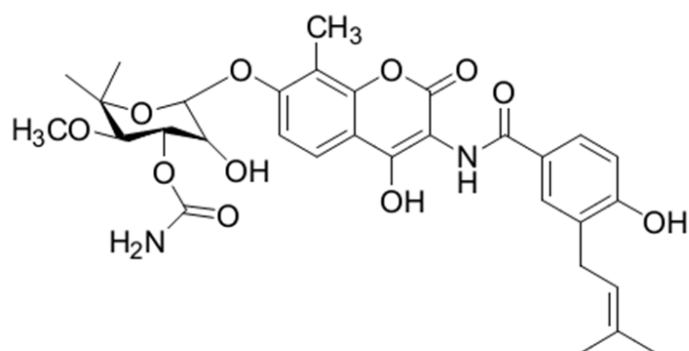


robustin

Several papers have been published on various biological and pharmacological properties of 4-hydroxycoumarin derivatives such as antimicrobial, anticancer and anticoagulant activity as follows:

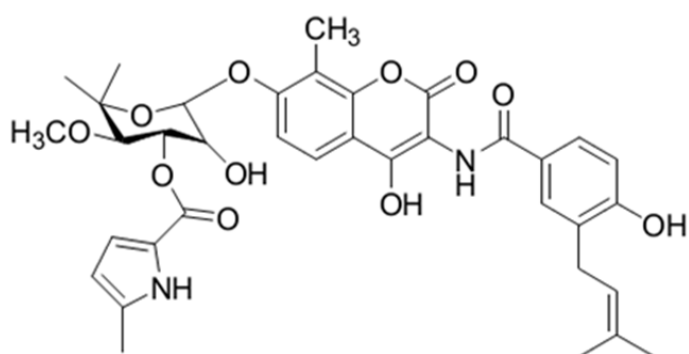
1.2.1.1 Antimicrobial Activity

Novobiocin, clorobiocin and coumermycin A1 are 4-hydroxycoumarin derivatives isolated from *Streptomyces* species. They have been more intensively studied since their pharmacological action as antibiotic drugs.¹⁰ Novobiocin could bind to human and bovine serum albumins. It totally bound after incubation for 30 min at 37 °C, albumin has binding ability for many drugs.

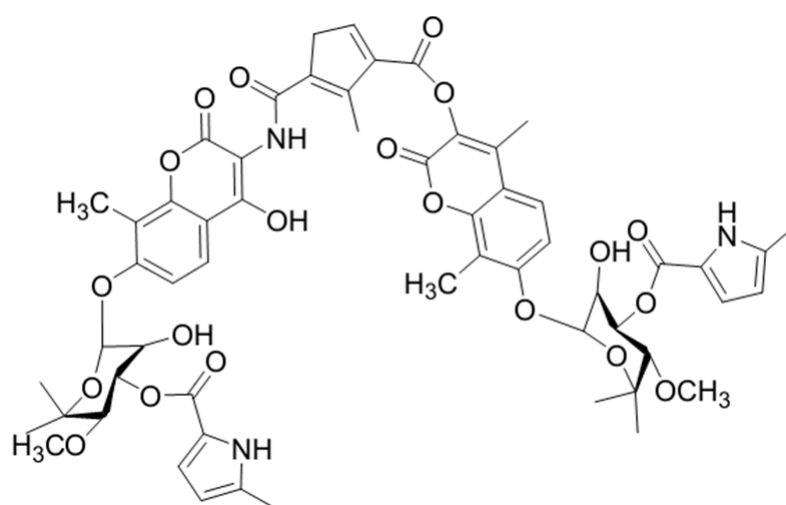


novobiocin

The newer antibiotic clorobiocin and coumermycin A1 are similar mode of action to novobiocin.



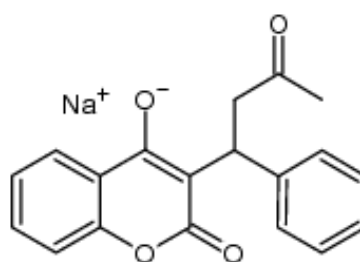
clorobiocin



coumermycin A1

1.2.1.2 Anticancer Activity

Sodium warfarin is widely used for the treatment of many types of cancers. This compound is known for inhibiting tumor spread and stimulating granulocytes, lymphocytes and macrophages.¹¹



sodium warfarin

1.2.1.3 Anticoagulant activity

Warfarin is an oral anticoagulant belonging to 4-hydroxycoumarin class. It is the best known as drug for therapy and prevention of thromboembolic. Dicoumarol is similar to warfarin. It is known to have anticoagulant effect on blood that functions as a vitamin K antagonist.

1.2.2 Dicoumarols

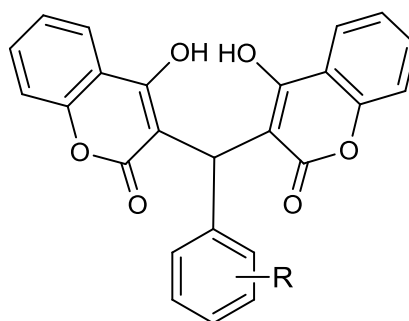
Dicoumarol, a biscoumarin class, was first studied in Canadian cattle because of the ingestion of moldy sweet clovers hay. This compound is best known for its anticoagulant effect on blood.¹² For example, the treatment and prophylaxis of thromboembolic disorder in veins and arteries by production abnormal prothrombins and as an antagonist of vitamin K. Moreover, many studies have interested to explore other activities of dicoumarols and their derivatives.

1.2.2.1 Antimicrobial Activity

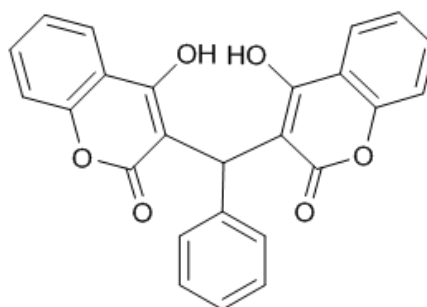
Previous studies have focused on the inhibition of bacterial growth and antifungal activity using naturally occurring coumarins. In 1945, Goth was the first who found the antibacterial activity of dicoumarol to inhibit the growth of many strains of bacteria.⁷

In 1966, Dadák and Hodak tested the antibacterial activity of ten natural coumarins including dicoumarol with two types of bacteria. One type is gram-positive bacteria: *Staphylococcus*, *Micrococcus* and *Bacillus*. The other type is gram-negative bacteria: *Escherichia coli*, *Aerobacter aerogenes* and *Serratia marcescens* by the paper disc method. The results displayed that all derivatives reported certain coumarin derivatives could inhibit selectively against gram-positive microorganisms.⁷

In 2008, Hamdi synthesized 8 dicoumarol derivatives and tested their activity against *Staphylococcus aureus*, *Propionibacterium acne* and *Staphylococcus epidermidis*. The results showed that most compounds are potent against *Staphylococcus aureus*. The minimum inhibitory concentrations (MICs) of all compounds were between 2.6 and 25.5 mg/mol. The most active compound was 3,3'-(phenylmethylene)bis-(4-hydroxy-2H-chromen-2-one). In addition this compound showed good antifungal activities against *P. acnes* and *S. epidermidis*.³

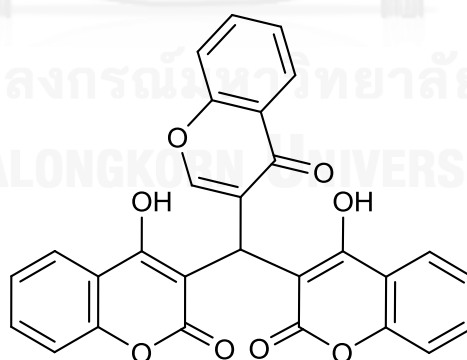


R: H, OCH₃, NO₂, OH, CH₃



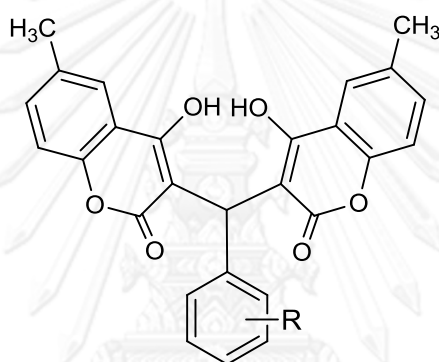
3,3'-(phenylmethylene)bis(4-hydroxy-2H-chromen-2-one)

In 2011, Siddiqui *et al.* synthesized 4 dicoumarols and tested for their antibacterial and antifungal activities. These compounds were screened for their antibacterial activity against *Escherichia coli*, methicillin-resistant *Staphylococcus aureus*, *Pseudomonas aeruginosa*, *Streptococcus pyogenes* and *Klebsiella pneumonia* by the disk diffusion method. The results showed that all compounds have good antibacterial activity with MICs between 12.5 and 50 mg/mL. Antifungal activity was screened by disk diffusion method against *Candida albicans*, *Aspergillus fumigatus*, *Penicillium marneffeii* and *Trichophyton mentagrophytes*. All compounds exhibited good fungicidal activity. Among the studied compounds, 1-(4-oxo-4H-1-benzopyran-3-yl)-1,1-bis(4-hydroxy-1-benzopyran-2-one-3-yl)methane displayed the most potent antibacterial as well as antifungal activities.¹³



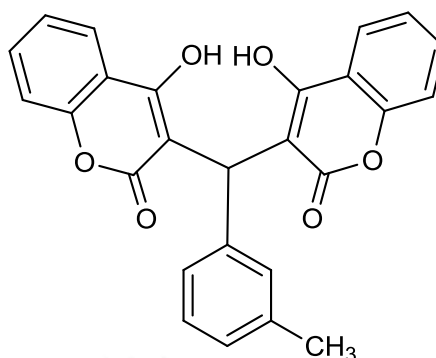
1-(4-oxo-4H-1-benzopyran-3-yl)-1,1-bis(4-hydroxy-1-benzopyran-2-one-3-yl)methane

In 2013, Dholariya and coworkers prepared 6 dicoumarols (the structures shown below) and tested for their antimicrobial activities. The compounds were screened for their antibacterial activity against *Bacillus subtilis*, *Streptococcus pyogenes*, *Escherichia coli* and *Pseudomonas aeruginosa* and compared to standard drugs ciprofloxacin and norfloxacin by using Kirby–Bauer disk diffusion method according to the guidelines of clinical and laboratory standards institute and measured MIC. MIC of all compounds were between 70 to 400 mg/mol. Moreover, these compounds were tested for antifungal activity against *Candida albicans*, *Aspergillus niger* and compared to standard drugs ciprofloxacin and norfloxacin. These compounds showed good antibacterial and antifungal activities comparing to standard drugs.¹⁴



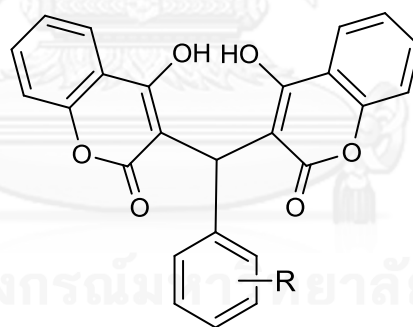
R: H, OH, Cl, NO₂

In 2013, Li *et al.* synthesized 4 dicoumarols and verified by single-crystal X-ray crystallography. These compounds were evaluated for their antibacterial activity against *Staphylococcus aureus* (*S. aureus* ATCC 29213), methicillin-resistant *S. aureus* (MRSA XJ 75302), vancomycin-intermediate *S. aureus* (Mu50 ATCC 700699) by measuring the minimum inhibitory concentration. 3,3'-(3-methylphenylmethylene)bis-(4-hydroxy-2H-chromen-2-one) displayed the most potent antibacterial activity.¹⁵



3,3'-(3-methylphenylmethylene)bis-(4-hydroxy-2H-chromen-2-one)

Besides the international publication, in Thailand Sirisuksukon synthesized fifty five dicoumarol and its derivatives by condensation of 4-hydroxycoumarin with different aldehydes and tested with seven bacteria: *Escherichia coli*, *Bacillus cereus*, *Staphylococcus aureus*, *Salmonella derby*, *Escherichia coli* O157:H7, *Listeria monocytogenes* and Flat sour spoilage by disk diffusion method. The results showed that most dicoumarols selectively inhibited four bacteria including *Bacillus cereus*, *Staphylococcus aureus*, *Listeria monocytogenes* and Flat sour spoilage.¹⁶

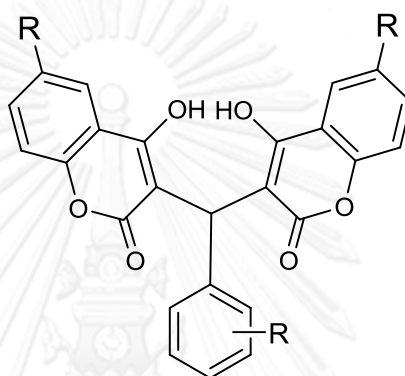


R: H, Cl, NO₂, OH, CH₃, OCH₃, etc

The most active compound was 3,3'-(phenylmethylene)bis-(4-hydroxy-2H-chromen-2-one) as a reference compound. Moreover, the relationship between antibacterial activity and dicoumarol derivatives based on substituent on a benzene ring of dicoumarols were divided into various types. In the case of nitro group, the substituent at the *ortho* position displayed higher activity than others. For the series of halogen group, chloro group at the *ortho* position showed the highest activity.

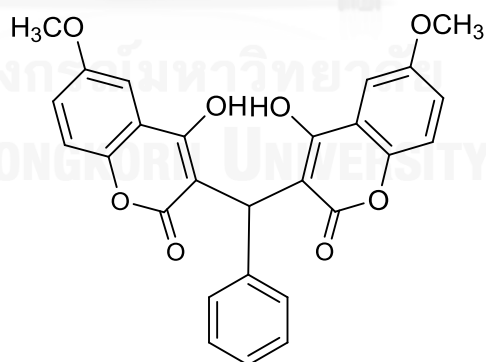
With various substituents on benzene ring such as 3-methoxy-4-hydroxy group, the highest activity was observed.

Worakijthamrongchai prepared sixteen dicoumarols and tested with seven bacteria: *Escherichia coli*, *Bacillus cereus*, *Staphylococcus aureus*, *Salmonella derby*, *Escherichia coli* O157:H7, *Listeria monocytogenes* and Flat sour spoilage by disk diffusion method.



R: H, Cl, NO₂, CH₃, OCH₃, etc

The results showed that these compounds selectively inhibited against four bacteria including *Bacillus cereus*, *Staphylococcus aureus*, *Listeria monocytogenes* and Flat sour spoilage. The most active compound was 3,3'-(benzylidene)*bis*-4-hydroxy-6-methoxycoumarin.¹⁷



3,3'-(benzylidene)*bis*-4-hydroxy-6-methoxycoumarin

Dicoumarols and coumarin-based inhibitors exhibited a broad spectrum of activity against gram positive bacteria.¹⁸ They have been shown to impede the growth of several bacteria strains for instance *Staphylococcus aureus*, *Bacillus anthracis* and *Streptococcus pyogenes*. Another interesting property of dicoumarols lies in the effective anticancer activity.¹⁹ Particularly, several evidences have shown that dicoumarol appears to be the most potent inhibitor which competes with NAD(P)H coenzyme for binding to the two-electron reduction quinone oxidoreductase,²⁰ nitroreductase²¹ and azo-dyes azoreductase,²² a ubiquitous flavoprotein found widely in various organisms. This flavoprotein is an antioxidant enzyme which plays a role in cellular protection by preventing the formation of free radical oxygen/nitrogen such as superoxide (O_2^-), hydroxyl radical ($HO\cdot$) and nitric oxide ($NO\cdot$). These reactive oxygen and nitrogen species (ROS and RNS) are toxic to cells. Inhibition of the redox flavoprotein by dicoumarol generates a high-level of ROS and RNS which increase cellular toxicity and inhibit cell division.

1.2.2.2 Anticoagulant Activity

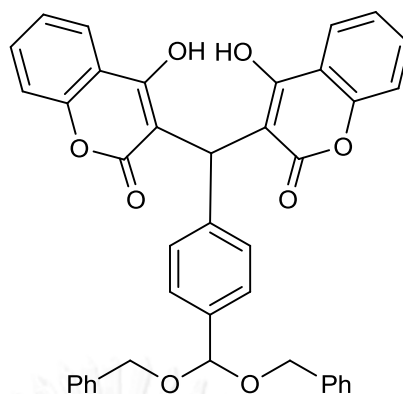
Guminska *et al.* studied anticoagulant activity of 3,3'-(halobenzylidene)bis-4-hydroxycoumarins as compared with that of dicoumarol in rabbits. They reported that all *para* position of halide-substituted derivatives were more active anticoagulants than *ortho* position and *meta* position compounds. Moreover, chloro substituents were better than fluoro and iodo ones.



R: F, Cl, Br, I

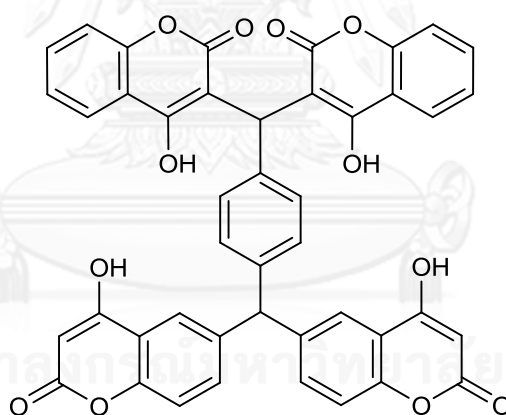
1.2.2.3 Anti HIV Activity

The structures of HIV-1 integrase inhibitors commonly contain two aryl units divided by a central linker. Mostly, at least one of these aryl moieties has to consist of 1,2-dihydroxy substituents in order to express high inhibitory potency. Substituents on a phenyl ring would increase lipophilicity and improve potency.²³



the structures of HIV-1 integrase inhibitor

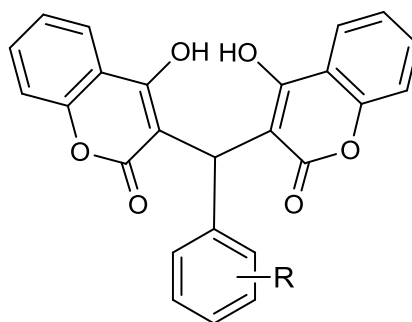
Mazumder *et al.* reported most of dimeric coumarin consisting moieties for potential antiviral, antiprotease and anti integrase activity. They concluded that NSC 158393 consisted of four 4-hydroxycoumarin residues. It displayed the most sufficient in micromolar concentrations. So, NSC 158393 may express necessary elements of the antiintegrase coumarin pharmacophore.



NSC 158393

1.2.2.4 Antioxidant Activity

Hamdi and coworkers reported that dicoumarol derivatives could inhibit and display antiradical activity by reacting with ABTS⁺. Moreover, it could help to increase the overall antioxidant capacity of an organism.



R: H, OCH₃, NO₂, OH, CH₃

1.3. Computational Study

In the past, advanced synthesis and high-throughput screening (HTS) have changed the lead discovery process in chemical pharmaceutical industries. Molecular modeling techniques are widely used to discover drug candidates such as molecular docking and 3D QSAR. Structure aided drug design is helpful for traditional chemistry with the techniques of X-ray crystallography, nuclear magnetic resonance, molecular modeling, computational chemistry, small molecular 3-dimensional database search and the ab initio design of ligands. Many drug design processes depend on the target molecule. There are many advantages for design of inhibitors on the structure of enzyme active site. First the 3-dimensional structure is identified. Second, molecular interaction on target site is resolved. Finally a new ligand with better binding is found and improved shape that fits better into the active site and charge distribution proper for increased interaction energies.

In 2008, Ito compared the active sites of dicoumarol in AzoR which are a homodimeric enzyme, NQO1 of human (Protein Data Bank accession code 2F1O) and NQO1 of rat in complex with duroquinone (Protein Data Bank accession code 1QRD) as shown in Figure 1.1. Their intermolecular forces of these residues are

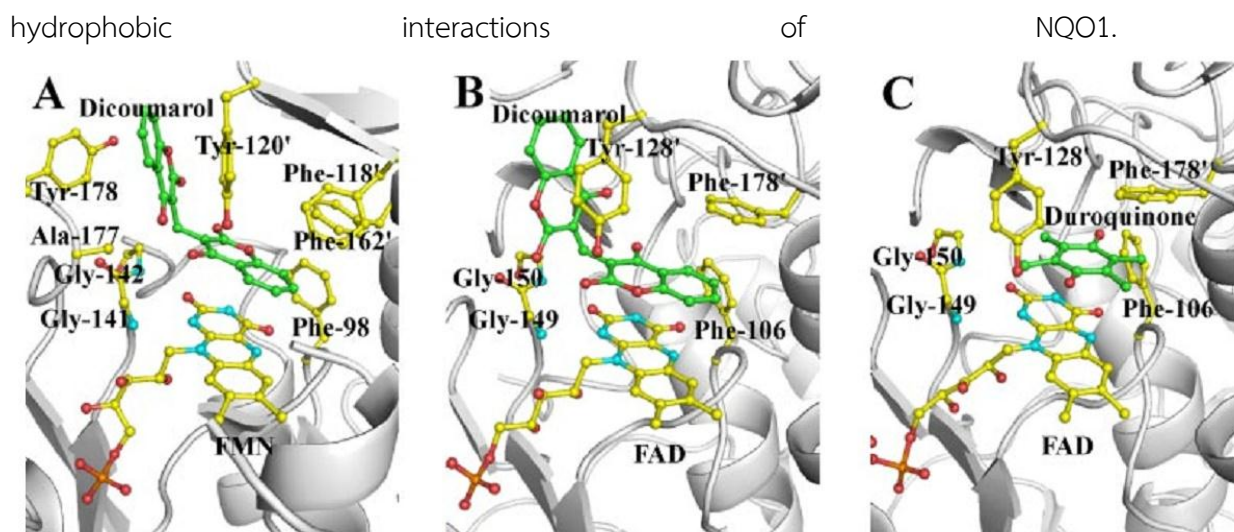


Figure 1.1 A Azor in complex with dicoumarol B NQO1 of human in complex with dicoumarol C NQO1 of rat in complex with duroquinone

In previous research of Nolan in 2009, a series of dicoumarols were studied in computational, synthetic, and biological field. Dicoumarols could be competitive NQO1 inhibitors. For docking studies, two preferred poses were suggested that the first pose has coumarin ring oxygen oriented in the same direction as in the crystallographic toward the glycerol moiety of FAD (pose A). Another pose has O1 pointing in the opposite direction (pose B) in Figure 1.2 Tyr 128 and His 161 is amino acid that found in polar active site.

In previous research of Nolan in 2009, a series of dicoumarols was studied in computational, synthetic, and biological field. Dicoumarols could be competitive NQO1 inhibitors. For docking studies, two preferred poses as presented in Figure 1.2 were suggested that the first pose have a coumarin ring oxygen oriented in the same direction as in the crystallographic toward the glycerol moiety of FAD (pose A). The other has O1 pointing in the opposite direction (pose B).

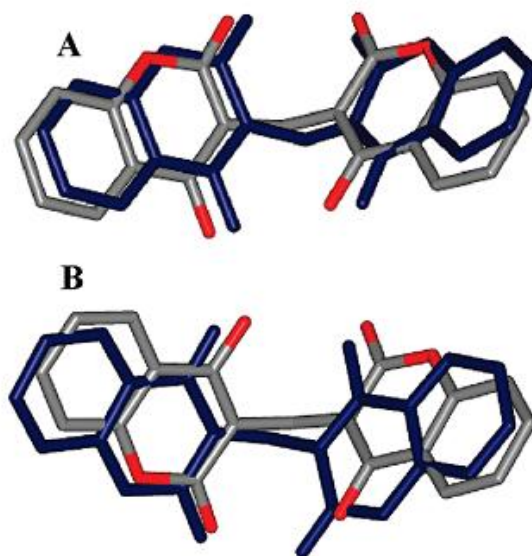


Figure 1.2 The possible arrangements of dicoumarols : A pose A B pose B

The antiproliferative mechanism of action of dicoumarol might be *via* a major suppression of NAD(P)H-dependent flavoprotein activity. This hypothesis is also relied on the available 3D crystal structures of dicoumarol-oxidoreductase complexes such as human NQO1 (pdb 2F1O) in Figure 1.3, nitroreductase (pdb 1OQO) and azoreductase (pdb 2Z9C) from *Escherichia coli*. From the crystallographic data, these proteins share great similarities in the secondary structure organization and the tertiary fold. They are homodimeric proteins with similar quaternary structure arrangement of the two monomers, providing two catalytic sites at the dimer interface. In each binding pocket, dicoumarol and flavin molecules interact with the surrounding residues of both subunits in Figure 1.4. Based on these structural studies, the results provided useful information about the potential and common target proteins for dicoumarol.



Figure 1. 3 structure of the hNQO1

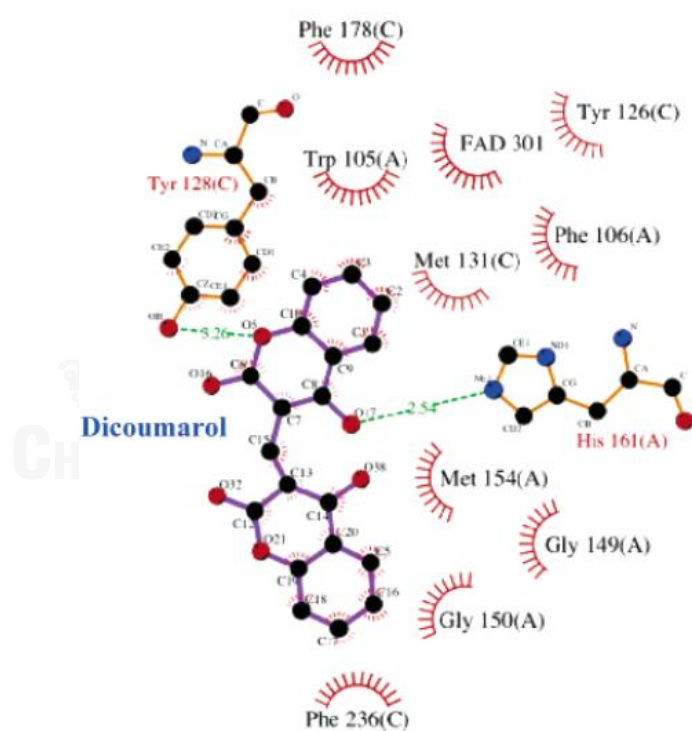


Figure 1. 4 dicoumarol/hNQO1 interactions

3. Aims of Research

Due to the evolution of antibiotic resistance to existing drugs, the development of novel antibacterial drugs is essential. In search for more active compounds, it has been shown that the substitution of phenyl ring at the methylenebis position of dicoumarol exhibited interesting biological activity. This study focused on the synthesis and the antibacterial activity of a series of dicoumarol derivatives containing 3,3'-phenylmethylene-bis-4-hydroxycoumarins. Dicoumarols have been synthesized from the condensation reaction of 4-hydroxycoumarin with benzaldehydes. The synthesized compounds were tested for antibiotic susceptibility against gram-positive *S. aureus* and gram-negative *E. coli* bacteria through disk diffusion assay. The antibacterial activity tested against *E. coli* cells was used as a control. Since their antibacterial mode of action is still poorly understood, using of existing protein sequences and structural information available in databases was made to identify the potent antibiotic target. A molecular modeling approach was employed to reveal the inhibition mechanism of the synthesized compounds on the NAD(P)H-dependent flavoprotein, a hypothetical protein target for dicoumarol. In the study, molecular docking was used to predict the binding mode of dicoumarol to the protein target and a 3D QSAR approach was carried out for the analysis of structural features of dicoumarols as antibacterial activity. Understanding the molecular mechanism of drug action can provide the basis for the rational design of effective drugs.

The objective of the research can be summarized as follows:

1. Synthesis of dicoumarol and its derivatives
2. Antibacterial susceptibility testing against gram-positive and gram-negative bacteria
3. Investigation of the protein-ligand interactions using molecular docking and of structure-activity relationship using 3D QSAR.

CHAPTER II

MATERIALS AND METHODS

2.1 Chemicals

Chemicals and reagents used were of analytical grade from Sigma-Aldrich company and used without further purification. All solvents used in this research were purified using standard methodology except for those which were reagent grades.

2.2 Instruments and Equipment

The ^1H NMR spectra of the synthesized compounds were obtained on a Varian nuclear magnetic resonance spectrometer, model Mercury plus 400 NMR spectrometer which was operated at 400 MHz for ^1H nuclei. The NMR samples were dissolved in CDCl_3 with tetramethylsilane (TMS) as an internal reference or DMSO-d_6 . The chemical shifts were assigned by comparison with residue solvent protons.

2.3 Hardware

- Personal computer (PC)
- Notebook
- High-performance computer cluster "Pheonix" located at Computational Chemistry Unit Cell, Department of Chemistry, Faculty of Science, Chulalongkorn University.

2.4 Software

- Discovery Studio 2.5
- AMBER 10 software package
- Autodock vina
- Gaussian 03 program
- AutoDock Tools
- VMD software
- SYBYL (Tripos International, Missouri, USA).

2.5 Synthesis of Dicoumarols

The synthesis of dicoumarol and its derivatives was based on the previously described method.

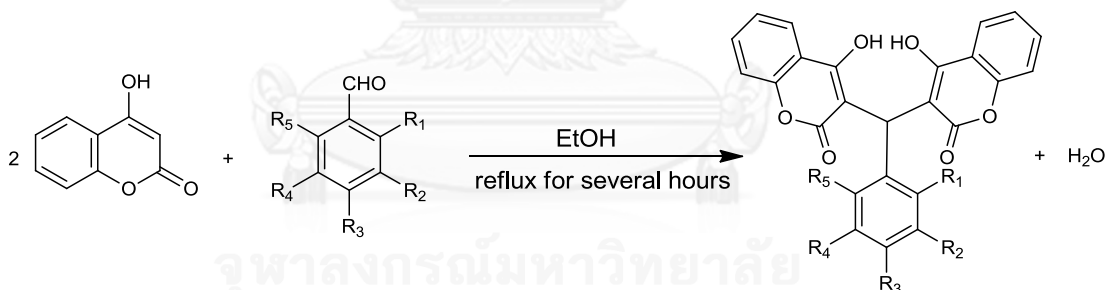
Synthesis of dicoumarol

Dicoumarol was synthesized by dissolving 4-hydroxycoumarin 1.00 g (2.97 mmol) in 300 mL of boiling water, the solution was allowed to cool to 70 °C and 10 mL of 40% aqueous formaldehyde was added with stirring. The mixture was then chilled, the crude product was filtered off and washed well with water, dried and recrystallized with EtOH.



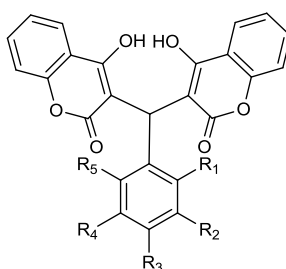
Synthesis of dicoumarol derivatives (3,3'-phenylmethylene-bis-4-hydroxycoumarins)

A series of nineteen dicoumarols with various substituents were synthesized by mixing 4-hydroxycoumarin and selected aromatic aldehydes with different substituents at *ortho*, *meta* or *para* (2:1 ratio of molar equivalent). The mixture was dissolved in EtOH. Each mixture was refluxed until the solid began to precipitate. After cooling, the product was filtered and recrystallized with EtOH. The purified compounds were identified by NMR spectrometer.



All synthesized compounds are listed as shown in Table 2.1.

Table 2. 1 The structures of synthesized dicoumarol and derivatives.



Compound	R ₁	R ₂	R ₃	R ₄	R ₅
1					
2	Cl	H	Cl	H	H
3	H	Cl	Cl	H	H
4	Cl	H	H	H	H
5	H	Cl	H	H	H
6	H	H	Cl	H	H
7	H	H	Br	H	H
8	H	H	H	H	H
9	H	H	Me	H	H
10	H	H	t-Bu	H	H
11	H	H	OH	H	H
12	H	NO ₂	H	H	H
13	H	OH	H	H	H
14	H	OMe	OH	H	H
15	H	OMe	OH	OMe	H
16	H	OMe	OMe	OMe	H
17	H	OMe	OMe	H	H
18	H	H	OMe	H	H
19	OMe	H	H	H	H
20	OMe	H	OMe	H	H

3,3'-methylene-bis-4-hydroxy-2H-chromen-2-one⁵ (1) solid, C₁₉H₁₂O₆, 85% yield, ¹H NMR (400 MHz, CDCl₃) δ (ppm): 11.32 (s, 2H), 7.99 (d, *J* = 7.9 Hz, 2H), 7.58 (t, *J* = 7.8 Hz, 2H), 7.50 – 7.30 (m, 4H), 3.84 (s, 2H).

3,3'-(2,4-dichlorophenylmethylene)bis-(4-hydroxy-2H-chromen-2-one)¹⁶ (2) solid, C₂₅H₁₄Cl₂O₆, 72% yield, ¹H NMR (400 MHz, CDCl₃) δ 11.70 (s, 1H), 11.95 (s, 1H), 8.05 (d, *J* = 1.3 Hz, 1H), 8.03 (d, *J* = 1.2 Hz, 1H), 7.64 (t, *J* = 7.2 Hz, 2H), 7.34 – 7.47 (m, 6H), 7.29 (s, 1H), 6.11 (s, 1H)

3,3'-(3,4-dichlorophenylmethylene)bis-(4-hydroxy-2H-chromen-2-one)¹⁶ (3) solid, C₂₅H₁₄Cl₂O₆, 76% yield, ¹H NMR (400 MHz, CDCl₃) δ 11.58 (s, 1H), 11.31 (s, 1H), 8.08 (d, *J* = 7.8 Hz, 1H), 8.01 (d, *J* = 7.7 Hz, 1H), 7.65 (t, *J* = 7.6 Hz, 2H), 7.48 – 7.36 (m, 4H), 7.27 (d, *J* = 8.7 Hz, 2H), 7.07 (s, 1H), 6.01 (s, 1H).

3,3'-(2-chlorophenylmethylene)bis-(4-hydroxy-2H-chromen-2-one)¹⁶ (4) solid, C₂₅H₁₅ClO₆, 78% yield, ¹H NMR (400 MHz, CDCl₃) δ 11.64 (s, 1H), 10.92 (s, 1H), 8.05 (d, *J* = 6.9 Hz, 1H), 8.00 (d, *J* = 6.8 Hz, 1H), 7.62 (t, *J* = 7.8 Hz, 2H), 7.46 (d, *J* = 7.10 Hz, 1H), 7.42– 7.33 (m, 4H), 7.27 (m, 3H), 6.14 (s, 1H).

3,3'-(3-chlorophenylmethylene)bis-(4-hydroxy-2H-chromen-2-one)¹⁶ (5) solid, 80% yield, ¹H NMR (400 MHz, CDCl₃) δ 11.57 (s, 1H), 11.29 (s, 1H), 8.06 (d, *J* = 7.9 Hz, 1H), 8.00 (d, *J* = 7.9 Hz, 1H), 7.64 (t, *J* = 7.3 Hz, 2H), 7.42-7.39 (m, 4H), 7.25 (d, *J* = 6.0 Hz, 3H), 7.11 (d, *J* = 4.0 Hz, 1H), 6.05 (s, 1H).

3,3'-(4-chlorophenylmethylene)bis-(4-hydroxy-2H-chromen-2-one)¹⁶ (6) solid, C₂₅H₁₅ClO₆, 78% yield, ¹H NMR (400 MHz, CDCl₃) δ 11.54 (s, 1H), 11.32 (s, 1H), 8.07 (d, *J* = 7.8 Hz, 1H), 7.99 (d, *J* = 7.8 Hz, 1H), 7.64 (t, *J* = 7.1 Hz, 2H), 7.49 – 7.33 (m, 4H), 7.28 (d, *J* = 8.0 Hz, 2H), 7.15 (d, *J* = 7.9 Hz, 2H), 6.04 (s, 1H).

3,3'-(4-bromophenylmethylene)bis-(4-hydroxy-2H-chromen-2-one)¹⁶ (7) solid, C₂₅H₁₅BrO₆, 75% yield, ¹H NMR (400 MHz, CDCl₃) δ 11.54 (s, 1H), 11.32 (s, 1H), 8.07 (d, *J* = 7.6 Hz, 1H), 7.99 (d, *J* = 7.4 Hz, 1H), 7.64 (t, *J* = 7.8 Hz, 2H), 7.48 – 7.32 (m, 6H), 7.10 (d, *J* = 8.4 Hz, 2H), 6.02 (s, 1H).

3,3'-(phenylmethylene)bis-(4-hydroxy-2H-chromen-2-one)^{3c} (8) solid, C₂₅H₁₆O₆, 71% yield, ¹H NMR (400 MHz, CDCl₃) δ 11.54 (s, 1H), 11.31 (s, 1H), 8.09 (d, *J* = 4.4 Hz, 1H), 8.04 (d, *J* = 4.8 Hz, 1H), 7.65 (t, *J* = 7.8 Hz, 2H), 7.47 – 7.25 (m, 9H), 6.13 (s, 1H).

3,3'-(4-methylphenylmethylene)bis-(4-hydroxy-2H-chromen-2-one)³ (9) solid, C₂₆H₁₈O₆, 82% yield, ¹H NMR (400 MHz, CDCl₃) δ 11.52 (s, 1H), 11.29 (s, 1H), 8.07 (d, *J* = 6.5 Hz, 1H), 8.00 (d, *J* = 6.8 Hz, 1H), 7.62 (t, *J* = 7.8 Hz, 2H), 7.42-7.35 (m, 4H), 7.11 (m, 4H), 6.06 (s, 1H), 2.33 (s, 3H).

3,3'-(4-tertbutylphenylmethylene)bis-(4-hydroxy-2H-chromen-2-one)¹⁶ (10) solid, C₂₉H₂₄O₆, 85% yield, ¹H NMR (400 MHz, CDCl₃) δ 11.50 (s, 1H), 11.28 (s, 1H), 8.07 (d, *J* = 7.3 Hz, 1H), 8.00 (d, *J* = 7.2 Hz, 1H), 7.63 (t, *J* = 8.5 Hz, 2H), 7.46 – 7.35 (m, 4H), 7.33 (d, *J* = 8.5 Hz, 2H), 7.14 (d, *J* = 8.0 Hz, 2H), 6.06 (s, 1H), 1.30 (s, 9H).

3,3'-(4-hydroxyphenylmethylene)bis-(4-hydroxy-2H-chromen-2-one)¹⁶ (11) solid, C₂₅H₁₆O₇, 74% yield, ¹H NMR (400 MHz, CDCl₃) δ 11.47 (s, 1H), 11.30 (s, 1H), 8.05 (d, *J* = 4.6 Hz, 1H), 7.99 (d, *J* = 4.9 Hz, 1H), 7.62 (t, *J* = 7.6 Hz, 2H), 7.41-7.39 (m, 4H), 7.06 (d, *J* = 8.0 Hz, 2H), 6.78 (d, *J* = 8.2 Hz, 2H), 6.03 (s, 1H), 5.47 (s, 1H).

3,3'-(3-nitrophenylmethylene)bis-(4-hydroxy-2H-chromen-2-one)¹⁶ (12) solid, C₂₅H₁₅NO₈, 87% yield, ¹H NMR (400 MHz, CDCl₃) δ 11.58 (s, 1H), 11.39 (s, 1H), 8.00 (d, *J* = 7.7 Hz, 2H), 8.07 (s, 1H), 8.00 (d, *J* = 7.7 Hz, 1H), 7.67 (t, *J* = 7.0 Hz, 2H), 7.58 (d, *J* = 7.7 Hz, 1H), 7.52 (t, *J* = 7.9 Hz, 1H), 7.48 – 7.36 (m, 4H), 6.13 (s, 1H).

3,3'-(3-hydroxyphenylmethylene)bis-(4-hydroxy-2H-chromen-2-one)²⁴ (13) solid, C₂₅H₁₆O₇, 84% yield, ¹H NMR (400 MHz, CDCl₃) δ 11.59 (s, 1H), 11.27 (s, 1H), 8.05 (s, 2H), 7.66 (t, *J* = 7.8 Hz, 2H), 7.22 (t, *J* = 7.8 Hz, 1H), 6.85-6.71 (m, 3H), 7.50 – 7.35 (m, 4H), 6.07 (s, 1H).

3,3'-(4-hydroxy-3-methoxyphenylmethylene)bis-(4-hydroxy-2H-chromen-2-one)²⁵ (14) solid, C₂₆H₁₈O₈, 83% yield, ¹H NMR (400 MHz, CDCl₃) δ 11.52 (s, 1H), 11.29 (s, 1H), 8.06 (d, *J* = 6.8 Hz, 1H), 8.00 (d, *J* = 6.7 Hz, 1H), 7.63 (t, *J* = 7.8 Hz, 2H), 7.41-7.38 (m, 4H), 6.86 (d, *J* = 8.3 Hz, 1H), 6.77 – 6.65 (m, 2H), 6.06 (s, 1H), 5.58 (s, 1H), 3.78 (s, 3H)

3,3'-(4-hydroxy-3,5dimethoxyphenylmethylene)bis-(4-hydroxy-2H-chromen-2-one)²⁶ (15) solid, C₂₇H₂₀O₉, 87% yield, ¹H NMR (400 MHz, CDCl₃) δ 11.53 (s, 1H), 11.29 (s, 1H), 8.04 (d, *J* = 16.0 Hz, 2H), 7.67 (t, *J* = 7.7 Hz, 2H), 7.42-7.37 (m, 4H), 6.41 (s, 2H), 6.07 (s, 1H), 5.50 (s, 1H), 3.75 (s, 6H).

3,3'-(3,4,5-trimethoxyphenylmethylene)bis-(4-hydroxy-2H-chromen-2-one)³ (16) solid, C₂₈H₂₂O₉, 88% yield, ¹H NMR (400 MHz, CDCl₃) δ 11.56 (s, 1H), 11.29 (s, 1H), 8.04 (d, *J* = 14.6 Hz, 2H), 7.64 (t, *J* = 7.8 Hz, 2H), 7.42-7.40 (m, 4H), 6.41 (s, 2H), 6.07 (s, 1H), 3.84 (s, 3H), 3.71 (s, 6H).

3,3'-(3,4-dimethoxyphenylmethylene)bis-(4-hydroxy-2H-chromen-2-one)¹⁶ (17)

solid, C₂₇H₂₀O₈, 83% yield, ¹H NMR (400 MHz, CDCl₃) δ 11.53 (s, 1H), 11.30 (s, 1H), 8.07 (d, *J* = 5.1 Hz, 1H), 8.00 (d, *J* = 5.7 Hz, 1H), 7.63 (t, *J* = 7.8 Hz, 2H), 7.43-7.41 (m, 4H), 6.79 (dd, *J* = 21.3, 8.9 Hz, 2H), 6.70 (s, 1H), 6.07 (s, 1H), 3.87 (s, 3H), 3.73 (s, 3H).

3,3'-(4-methoxyphenylmethylene)bis-(4-hydroxy-2H-chromen-2-one)³ (18)

solid, C₂₆H₁₈O₇, 81% yield, ¹H NMR (400 MHz, CDCl₃) δ 11.51 (s, 1H), 11.30 (s, 1H), 8.05 (d, *J* = 13.8 Hz, 2H), 7.64 (t, *J* = 7.8 Hz, 2H), 7.42 (d, *J* = 8.3 Hz, 4H), 7.14 (d, *J* = 8.3 Hz, 2H), 6.87 (d, *J* = 7.8 Hz, 2H), 6.06 (s, 1H), 3.81 (s, 3H).

3,3'-(2-methoxyphenylmethylene)bis-(4-hydroxy-2H-chromen-2-one)¹⁶ (19)

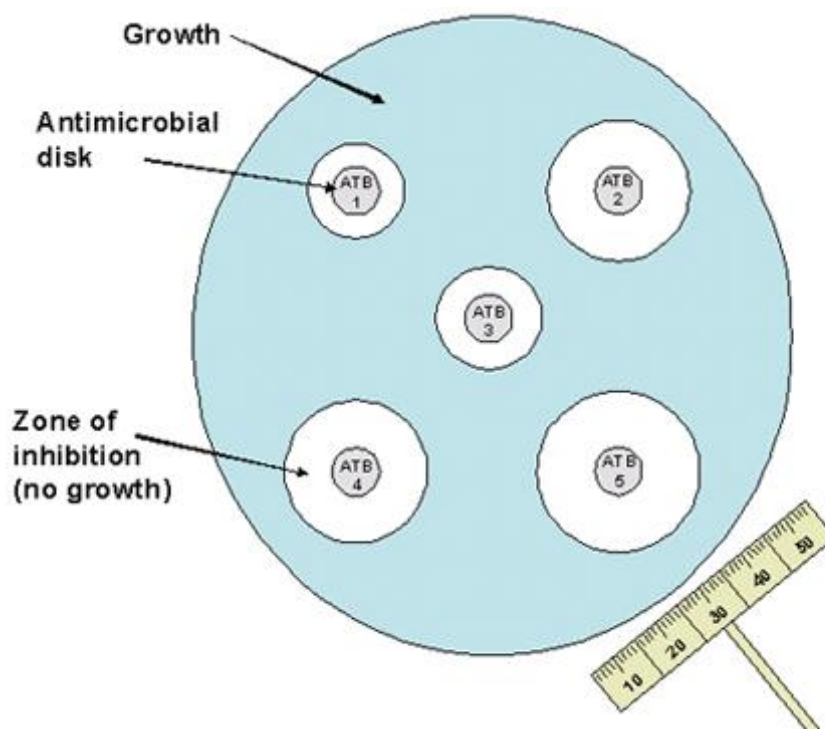
solid, C₂₆H₁₈O₇, 81% yield, ¹H NMR (400 MHz, CDCl₃) δ 11.22 (s, 1H), 8.01 (d, *J* = 7.9 Hz, 2H), 7.59 (t, *J* = 7.8 Hz, 2H), 7.48 – 7.21 (m, 4H), 6.94 (t, *J* = 7.6 Hz, 3H), 6.85 (d, *J* = 8.1 Hz, 1H), 6.08 (s, 1H), 3.57 (s, 3H).

3,3'-(2,4-dimethoxyphenylmethylene)bis-(4-hydroxy-2H-chromen-2-one)¹⁶ (20)

solid, C₂₇H₂₀O₈, 89% yield, ¹H NMR (400 MHz, CDCl₃) δ 11.20 (s, 1H), 8.01 (d, *J* = 7.7 Hz, 2H), 7.59 (t, *J* = 7.1 Hz, 2H), 7.46 – 7.31 (m, 4H), 7.16 (d, *J* = 8.5 Hz, 1H), 6.50 – 6.39 (m, 2H), 6.01 (s, 1H), 3.79 (s, 3H), 3.55 (s, 3H).

2.6 Antibacterial Susceptibility Testing

The bioassay was carried out by disk diffusion method. The purified dicoumarol and its derivatives were tested with gram-positive *Staphylococcus aureus* ATCC-6538 and *Bacillus subtilis* ATCC-6633, and gram-negative *Escherichia coli* ATCC-25922 and *Klebsiella sp.* TISTR-1843. A stock solution was prepared by dissolving 10 mg of the tested sample in 1000 μ L of DMSO. The concentration of sample was 10,000 ppm. A 20 μ L of each preparation were dropped into a 6 mm disk. After incubation at 37 °C for 24 h, the diameter of clear zone was measured. Penicillin G was used as positive control for *S. aureus* and chloramphenicol was used for *B. subtilis* while DMSO was used as negative control. The antibiotic susceptibility tests were undertaken twice.



(<http://www.cdc.gov/meningitis/lab-manual/chpt11-antimicrobial-suscept-testing.html>)

2.7 Molecular Modeling

2.7.1 Comparative Modeling of a Protein Target from *S. aureus*

Homology modeling of azoreductase *S. aureus* was built using Discovery Studio 2.5 (Accelrys Inc., San Diego, CA, USA). First, NCBI BLAST (Figure 2.1) to search for protein sequences from three crystal structures: human NQO1 (pdb 2F1O), nitroreductase (pdb 1OOQ) and azoreductase (pdb 2Z9C) from *E. coli* through identified protein-encoding genes in *S. aureus* genome in order to be primary information of recognition homologous proteins from *S. aureus*. Azoreductase with dicoumarol complex from *E. coli* was the most similar to complete sequence information. The crystal structure of *E. coli* azoreductase was therefore used as template of *S. aureus*. Sequence alignment and comparative modeling were carried out using Discovery Studio 2.5. The best *S. aureus* protein structure with lowest DOPE (density optimization potential energy) score was selected and subjected to structure validation using Procheck. The presence of dicoumarol and flavin mononucleotide (FMN) was next optimized for energy minimization using AMBER 10 software.²⁶ Finally, the structure of the protein-dicoumarol-FMN complex was prepared by

superimposing the model onto the template structure. The force field parameters of FMN were brought from Lugsanangarm *et al.* while those of dicoumarol were developed using the same protocol as described in previous literature.

BLAST® Basic Local Alignment Search Tool

Home Recent Results Saved Strategies Help

NCBI/ BLAST/ blastp suite

blastn blastp blastx tblastn tblastx

Enter Query Sequence

Enter accession number(s), gi(s), or FASTA sequence(s) [Clear](#) Query subrange [Query subrange](#)

2Z9C_A From To

Or, upload file No file selected.

Job Title Enter a descriptive title for your BLAST search

Align two or more sequences

Choose Search Set

Database Non-redundant protein sequences (nr)

Organism Enter organism name or id--completions will be suggested Exclude +
Enter organism common name, binomial, or tax id. Only 20 top taxa will be shown.

Exclude Models (XM/XP) Uncultured/environmental sample sequences

Entrez Query aureus Enter an Entrez query to limit search

Program Selection

Algorithm

blastp (protein-protein BLAST)

PSI-BLAST (Position-Specific Iterated BLAST)

PHI-BLAST (Pattern Hit Initiated BLAST)

DELTA-BLAST (Domain Enhanced Lookup Time Accelerated BLAST)

Choose a BLAST algorithm

BLAST Search database Non-redundant protein sequences (nr) using Blastp (protein-protein BLAST)

Show results in a new window

Figure 2. 1 NCBI BLAST search

2.7.2 Molecular Docking Study of Dicoumarols for Antibacterial Activity

Molecular docking approach was performed to investigate the binding mode of dicoumarols to target protein. Dicoumarols were docked around residues of the *S. aureus* flavoprotein using Autodock vina. 3D structures of all synthesized dicoumarol derivatives were constructed and optimized at the semi-empirical AM1 level using the Gaussian 03 program. For the target protein, a dicoumarol molecule and all hydrogen atoms of the energy-minimized comparative model were deleted while the FMN molecule was remained in the binding pocket of the receptor during the docking simulation. The protein and all ligands were assigned gasteiger partial charges, atom types and polar hydrogen using AutoDock Tools (ADT).²⁷ Then, the torsional bonds of ligands were set free. The location of dicoumarol in the crystal structure was evaluated center of 40×40×40 Å grid box. The exhaustiveness parameter was set to 64. The root-mean square deviation (RMSD) of the top ten conformations from crystal structure was ranked in agreement with the binding energy and clustered on the basis. For each compound, the docked poses that adopt an orientation similar to that of the experimental X-ray structure (RMSD < 3Å) was chosen as a representative bound conformation. After that, VMD software was used to analyze and visualize the structures of protein and dicoumarol.

2.7.3 Physicochemical Properties of the Synthesized Compounds

3D structures of all synthesized dicoumarol derivatives were constructed and optimized at the semi-empirical AM1 level using the Gaussian 03 program. The physicochemical properties of the synthesized compounds can be computed by using its additive property and many molecular modeling softwares are available. For this study, molecular weight, lipophilicity, donate hydrogen atoms and accept hydrogen atoms were calculated by Discovery Studio program.

2.7.4 Quantitative Antibacterial Structure Activity Relationship (QSAR) Study

All synthesized dicoumarol derivatives and their inhibition zones were used to construct CoMFA and CoMSIA models using the program SYBYL (Tripos International, Missouri, USA). The training set of 14 dicoumarol derivatives was selected on the basis of structural diversity and wide range of activity and the test set contained 5 compounds (Table 2.1). Model building of the compounds was already described in the previous section (molecular docking). Atomic charges of the compounds were assigned according to Gasteiger–Huckel method²⁸. Structural alignment of the compounds was performed using the SYBYL automatic alignment feature. For

CoMFA, steric and electrostatic fields of the compounds were automatically computed using the standard CoMFA method with default parameters. Analogously, the calculated CoMSIA fields are associated with five descriptors including steric, electrostatic, hydrophobic, hydrogen bond donor and hydrogen bond acceptor. The partial least squares (PLS) analysis was carried out using the “leave-one-out” cross-validation protocol to choose the optimum number of components (ONC) that does not exceed one-third of the number of the training compounds but yields the highest cross-validated correlation coefficient (q^2). Subsequently, non-cross-validation analysis was performed with the same ONC to calculate the conventional correlation coefficient (r^2), standard error of estimation (SEE) and F-values.



CHAPTER III

RESULTS AND DISCUSSION

This chapter presents information regarding chemicals, general procedure, antibacterial susceptibility testing, and molecular modeling which consists of homology modeling, molecular docking and QSAR. The details of each step are described below.

3.1 Synthesis of Dicoumarols

Many methods to synthesize dicoumarols have been reported in literatures. In this research, dicoumarol and nineteen dicoumarol derivatives (Figure 3.1, see also Table 2.1) were synthesized from the condensation reaction between two mole equivalents of 4-hydroxycoumarin and one mole equivalent of corresponding aldehydes in EtOH for 24 h. In the preparation of dicoumarol, formaldehyde was reacted with 4-hydroxycoumarin in hot water.

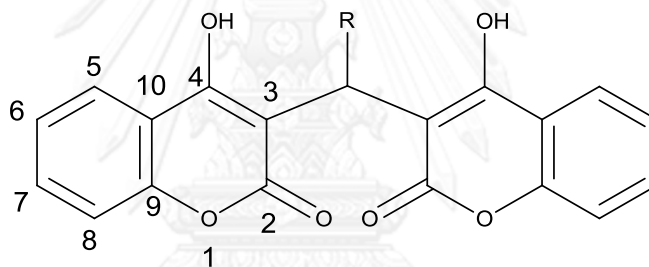


Figure 3. 1 Labeling of dicoumarol core structure

The synthesized compounds were attained in good to excellent yield. The physical properties and yields of all dicoumarol derivatives were in the range of 70-90% (Table 3.1). From the selected ^1H NMR spectrum of compound **1** (Figure 3.2), 2H integration of H-5 was detected as doublet around δ 7.90 ppm ($J = 7.9$ Hz) and 2H integration of H-6 was seen as triplet around δ 7.58 ppm ($J = 7.8$ Hz). The overlapped 4H integration of H-7 and H-8 around δ 7.30-7.50 ppm was detected. The typical 2H integration of CH methylene bridge was observed in δ 3.84 ppm depending on the substituent (R) at the bridge carbon.

Table 3. 1 Physical property and % yield of synthesized dicoumarols

Compound	Appearance	% Yield
1	white powder	85
2	white powder	72
3	white amorphous	76
4	white amorphous	78
5	white amorphous	80
6	white mirror crystal	78
7	white powder	75
8	small white crystal	71
9	white powder	82
10	white crystal	85
11	brown amorphous	74
12	white crystal	87
13	white crystal	84
14	white amorphous	83
15	white powder	87
16	white amorphous	88
17	white powder	83
18	white powder	81
19	white amorphous	81
20	yellow powder	89

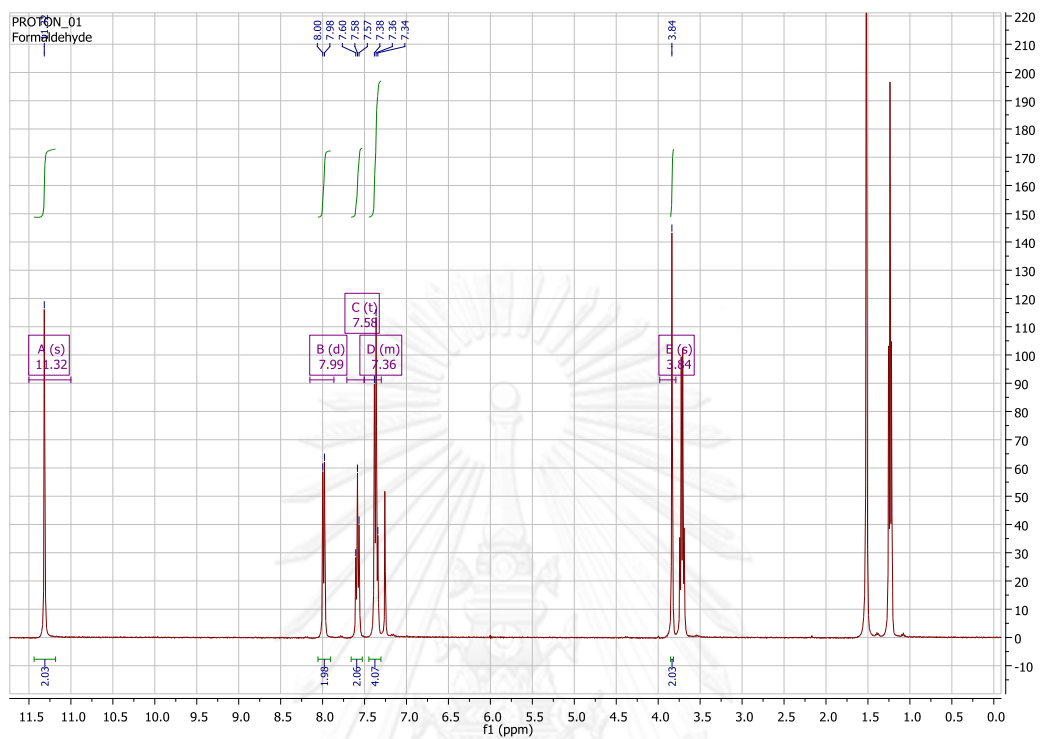


Figure 3. 2 The ^1H NMR spectrum of compound 1

The feature and pattern of signals in the ^1H NMR spectra of dicoumarols was tabulated in Table 3.2.

Table 3. 2 The ^1H NMR spectral assignments of synthesized dicoumarols

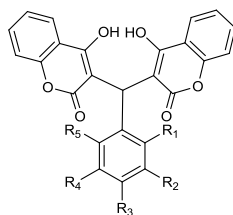
Compound	Chemical shift (ppm)					
	H-5	H-6	H-7,H-8	CH- bridge	4-OH	Others
1	7.99(d)	7.58(t)	7.50- 7.30(m)	3.84(s)	11.32(s)	-
2	8.05(d) 8.03(d)	7.64(t)	7.34- 7.47(m)	6.11(s)	11.70(s), 11.95(s)	7.34-7.47(m), 7.29(s) (Ar-H)
3	8.08(d) 8.01(d)	7.65(t)	7.48- 7.36(m)	6.01(s)	11.58(s), 11.31(s)	7.27(d), 7.07(s)(Ar-H)
4	8.05(d) 8.00(d)	7.62(t)	7.42- 7.33(m)	6.14(s)	11.64(s), 10.92(s)	7.46(d), 7.27(m) (Ar-H)
5	8.06(d) 8.00(d)	7.64(t)	7.42- 7.39(m)	6.05(s)	11.57(s), 11.29(s)	7.25(d), 7.11(s)(Ar-H)
6	8.07(d) 7.99(d)	7.64(t)	7.49- 7.33(m)	6.04(s)	11.54(s), 11.32(s)	7.28(d), 7.15(d)(Ar-H)
7	8.07(d) 7.99(d)	7.64(t)	7.48- 7.32(m)	6.02(s)	11.54(s), 11.32(s)	7.48-7.32(m), 7.10(d)
8	8.09(d) 8.04(d)	7.65(t)	7.47- 7.25(m)	6.13(s)	11.54(s), 11.31(s)	7.47-7.25(m)
9	8.07(d) 8.00(d)	7.62(t)	7.42- 7.35(m)	6.06(s)	11.52(s), 11.29(s)	2.33(s)(CH ₃), 7.11(m) (Ar-H)
10	8.07(d) 8.00(d)	7.63(t)	7.46- 7.35(m)	6.06(s)	11.50(s), 11.28(s)	1.30(s)(CH ₃), 7.14(d), 7.33(d) (Ar-H)
11	8.05(d) 7.99(d)	7.62(t)	7.41-7.39(m)	6.03(s)	11.47(s), 11.30(s)	5.47(OH), 6.78(d), 7.06(d)(Ar-H)
12	8.07(d) 8.00(d)	7.67(t)	7.48- 7.36(m)	6.13(s)	11.58(s), 11.39(s)	7.52(t), 7.58(d)(Ar-H), 8.00(d), 8.07(s)

13	8.05(s)	7.66(t)	7.50- 7.35(m)	6.07(s)	11.59(s), 11.27(s)	6.85-6.71(m), 7.22(t)(Ar-H)
14	8.06(d) 8.00(d)	7.63(t)	7.41- 7.38(m)	6.06(s)	11.29(s), 11.52(s)	5.58(s)(OH), 6.86(d), 6.77-6.65(m)(Ar-H)
15	8.04(d)	7.67(t)	7.42- 7.37(m)	6.07(s)	11.53(s), 11.29(s)	3.75(s)(OCH ₃), 5.50(s)(OH), 6.41(s) (Ar-H)
16	8.04(d)	7.64(t)	7.42-7.40 (m)	6.07(s)	11.56(s), 11.29(s)	3.84(s)(OCH ₃), 3.71(s)(OCH ₃), 6.41(s)(Ar-H)
17	8.07(d) 8.00(d)	7.63(t)	7.43- 7.41(m)	6.07(s)	11.53(s), 11.30(s)	3.87(s)(OCH ₃), 3.73(s)(OCH ₃), 6.70(s), 6.79(dd) (Ar-H)
18	8.05(s)	7.64(t)	7.43- 7.37(m)	6.06(s)	11.51(s), 11.30(s)	3.81(s), 7.14(d), 6.87(d) (Ar-H)
19	8.01(d)	7.59(t)	7.48- 7.21(m)	6.08(s)	11.22(s)	3.57(s)(OCH ₃), 6.85(d), 6.94(t), 7.48-7.21(m) (Ar-H)
20	8.01(d)	7.59(t)	7.46- 7.31(m)	6.01(s)	11.20(s)	3.55(s), 3.79(s) (OCH ₃), 7.16(d), 6.50-6.39(m)(Ar-H)

3.2 Antibacterial Susceptibility Testing

Four bacteria were selected for testing with synthesized dicoumarols and commercially available antibiotic drug. These bacteria can be classified into two groups: gram-positive bacteria, *Staphylococcus aureus* and *Bacillus subtilis*, and gram-negative bacteria, *Escherichia coli* and *Klebsiella* sp. The antibacterial activity testing was performed using the standard paper-disc method. The concentration of sample was 10,000 ppm. All bacteria testings were performed by incubation at 37°C for 24 h at microbiology laboratory' 4th floor, Tab Building, Faculty of Science, Chulalongkorn University. The antibiotic susceptibility was determined by measuring the diameter of inhibition zone. The antibacterial activities of twenty dicoumarols are shown in Table 3.3.

Table 3.3 Antibacterial activities of synthesized dicoumarol and its derivatives



Compound	R ₁	R ₂	R ₃	R ₄	R ₅	Inhibition zone (mm) ^a			
						<i>S. aureus</i>	<i>B. subtilis</i>	<i>E. coli</i>	<i>Klebsiella</i> sp.
1						28	32	nz	nz
2	Cl	H	Cl	H	H	26	32	nz	nz
3	H	Cl	Cl	H	H	23	28	nz	nz
4	Cl	H	H	H	H	24	29	nz	nz
5	H	Cl	H	H	H	26	28	nz	nz
6	H	H	Cl	H	H	25	29	nz	nz
7	H	H	Br	H	H	24	28	nz	nz
8	H	H	H	H	H	23	29	nz	nz
9	H	H	Me	H	H	23	25	nz	nz
10	H	H	<i>t</i> -Bu	H	H	20	20	nz	nz
11	H	H	OH	H	H	20	26	nz	nz
12	H	NO ₂	H	H	H	24	25	nz	nz
13	H	OH	H	H	H	19	38	nz	nz
14	H	OMe	OH	H	H	22	22	nz	nz
15	H	OMe	OH	OMe	H	23	22	nz	nz
16	H	OMe	OMe	OMe	H	16	23	nz	nz
17	H	OMe	OMe	H	H	18	22	nz	nz
18	H	H	OMe	H	H	19	27	nz	nz
19	OMe	H	H	H	H	21	31	nz	nz
20	OMe	H	OMe	H	H	19	28	nz	nz
21	Positive control ^b					40	35	nt	27
22	DMSO					nz	nz	nz	nz

^aThe antibacterial activities tests were undertaken twice. Average values are reported. nz: no inhibition zone, nt: not test, ^bPositive control is penicillin G for *S. aureus* while chloramphenicol was used for *B. subtilis*. and *Klebsiella* sp.

Table 3.3 reveals antibacterial activities of twenty dicoumarols. It was found that all synthesized dicoumarols selectively inhibited against gram-positive bacteria. Penicillin G (10 µg, Oxoid) was used as a positive control for *S. aureus* and *E. coli* and displayed 40 mm of inhibition zone as shown in Figure 3.3 (A) while chloramphenicol (30 µg , Oxoid) was used for *B. subtilis* and *Klebsiella* sp. with found 35 mm of inhibition zone as shown in Figure 3.3 (B). The synthesized compounds considerably inhibited against *S. aureus* with a range of clear zone from 16 to 28 mm. For *B. subtilis*, a range of clear zone was 20 to 32 mm. However, there was no inhibition observed for *E. coli* strain and *Klebsiella* sp. in Figures 3.4, 3.5, 3.6 and 3.7. These results are consistent with the previous report that dicoumarols were selectively against gram-positive microorganisms. This study is a process for screening a new antibacterial drug for treatment bacterial disease. One of possible explanations was due to a permeability barrier to dicoumarol molecule since structures and properties of cell membranes between the two bacterial cells are different. The presence of outer membrane of peptidoglycan in *E. coli* may prevent the transport of dicoumarols into the cell. There is yet no evidence for the relationship between molecular properties of the tested compounds and their transportation across the membrane.



Figure 3. 3 positive control (A) penicillin G (B) chloramphenicol

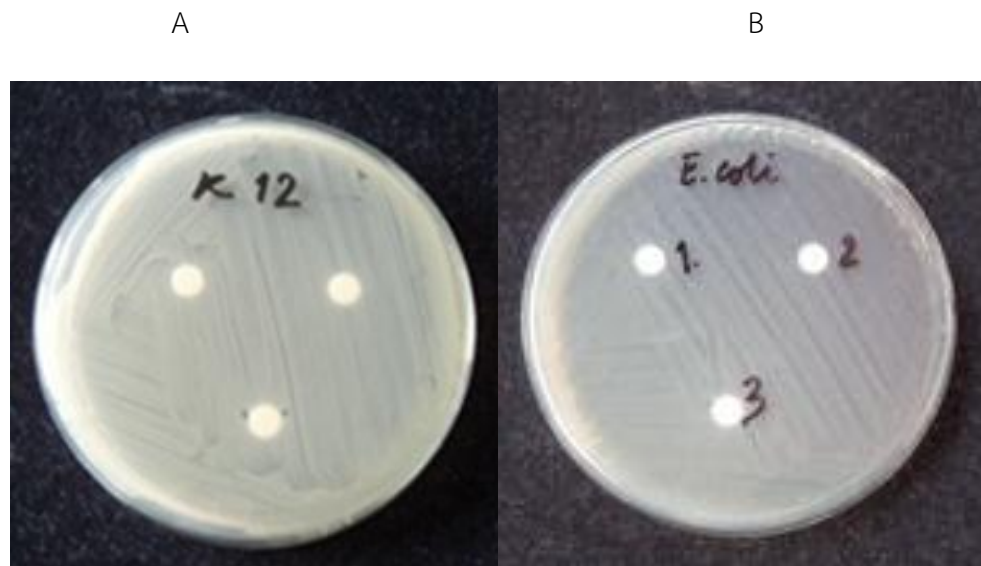


Figure 3. 4 no inhibition zone for (A) *E.coli* (B) *Klebsiella* sp.



Figure 3. 5 Inhibition tests of sample on *B. subtilis* for 24 h., incubated at 37°C

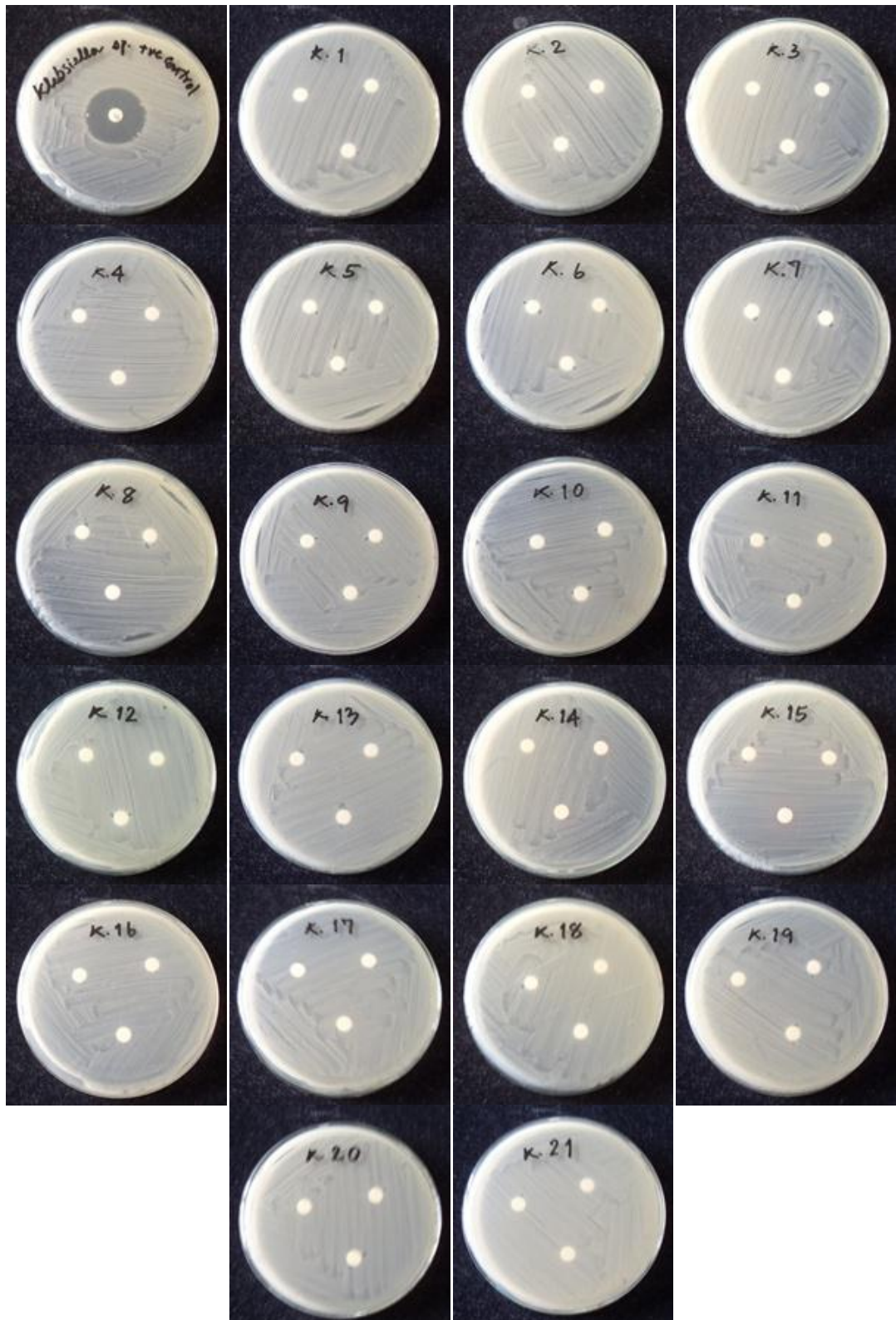


Figure 3. 6 Inhibition tests of samples on *Klebsiella* sp. for 24 h, incubated at 37°C

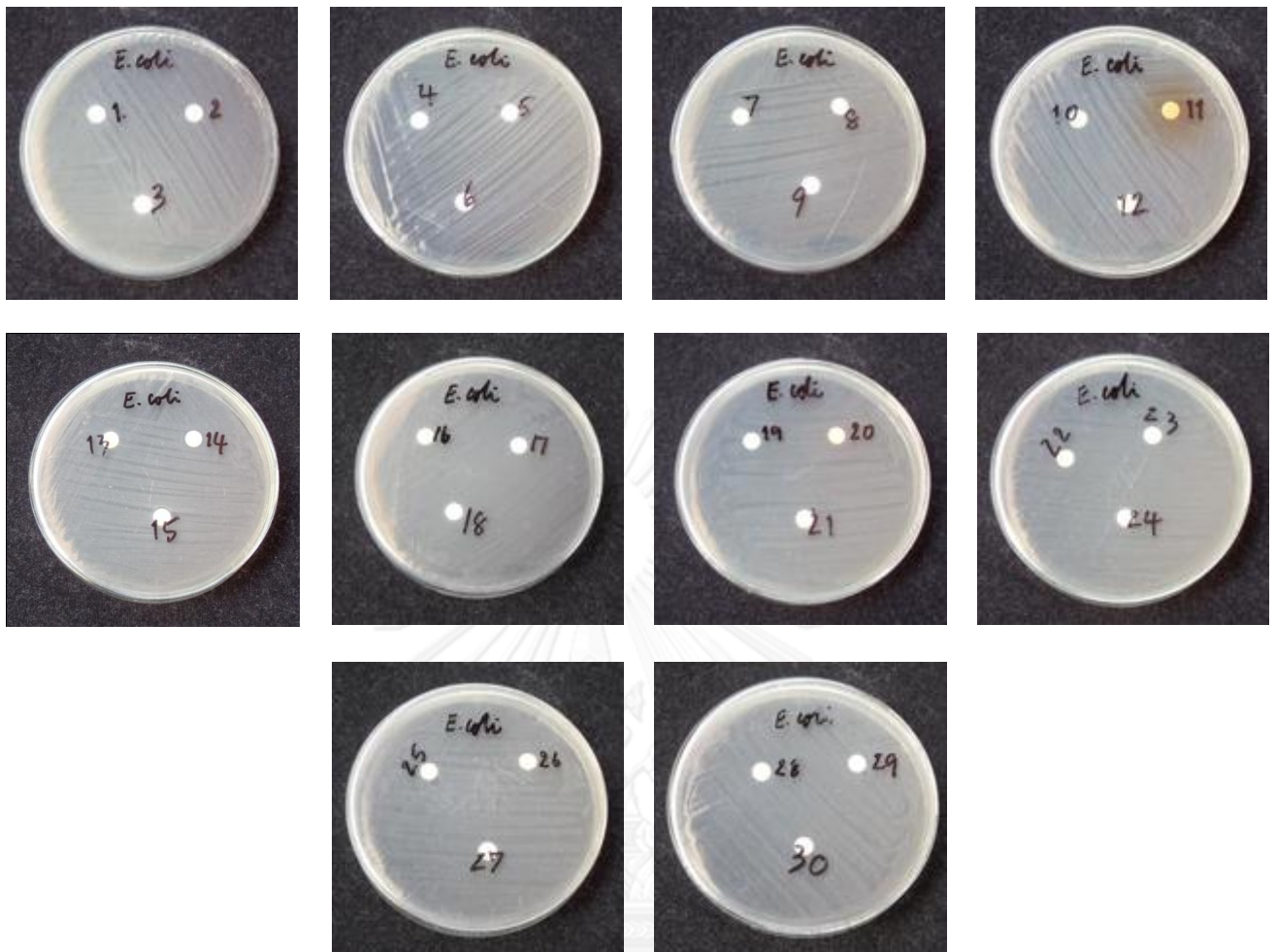


Figure 3. 7 Inhibition tests of sample on *E. coli* for 24 h, incubated at 37°C

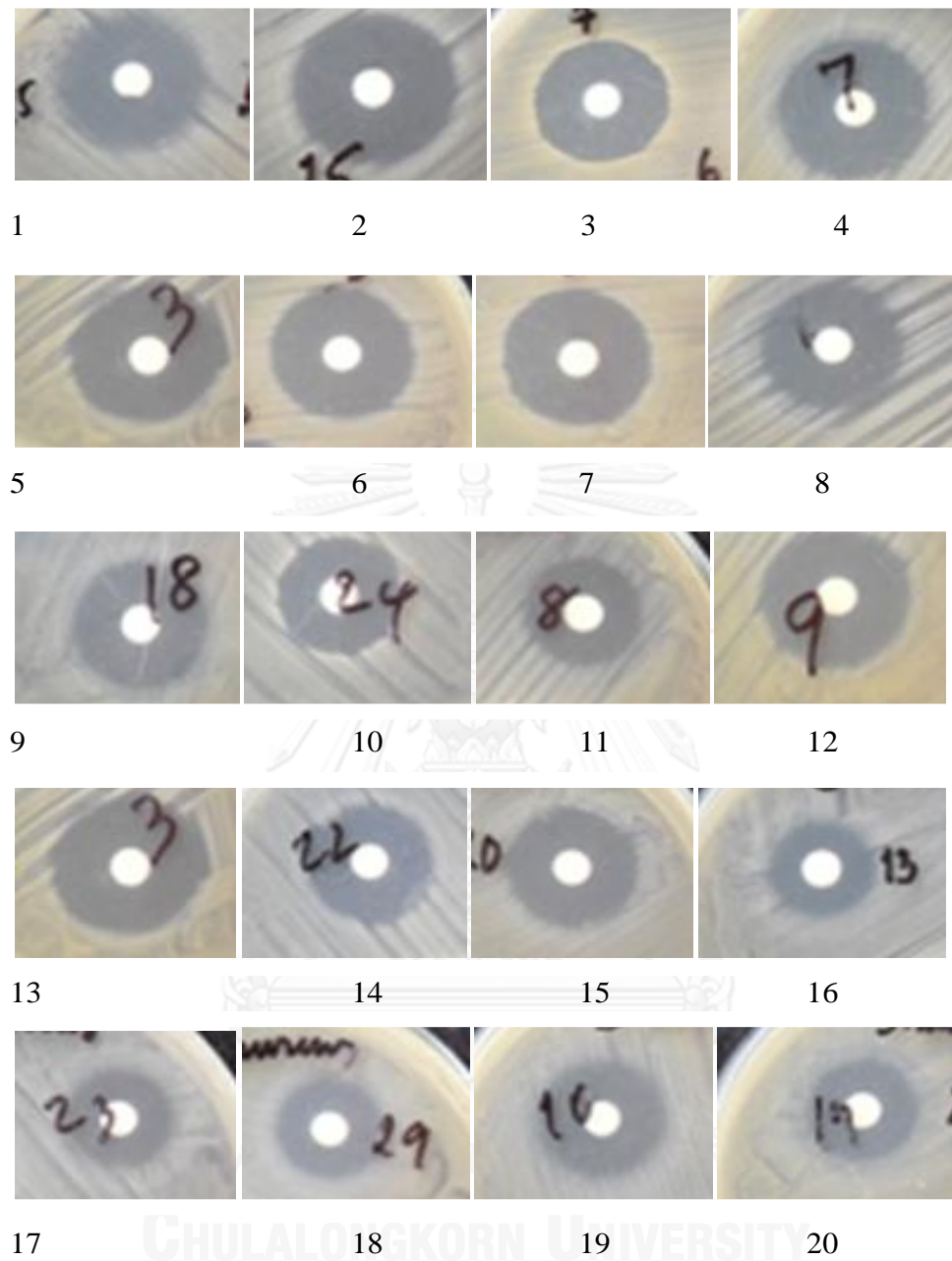


Figure 3. 8 Inhibition tests of sample on *S. aureus* for 24 h, incubated at 37°C

The parent dicoumarol without the substituted phenyl ring exhibited the highest antibacterial activity with an average clear zone of 28 mm. Addition of the benzene ring at the methylene bridge position did not increase the activity. Structure-activity relationship analysis of dicoumarol derivatives revealed that the effect of halide-substituted benzene ring of the derivatives (compounds **2** to **6**) on the inhibition zone was relatively high with respect to the substitution with nitro, methyl, methoxy and hydroxyl groups. Especially, the antibacterial activity of the compound with three methoxy substitutions (compound **16**) was the lowest among the active compounds in Figure 3.8. Moreover, the addition of steric or bulky hydrophobic groups at the *para* position tended to diminish the inhibition zone of dicoumarol against *S. aureus*.

For *B. subtilis*, the results showed that compound **13** exhibited the highest antibacterial activity with an average clear zone of 38 mm. The parent dicoumarol without the substituted phenyl ring (compound **1**) and compound **2** gave the same inhibition zone (32 mm). Among a variety of *tert*-butyl group substituents at *para* position, compound **10** showed the lowest activity against *B. subtilis* and *S. aureus* (20 mm). Steric or bulky hydrophobic properties at the *para* position tend to decrease the inhibition zone of dicoumarol against both *B. subtilis* and *S. aureus* cells. Moreover, halide-substituted benzene ring of the derivatives (compounds **2** to **6**) tended to increase the activity in Figure 3.5.

3.3 Structure Antibacterial Activity against *S. aureus* Relationship Analysis of Dicoumarol Derivatives

All synthesized dicoumarols could be classified into two types according to substituent present as follows: 1) electron withdrawing group (Cl, Br, and NO₂) 2) electron donating group (OMe, Me, *t*-Bu and OH). The relationship between structures of the synthesized derivatives and their corresponding antibacterial activity could be explained in terms of electronic and steric effects of the substituent. In case of the electronic effect, it was observed that most of dicoumarols bearing electron withdrawing substituents showed higher activity than those containing electron donating substituents. The inhibition zones of the substituted halide and nitro groups of CID were observed in a range from 24 to 26 mm whereas the inhibition zones of the derivatives containing methoxy and hydroxyl groups were around 18-22 mm. The effects of individual substituted group on the antibacterial susceptibility can be analyzed as follows:

3.3.1 Effect of *Mono*-substitution on Antibacterial Activity

-*ortho* substitution

Compound **4** with –Cl substitution at *ortho*-position showed higher activity than the compound **19** with methoxy substitution of compounds **19** and **20**. For electrostatic effect, *ortho* substitution with an electron-withdrawing group represented higher activity for antibacterial properties than electron-donating group.

-*meta* substitution

Compound **5** with –Cl substitution at *meta*-position displayed higher activity than compound **12** with –nitro substitution and compound **13** with hydroxy group, respectively. The results showed the electrostatic effect of *ortho* and *meta*-position suggested that substitution with an electron-withdrawing group display higher activity for antibacterial properties than those containing electron-donating groups.

-*para* substitution

The antibacterial properties of these series showed the compound **6** with –Cl substitution at *para*-position and –Br substitution were higher activity than the compound **9** with methyl group, the compound **10** with *tert*-butyl substitution and the compound **18** with methoxy substitution, respectively.

The effect of mono-substitution on the antibacterial susceptibility may be arranged from the greatest to the smallest as follows: Halogen > NO₂ > H = Me > *t*-Bu = OH > OMe.

For-*para* substitution, compounds **6** and **7** with an electron-withdrawing group generally revealed higher activity for antibacterial properties than electron-donating group. In this series, the steric effect may be observed for compound **10** with *tert*-butyl substitution being less activity than compound **9** with methyl substitution.

3.3.2 Effect of *di*-substitution on the antibacterial activity

The di-substitution at the benzene ring of the synthesized derivatives such as the compound **2** with 2,4-dichloro group increased antibacterial activity. Moreover, compound **3** with 3,4-dichloro group showed higher activity than compound **14** with 4-hydroxy-3-methoxy group, compound **20** with 2,4-dimethoxy group and compound **17** with 3,4-dimethoxy group, respectively. The tendency showed that the

compound with an electron-withdrawing group gave higher activity for antibacterial properties than that with electron-donating group. The results were similar to those found in the mono-substitution.

The effect of di-substituted group on the antibacterial susceptibility may be arranged from the greatest to the smallest as follows: 2,4-dichloro>3,4-dichloro>4-hydroxy-3-methoxy>3,4-dimethoxy.

3.4 Structure-Activity Relationship Analysis of Dicoumarol Derivatives against *B. subtilis*

The inhibition zone of *B. subtilis* was the same trend as *S. aureus* except hydroxyl substituents displayed high activity against *B. subtilis*. For electrostatic effect, most of dicoumarols bearing electron withdrawing substituents showed higher activity than those containing electron donating substituents. For steric effect, bulky substituents at *para* position tended to decrease the inhibition zone of dicoumarol against both *B. subtilis* and *S. aureus*.

3.5 Exploring Putative Target and Binding Site of Dicoumarols

Analysis of the NAD(P)H-dependent oxidoreductase proteins from *S. aureus* genome through NCBI database was utilized to identify potential antibacterial targets including quinone reductase, nitroreductase, flavin reductase and FMN oxidoreductase. The hit proteins from the search were subsequently screened to identify the protein target, of which the 3D structure is available as a template. The database of multiple sequence alignments of *Staphylococcus aureus*, *Bacillus subtilis*, *Escherichia coli* and *Klebsiella sp.* were prepared by service in www.unitprot.org as shown in Figure 3.9.

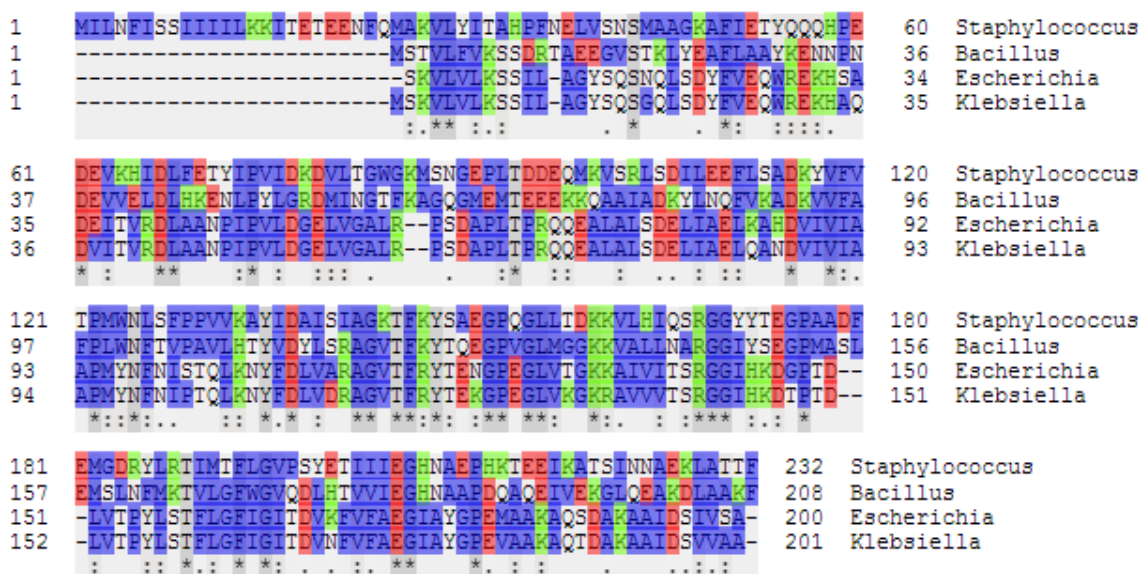


Figure 3.9 Amino acid sequence alignment of azoreductase from *S. aureus*, *B. subtilis*, *E. coli* and *Klebsiella sp.*

A comparative model of NAD(P)H-dependent flavoprotein from *S. aureus* (A9635) was constructed based on the 3D structure of dicoumarol-binding azoreductase (2Z9C) with 34% of sequence identity (Figure 3.10). The model is a homodimer of ternary complex containing enzyme, FMN and dicoumarol (Figure 3.11). Each monomer contains 206 out of 232 residues of the full-length protein. Dicoumarol is located at the dimer interface and interacts with active site residues of both chains.

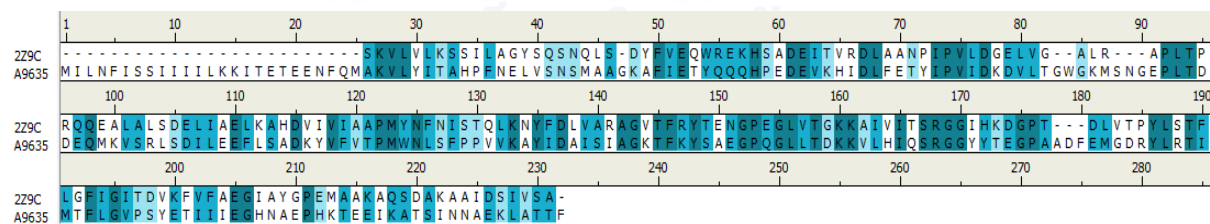


Figure 3.10 Amino acid sequence alignment of azoreductase from *E. coli* (2Z9C) and from *S. aureus* (A9635). Exactly conserved residues are in dark blue, and similar residues are in medium and light blue. The sequence identity is of 34%.

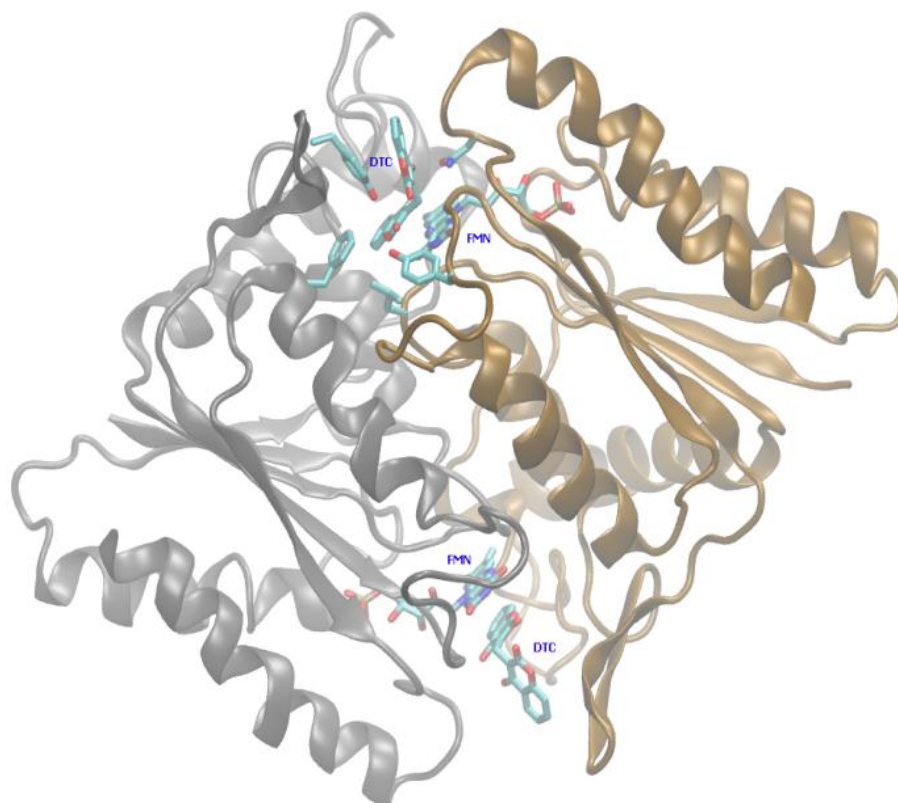


Figure 3. 11 Comparative model of *S. aureus* azoreductase in complex with FMN and dicoumarol.

To further validate the quality of the homology model, dicoumarol was docked into the enzyme binding pocket. The results showed that one of ten energetically most favorable docking poses adopted ligand orientation similar to that of the comparative model of the ternary complex, but differed slightly in the depth of the ligand position within the binding pocket (Figure 3.12). The docking model revealed sandwich-stacking interactions of dicoumarol with the FMN cofactor and the residues; Phe146A, Tyr148A, Phe193A, Gly170B and Asn208B (“A” and “B” indicate the protein chain) were mainly hydrophobic (Figure 3.13). Particularly, one of coumarin plane stacked between the isoalloxazine ring of FMN and the side chain of Tyr148A. The pi-pi stacking motif was similar to the binding mode of conserved residues found in the X-ray structures of human NQO1 quinone reductase and *E.coli* azoreductase. Thus, the conserved binding mode suggested that the *S. aureus* azoreductase be a potential protein target for antiproliferative activity of dicoumarols.

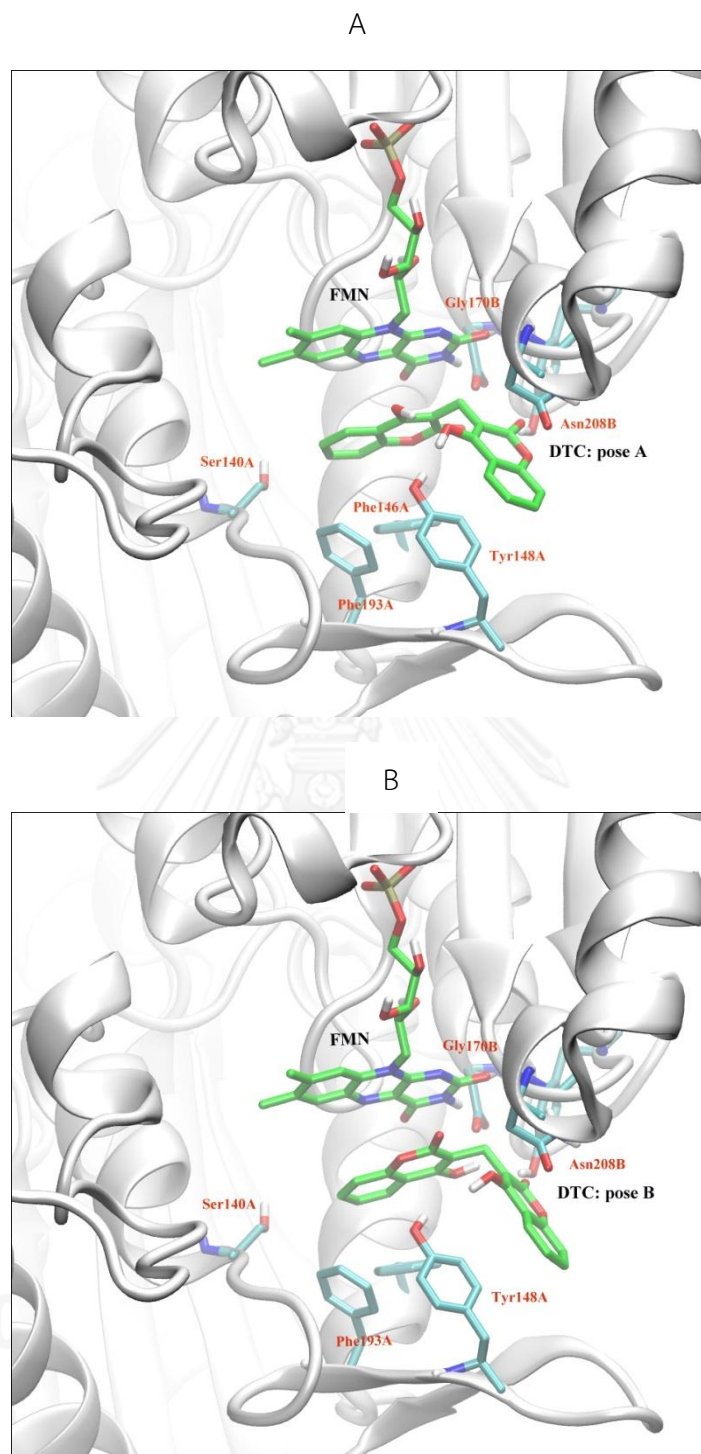


Figure 3. 12 Docked orientations and interactions of dicoumarol in the enzyme binding sites. (A) and (B) represented the ligand poses A and poses B, respectively. The surrounding conserved residues, FMN and dicoumarol molecules are in stick representation.

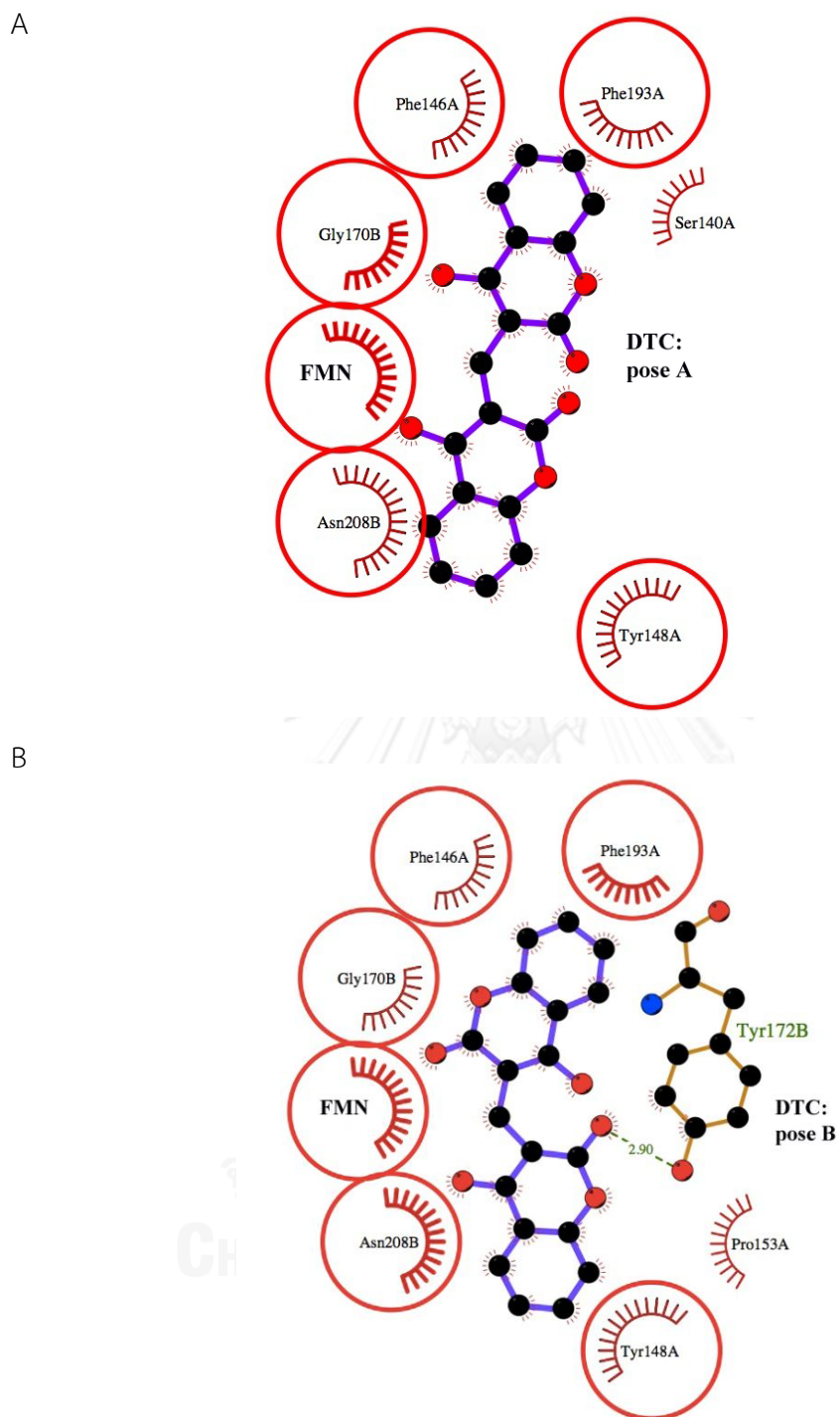


Figure 3. 13 (A) and (B) are schematic 2D diagrams of protein-ligand binding pose A and B, respectively. Spoked arcs represent residues making hydrophobic contacts with the ligand whereas dashed lines represent hydrogen bonds between the atoms involved. The 2D representation was created using the program LigPlot.

Further inspection of docking results illustrated an interesting binding mode of dicoumarols. Given the structure of the binding site, two coumarin rings possibly adopted two alternative orientations, denoted as poses A and B. As described in the previous paragraph, the ligand orientation of pose A was similar to that of the crystal structures. The pose B showed a very similar binding pose in a way that one of the two coumarin rings flipped approximately 180-degree with respect to pose A (Figure 3.13). The binding mode of the pose B revealed a similar pi-pi stacking motif, with additional hydrogen bonding between the hydroxyl hydrogen of the flipped coumarin ring and Tyr172B side chain. Considering molecular shape of the ligands, the two binding poses were similar. Ring flipping of the ligands had no obvious effect on the ring stacking interactions. This could be seen as the binding energies between the two poses were not significantly different (Table 3.4). At this point, these two possibilities could not be distinguished; however, the previous study by Nolan *et al.* also observed similar docked poses of dicoumarols in the active site of human NQO1.

Table 3. 4 Binding energy of dicoumarols

Compound	Binding energy	
	Pose A	Pose B
1	-9.3	-9.3
2	-	-8.9
3	-9.0	-8.8
4	-8.6	-
5	-9.4	-9.6
6	-9.0	-8.7
7	-8.9	-
8	-8.5	-8.5
9	-8.8	-8.8
10	-8.1	-9.5
11	-8.4	-8.5
12	-9.6	-9.3
13	-9.0	-8.8
14	-	-8.6
15	-8.2	-8.2
16	-8.6	-8.5
17	-	-8.4
18	-	-8.5
19	-8.3	-
20	-8.2	-

The docking studies of 19 dicoumarol derivatives suggested that the *S. aureus* azoreductase model possess a large binding cavity and accommodate larger ligands. For all docked conformations, these compounds possessed a similar orientation of coumarin rings with RMSD < 2Å. Most compounds bound in the binding pocket with a more shallow position than previously observed for the docked poses of the parent dicoumarol. A shift in position of the derivatives may be due to steric hindrance of the bulky benzene ring. By comparing the resulting ligand poses, the majority of the binding modes of all derivatives had fallen into two binding poses A and B similar to docking results of the parent compound. Both binding poses shared common interactions as the coumarin ring forms pi-pi stacking with the FMN cofactor and

Tyr148A. Inspection of these two ligand-receptor complexes identified several contact residues including Lys86A, Ser140A, Ile141A, Phe146A, Tyr148A, Phe36B, His206B, and Asn208B. It should be noted that the interactions of these residues were predominantly hydrophobic.

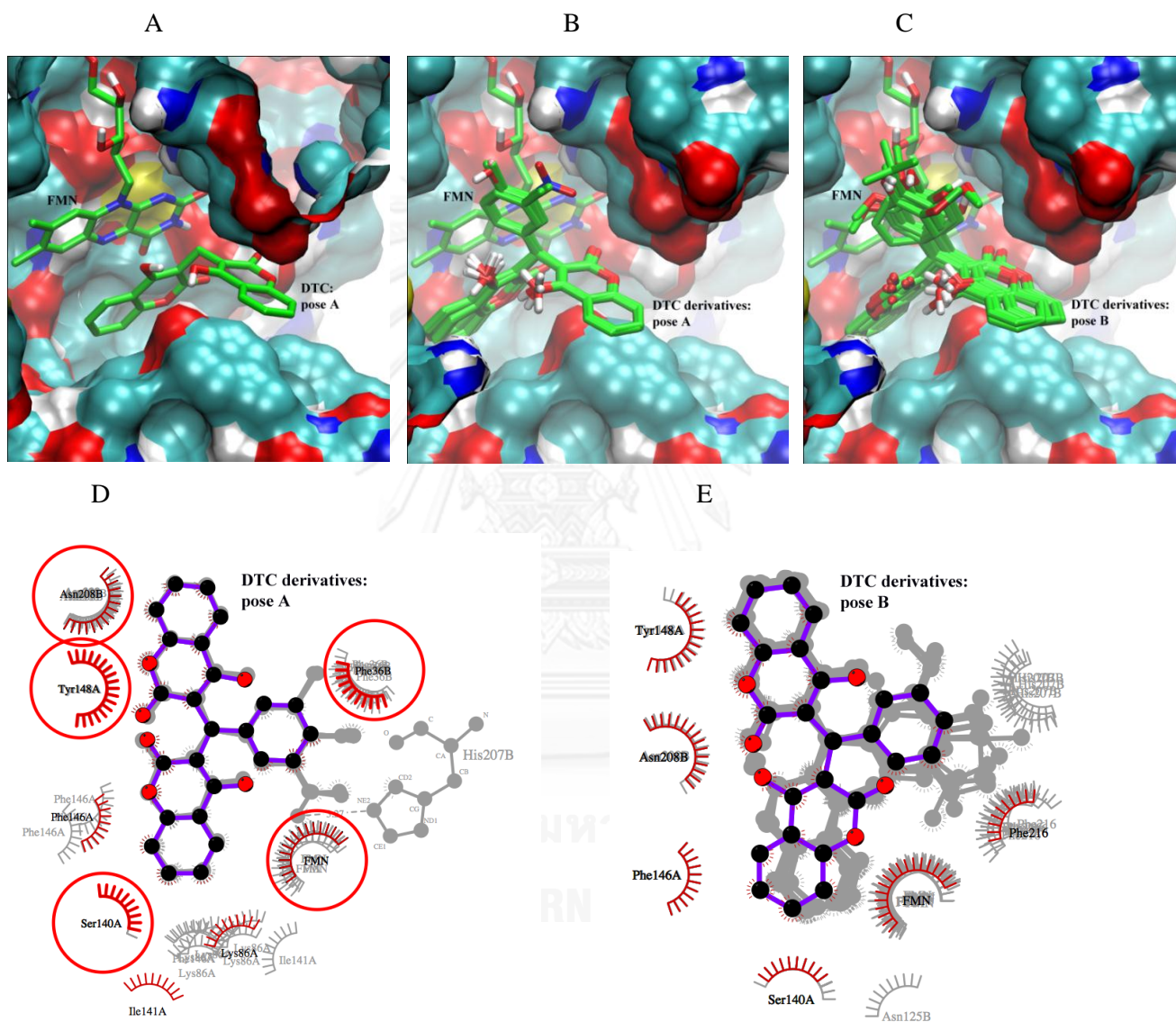


Figure 3.14 Docked orientations and interactions of dicoumarol derivatives in the enzyme binding site. (B) and (C) are the docking poses A and B of compound derivatives in comparison with the pose A of dicoumarol (A) in the pocket (surface representation). (D) and (E) are schematic 2D diagrams of protein-ligand binding pose A and B, respectively.

Analysis of docking results suggested the parent compound possess, on average, good binding energy when compare to its derivatives (Table 3.3). The good agreement between the experimental and the docking results supported the idea that adding a benzene ring at the methylenebis position could reduce antibacterial activity. However, no clear correlation could be established between the calculated binding energy and experimentally determined inhibition zone for the tested compounds. It should be noted that docking results from flexible ligand and rigid receptor had to be carefully interpreted because the active site might change slightly to make good contacts between the ligand and the receptor.

3.6 Physicochemical properties of the synthesized compounds

There are four criterions for Lipinski rule of five for good drug. Firstly, molecular weight of compound is less than 500. Secondly, the compound lipophilicity, present as a quantity known as log P (the logarithm of the partition coefficient between water and 1-octanol), is less than 5. Thirdly, the compound can donate hydrogen atoms to hydrogen bonds (the sum of hydroxyl and amine groups in a drug molecule) is less than 5. Finally, the compound can accept hydrogen atoms to form hydrogen bonds (the sum of oxygen and nitrogen atoms) is less than 10.

The Log P value can be computed by using its additive property and many molecular modeling softwares are available. For this study, Alog P value that is log of the octanol-water partition coefficient using Ghose and Crippen's method was calculated by Discovery Studio program. The ranges of Alog P value were 2.79 to 5.47 (almost compounds were less than 5). The ranges of molecular weight were 336 to 502 (almost compounds were less than 500). The ranges of hydrogen bond donor (HBD) were 2 to 3 (less than 5). Last physicochemical property, hydrogen bond acceptors (HBA) were 6 to 9 (the sum of oxygen and nitrogen atoms is less than 10). Almost physicochemical properties of dicoumarol followed Lipinski rule of five for good drug. Moreover, molecular volumes of dicoumarols that calculated from the 3D volume for each molecule using the current 3D coordinates were around 202 to 304. Molecular polar surface areas of dicoumarols which calculated the polar surface area for each molecule using a 2D approximation by Discovery Studio program were around 93 to 137. A possible relationship between physicochemical properties such as hydrophobicity and antibacterial activity of twenty dicoumarols was suggested. The results showed that the compound with high hydrophobicity exhibited a great antibacterial activity. High antibacterial activity of halide containing derivatives

(compounds 2 to 6) could be observed from the inhibition zone around 24-26 mm which correlated with high hydrophobicity (log P was around 4.74-5.40. While the derivatives with methoxy substituents (compounds 16 to 20) displayed low antibacterial activity: the inhibition zones were around 16-21 mm, correlating with high hydrophobicity (log P was around 4.02-4.04). The physicochemical properties of dicoumarol and its derivatives are collected in Table 3.5.

Table 3. 5 Physicochemical properties of dicoumarols

Compound	AlogP	MW (130- 725)	Molecular volume	HBD	HBA
1	2.79	336	202.36	2	6
2	5.40	481	288.11	2	6
3	5.40	481	286.4	2	6
4	4.74	446.5	272.68	2	6
5	4.74	446.5	267.53	2	6
6	4.74	446.5	268.22	2	6
7	4.82	491	282.97	2	6
8	4.07	412	254.84	2	6
9	4.56	426	267.19	2	6
10	5.47	468	300.46	2	6
11	3.83	428	261.36	3	7
12	2.72	457	273.37	2	6
13	3.83	428	259.99	3	7
14	3.81	458	279.2	3	8
15	3.80	488	304.58	3	9
16	4.02	502	313.5	2	9
17	4.04	472	316.58	2	6
18	4.06	442	296.69	2	7
19	4.06	442	270.62	2	7
20	4.04	472	290.86	2	8

Interestingly, the parent dicoumarol (compound **1**) and *m*-nitro-substituted benzene derivative (compound **12**) with low hydrophobicity (log P around 2.72-2.79) exhibited high antibacterial activity. Moreover, hydrogen bond interaction was an important factor of binding between enzyme and inhibitor, so ligpot program was used to analyze the interaction. This observation, both compounds may form hydrogen bond with the target enzyme in Figures 3.15 and 3.16. The hydrogen bond interaction between the hydroxyl hydrogen of the compound **1** in pose B and Tyr side chain. In addition, nitrogen of the compound **12** in pose B formed hydrogen bond with His.

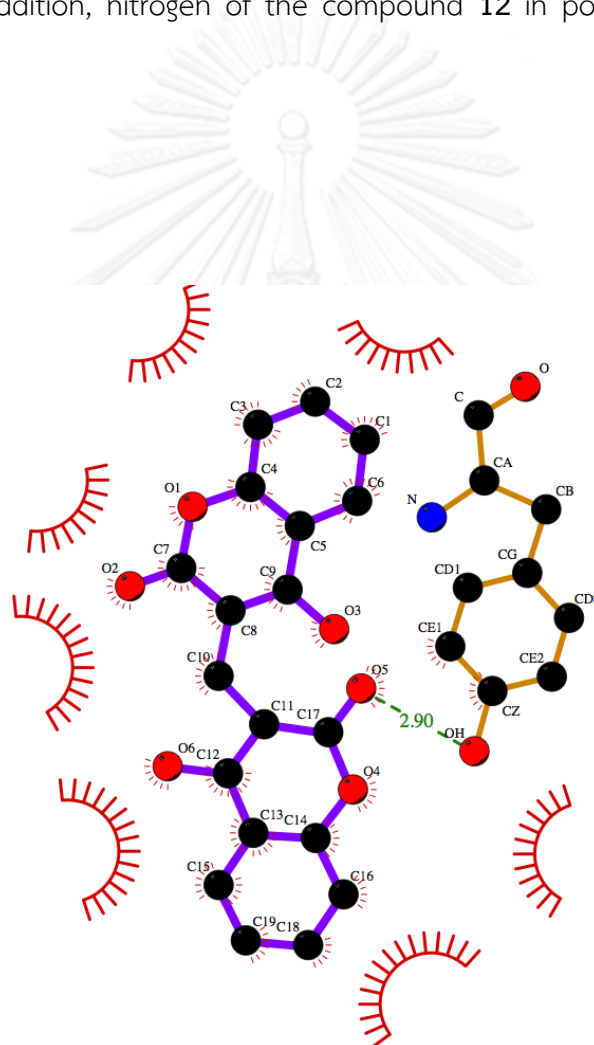


Figure 3.15 Docked orientations and interactions of compound **1** that formed hydrogen bond

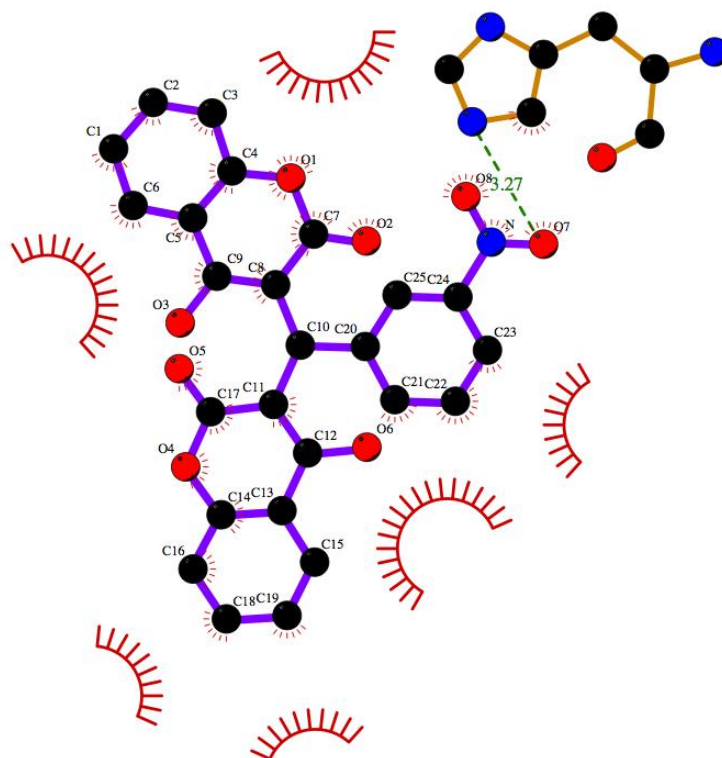


Figure 3. 16 Docked orientations and interactions of compound **12** that formed hydrogen bond

3.7 Analysis of 3D-QSAR: CoMFA and CoMSIA Analysis

Both CoMFA and CoMSIA are a 3D-QSAR (Quantitative-Structure Activity Relationship) approach, aiming to provide the relationship of biological activity and differences in the magnitudes of molecular fields surrounding the investigated receptor ligands. Molecular field of the CoMFA considers steric and electrostatic potentials that are computed based on Lennard-Jones and Coulombic equation, respectively. CoMSIA is similar to CoMFA-steric and -electrostatic fields, but adding hydrophobic, hydrogen-bond donor and acceptor fields into the molecular field potentials. The QSAR model can be employed for the prediction of the biological activities of new molecules.

In an attempt to extract a correlation between the structural properties and biological activities of dicoumarol derivatives, CoMFA and CoMSIA analyses of the synthesized compounds were performed. Compound **8** was chosen to align the molecular structures for CoMFA and CoMSIA data. Statistical results of CoMFA and CoMSIA studies are summarized in Table 3.6. For the CoMFA model, PLS analysis

showed q^2 value of 0.694 with 2 components and r^2 value of 0.894 with SEE of 0.929 and F-value of 46.3. The steric and electrostatic contributions were 59.2 and 40.8%, respectively. This indicated that the steric properties of the substituents had more impact on the antibacterial activity than the electrostatic properties.

Table 3. 6 Statistical results of CoMFA and CoMSIA models

Models	Descriptors	Statistical parameters					
		q^2	r^2	N	SEE	F	Field contribution (%)
CoMFA	S/E	0.694	0.894	2	0.929	46.3	59.2/40.8
CoMSIA	S/E/H/D/A	0.683	0.977	4	0.479	94.8	10.3/25.6/19.9/31.7/9.5

S, Steric field; E, Electrostatic field; H, Hydrophobic field; D, donor; A, acceptor ; q^2 , Cross-validated correlation coefficient; r^2 , Non-cross-validated correlation coefficient; N, Optimal number of components; SEE, standard error of estimate; F, F-test.

The PLS results of CoMSIA analysis showed q^2 of 0.683 with an optimized component number of 4. The non-cross-validation analysis of CoMSIA models gave a high r^2 value of 0.977 with a SEE of 0.479 and F-value of 94.8. The predominant field contributions from CoMSIA were electrostatic (25.6%) and hydrogen bond donor (31.7%), implying the importance of the electrostatic and hydrogen bond donor of the substituent for the activity. The other contributions, steric (10.3%), hydrophobic (19.9%) and the hydrogen bond acceptor (9.5%) gave minor effects.

The predicted inhibition zone *versus* their experimental data of training set and test set compounds are illustrated in Figure 3.17. Although both models gave a fairly good quality of the activity prediction with $q^2 > 0.6$ for the training set, the predictive quality of the test set was not great. An average deviation between the predicted and experimental inhibition zone was about 4 mm (Table 3.7). Particularly, the activities of the two compounds, **2** and **18**, were poorly predicted. The low number of data in the training set might be the cause of poor prediction. Compound **2** had the highest value in the set whereas compound **18** exhibited almost the lowest activity.

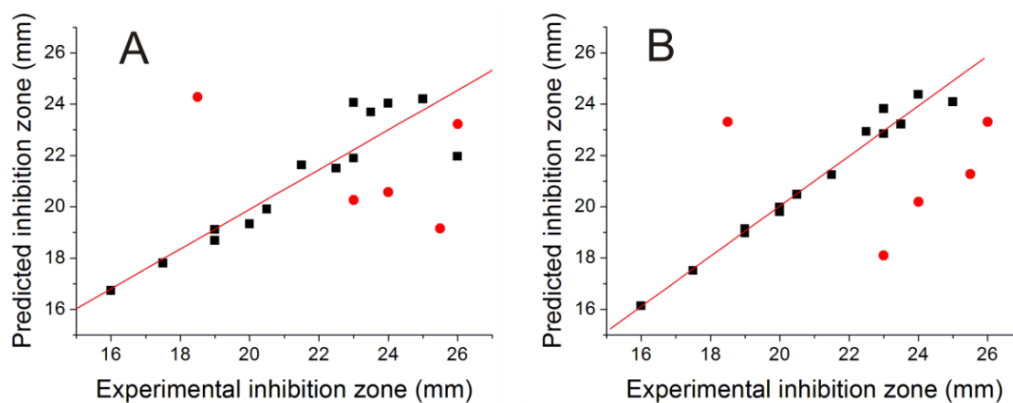


Figure 3. 17 Plots between the experimental and predicted biological activities of training (filled square) and test set (filled circle): (A) CoMFA plot and (B) CoMSIA plot

Table 3. 7 Experimental and predicted activities of test set compounds

CID	Inhibition zone (mm)	CoMFA		CoMSIA	
		Predicted (mm)	Residual (mm)	Predicted (mm)	Residual (mm)
2	26	19	7	21	5
4	24	21	3	20	4
5	26	23	3	23	3
15	23	20	3	18	5
18	19	24	5	23	4
		Avg	4	Avg	4

The effects of field contributions are illustrated by CoMFA and CoMSIA contour maps (Figure 3.18A-3.18B). An interpretation was focused on the effects of substituted phenyl ring to the antibacterial activity. For CoMFA, a green contour was found near the plane of substituted phenyl ring of compound while a yellow contour was located in the vicinity of the R_3 substituent. This indicated that the bulky substituents at the *para* position were unfavorable and might have negative effect on the activity of the compounds. Therefore, the activities of the compounds **10**, **16**, **17**, **18** and **20** were relatively low. For electrostatic maps, a red contour was found around the R_1 -position. This corresponded well with the methoxy substituent

at *ortho*-position of compounds **19** and **20** with an electron-donating group and hence these two compounds exhibited moderate and low activities, respectively.

For CoMSIA contour maps, steric and electrostatic were similar to those of CoMFA as shown by a yellow contour at the *para* position (inside a big green contour) and a red contour at the R₁-position (Figure 3.18C-3.18D). Hydrophobic contour map from CoMSIA is shown in Figure 3.15E. An orange contour found at the R₃-position suggested that a hydrophobic substituent at this site be expected to improve the activity. For hydrogen bond donor contour maps (Figure 3.18F), small purple contour located near the R₂ (or R₄) substituent indicated that the position required the hydrogen bond acceptor substituent. A magenta contour for hydrogen bond acceptor group suggested the R₁ substituent be in favor of hydrogen bond acceptor (Figure 3.18G).

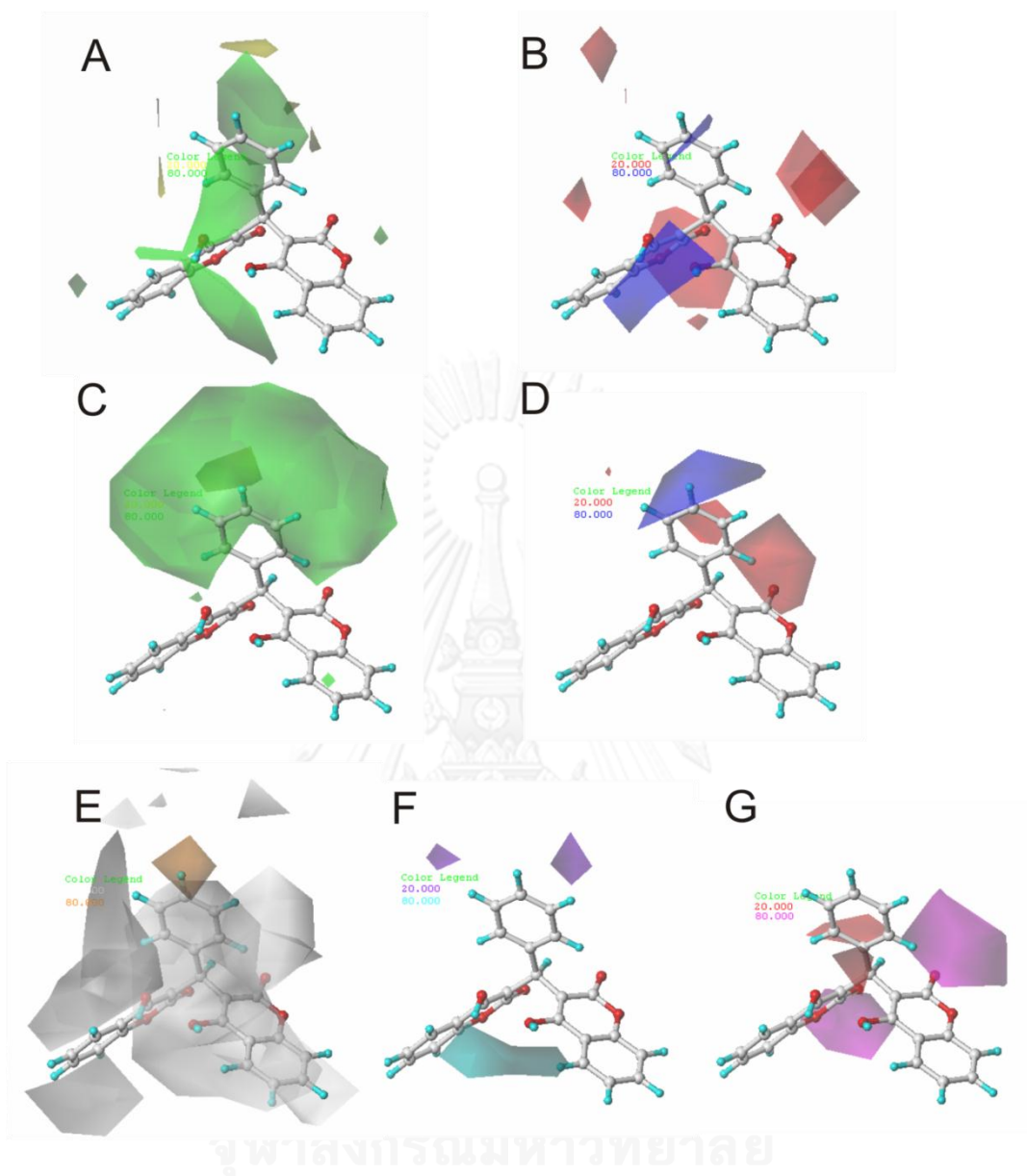


Figure 3. 18 The $\text{stdev} \times \text{coeff.}$ contour maps. (A) and (B) represent CoMFA steric and electrostatic, respectively. (C) to (F) represent CoMSIA steric, electrostatic, hydrophobic, hydrogen bond donor and hydrogen bond acceptor, respectively. Steric field is represented by green and yellow contour maps. Electrostatic field is represented by blue and red contour maps. Hydrophobic field is represented by orange and white contour maps. Hydrogen bond donor field is represented by cyan and purple contour maps. Hydrogen bond acceptor field is represented by magenta and red contour maps. All the contours represented the default 80% and 20% level contributions for favorable and unfavorable regions, respectively.

CHAPTER IV

CONCLUSION

During the course of this research, a series of 3,3'-phenylmethylene-bis-4-hydroxycoumarins containing ortho-, meta- and para-substituents on the benzene ring were synthesized via condensation reaction of 4-hydroxycoumarin with their selected aldehydes. Furthermore, dicoumarol was synthesized by dissolving 4-hydroxycoumarin in boiling water and added aqueous formaldehyde. The physical properties and yields of all dicoumarol derivatives were in the range of 70-90%. All structures were well characterized using $^1\text{H-NMR}$.

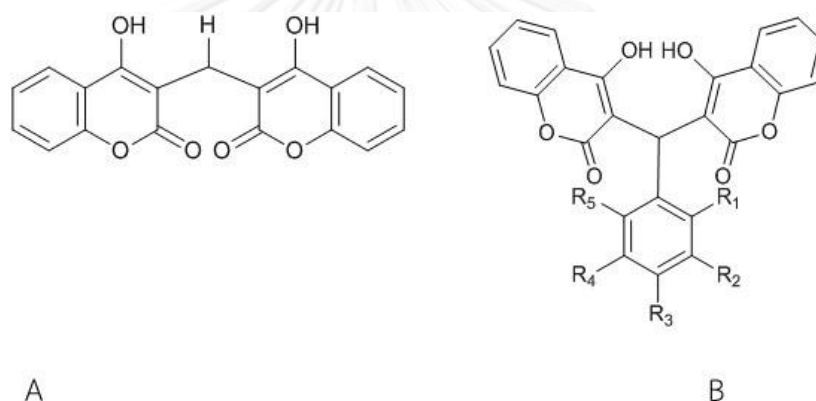


Figure 4. 1 The structures of synthesized compound (A) dicoumarol (B) derivatives of dicoumarol

In this research, the synthesized compounds were subsequently tested for cell growth inhibition against two bacterial types. One type is gram-positive bacteria: *Staphylococcus aureus* and *Bacillus subtilis*. The other type is gram-negative bacteria: *Escherichia coli* and *Klebsiella sp.* strains. The selectivity of these compounds for gram-positive bacteria is clearly demonstrated. One of possible explanations is due to a permeability barrier to dicoumarol molecule since the structures and properties of cell membranes between these two bacterial cells are different. The compounds are reasonable, although not great, as inhibitors of the growth of the gram positive bacteria compared to the parent dicoumarol. Structure-activity relationship analysis of dicoumarol derivatives reveals that the effect of halide-substituted benzene ring of the derivatives on inhibition zone is relatively higher than other functional groups. For most compounds, the substitutions of bulky benzene group on the methylenebis

position do not significantly increase the inhibitory. The structural bioinformatic approach was employed to identify a potential protein target from *S. aureus* and to better understand the mode of action of the synthesized compounds. This finding is broadly explained by the predicted poorer docked structure of the derivatives to a homology model of *S. aureus* flavoprotein.

The docking results showed that dicoumarol and derivatives bound to the active site of the enzyme in two possible orientations which were poses A and B. Their binding was characterized by predominant hydrophobic interactions. In addition, drug-likeness properties of the synthesized compounds were fallen in criterions for Lipinski rule.

3D QSAR analyses were employed to illustrate a relationship between the antibacterial activity and dicoumarol derivatives. Both CoMFA and CoMSIA models provided chemical and structural information insight into the effects of steric, electrostatic, hydrophobic, hydrogen-bond donor and acceptor fields around the substituted benzene ring of dicoumarol on biological activity. The findings of the study provided a better understanding of the inhibition mechanism of dicoumarols and may be useful guiding structural design of more effective antibacterial agents.

4.1 Propose for the Future Work

The discovery of a series of 3,3'-phenylmethylene-bis-4-hydroxycoumarins displaying antibacterial activity and 3D-QSAR study structural the antibacterial activity were highlighted. The investigation of disk diffusion method was well known as a preliminary indicator which could be used for further study on other sophisticated bioassays. Other functional groups substituted on these structures were still attractive so the structure activity relationship study of other types of molecule should be explored. From this research, more halide-substituted benzene ring of dicoumarol is suggested to synthesize. Moreover, the further research would be the study other biological activities such as antifungal activity, anti HIV activity, anticoagulant activity and relationship.

REFERENCES

1. Stahmann, M. A.; Huebner, C. F.; Link, K. P., Studies on the Hemorrhagic Sweet Clover Disease. V. Identification and Synthesis of the Hemorrhagic Agent *Journal of Biological Chemistry* **1941**, *138* (2), 513-527.
2. Holbrook, A. M.; Pereira, J. A.; Labiris, R.; McDonald, H.; Douketis, J. D.; Crowther, M.; Wells, P. S., Systematic overview of warfarin and its drug and food interactions. *Arch Intern Med* **2005**, *165* (10), 1095-1106.
3. Hamdi, N.; Puerta, M. C.; Valerga, P., Synthesis, structure, antimicrobial and antioxidant investigations of dicoumarol and related compounds. *Eur J Med Chem* **2008**, *43* (11), 2541-8.
4. Shaterian, H. R.; Honarmand, M., Uncatalyzed, One-pot Synthesis of 3,3'-(Benzylene)- bis(4-hydroxy-2H-chromen-2-one) Derivatives under Thermal Solvent-free Conditions. *Chinese Journal of Chemistry* **2009**, *27* (9), 1795-1800.
5. Nolan, K. A.; Doncaster, J. R.; Dunstan, M. S.; Scott, K. A.; Frenkel, A. D.; Siegel, D.; Ross, D.; Barnes, J.; Levy, C.; Leys, D.; Whitehead, R. C.; Stratford, I. J.; Bryce, R. A., Synthesis and biological evaluation of coumarin-based inhibitors of NAD(P)H: quinone oxidoreductase-1 (NQO1). *J Med Chem* **2009**, *52* (22), 7142-56.
6. Karmakar, B.; Nayak, A.; Banerji, J., Sulfated titania catalyzed water mediated efficient synthesis of dicoumarols—a green approach. *Tetrahedron Letters* **2012**, *53* (33), 4343-4346.
7. Dadak, V.; Hodak, K., Some relations between the structure and the antibacterial activity of natural coumarins. *Experientia* **1966**, *22* (1), 38-9.
8. Pelter, A.; Johnson, A. P., The structures of scandenin and lonchocarpic acid. *Tetrahedron Letters* **1964**, *5* (39), 2817-2822.
9. Falshaw, C. P.; Harmer, R. A.; Ollis, W. D.; Wheeler, R. E.; Lalitha, V. R.; Rao, N. V. S., Natural occurrence of 3-aryl-4-hydroxycoumarins. Part II. Phytochemical examination of *Derris scandens*(roxb.) benth. *Journal of the Chemical Society C: Organic* **1969**, (3), 374-382.
10. Brock, T. D., Effects of magnesium ion deficiency on *Escherichia coli* and possible relation to the mode of action of novobiocin *Science* **1962**, *3513* (136), 316-317.
11. Elgamel, M.; El-Tawil, B.; Fayez, M., The triterpenoid constituents of the leaves of *Ficus nitida* L. *Naturwissenschaften* **1975**, *62* (10), 486-486.

12. Heyward, R. C., The prototype compound for the oral anticoagulants 3,3'-methylene bis(4-hydroxycoumarin). *Journal of Chemistry Education* **1984**, *61*, 87.
13. Siddiqui, Z. N.; TN, M. M.; Ahmad, A.; Khan, A. U., Synthesis of 4-Hydroxycoumarin Heteroarylhybrids as Potential Antimicrobial Agents. *Archiv der Pharmazie* **2011**, *344* (6), 394-401.
14. Dholariya, H. R.; Patel, K. S.; Patel, J. C.; Patel, K. D., Dicoumarol complexes of Cu (II) based on 1, 10-phenanthroline: Synthesis, X-ray diffraction studies, thermal behavior and biological evaluation. *Spectrochimica Acta Part A: Molecular and Biomolecular Spectroscopy* **2013**, *108*, 319-328.
15. Li, M.-k.; Li, J.; Liu, B.-h.; Zhou, Y.; Li, X.; Xue, X.-y.; Hou, Z.; Luo, X.-x., Synthesis, crystal structures, and anti-drug-resistant *Staphylococcus aureus* activities of novel 4-hydroxycoumarin derivatives. *European Journal of Pharmacology* **2013**, *721* (1-3), 151-157.
16. Sirisuksakon, W. Synthesis of 3-substituted-4-hydroxycoumarins and their biological activities. Chulalongkorn University, 1999.
17. Worakijthamrongchai, R. Effect of substituents of 4-hydroxycoumarins on their biological activities. Chulalongkorn University, 2000.
18. Smyth, T.; Ramachandran, V. N.; Smyth, W. F., A study of the antimicrobial activity of selected naturally occurring and synthetic coumarins. *Int J Antimicrob Agents* **2009**, *33* (5), 421-6.
19. Cresteil, T.; Jaiswal, A. K., High levels of expression of the NAD(P)H:quinone oxidoreductase (NQO1) gene in tumor cells compared to normal cells of the same origin. *Biochem Pharmacol* **1991**, *42* (5), 1021-7.
20. Asher, G.; Dym, O.; Tsvetkov, P.; Adler, J.; Shaul, Y., The crystal structure of NAD(P)H quinone oxidoreductase 1 in complex with its potent inhibitor dicoumarol. *Biochemistry* **2006**, *45* (20), 6372-8.
21. Johansson, E.; Parkinson, G. N.; Denny, W. A.; Neidle, S., Studies on the nitroreductase prodrug-activating system. Crystal structures of complexes with the inhibitor dicoumarol and dinitrobenzamide prodrugs and of the enzyme active form. *Journal of Medicinal Chemistry* **2003**, *46* (19), 4009-4020.
22. Ito, K.; Nakanishi, M.; Lee, W. C.; Zhi, Y.; Sasaki, H.; Zenno, S.; Saigo, K.; Kitade, Y.; Tanokura, M., Expansion of substrate specificity and catalytic mechanism of azoreductase by X-ray crystallography and site-directed mutagenesis. *Journal of Biological Chemistry* **2008**, *283* (20), 13889-13896.

23. Zhao, H.; Neamati, N.; Hong, H.; Mazumder, A.; Wang, S.; Sunder, S.; Milne, G. W.; Pommier, Y.; Burke, T. R., Coumarin-Based Inhibitors of HIV Integrase 1. *Journal of medicinal chemistry* **1997**, *40* (2), 242-249.
24. Kancheva, V. D.; Boranova, P. V.; Nechev, J. T.; Manolov, I. I., Structure-activity relationships of new 4-hydroxy bis-coumarins as radical scavengers and chain-breaking antioxidants. *Biochimie* **2010**, *92* (9), 1138-1146.
25. Wattanasereekul, S. Structure-activity relationship of 4-hydroxycoumarins and related compounds. Chulalongkorn University
1998.
26. D.A. Case, T. A. D., T.E. Cheatham, III, C.L. Simmerling, J. Wang, R.E. Duke, R. Luo, R.C. Walker, W. Zhang, K.M. Merz, B. Roberts, S. Hayik, A. Roitberg, G. Seabra, J. Swails, A.W. Goetz, I. Kolossváry, K.F. Wong, F. Paesani, J. Vanicek, R.M. Wolf, J. Liu, X. Wu, S.R. Brozell, T. Steinbrecher, H. Gohlke, Q. Cai, X. Ye, J. Wang, M.-J. Hsieh, G. Cui, D.R. Roe, D.H. Mathews, M.G. Seetin, R. Salomon-Ferrer, C. Sagui, V. Babin, T. Luchko, S. Gusarov, A. Kovalenko, and P.A. Kollman, AMBER 10. University of California, San Francisco: San Francisco, 2008.
27. M. J. Frisch, G. W. T., H. B. Schlegel, G. E. Scuseria, M. A. Robb, J. R. Cheeseman, J. A. Montgomery, Jr., T. Vreven, K. N. Kudin, J. C. Burant, J. M. Millam, S. S. Iyengar, J. Tomasi, V. Barone, B. Mennucci, M. Cossi, G. Scalmani, N. Rega, G. A. Petersson, H. Nakatsuji, M. Hada, M. Ehara, K. Toyota, R. Fukuda, J. Hasegawa, M. Ishida, T. Nakajima, Y. Honda, O. Kitao, H. Nakai, M. Klene, X. Li, J. E. Knox, H. P. Hratchian, J. B. Cross, C. Adamo, J. Jaramillo, R. Gomperts, R. E. Stratmann, O. Yazyev, A. J. Austin, R. Cammi, C. Pomelli, J. W. Ochterski, P. Y. Ayala, K. Morokuma, G. A. Voth, P. Salvador, J. J. Dannenberg, V. G. Zakrzewski, S. Dapprich, A. D. Daniels, M. C. Strain, O. Farkas, D. K. Malick, A. D. Rabuck, K. Raghavachari, J. B. Foresman, J. V. Ortiz, Q. Cui, A. G. Baboul, S. Clifford, J. Cioslowski, B. B. Stefanov, G. Liu, A. Liashenko, P. Piskorz, I. Komaromi, R. L. Martin, D. J. Fox, T. Keith, M. A. Al-Laham, C. Y. Peng, A. Nanayakkara, M. Challacombe, P. M. W. Gill, B. Johnson, W. Chen, M. W. Wong, C. Gonzalez, and J. A. Pople *Gaussian 03*, Gaussian, Inc: Pittsburgh PA, 2003.
28. Marsili, J. G. a. M., Iterative Partial Equalization of Orbital Electronegativity - A Rapid Access to Atomic Charges. *Tetrahedron* **1980**, *36*, 3219-3228.

APPENDICES



จุฬาลงกรณ์มหาวิทยาลัย
CHULALONGKORN UNIVERSITY

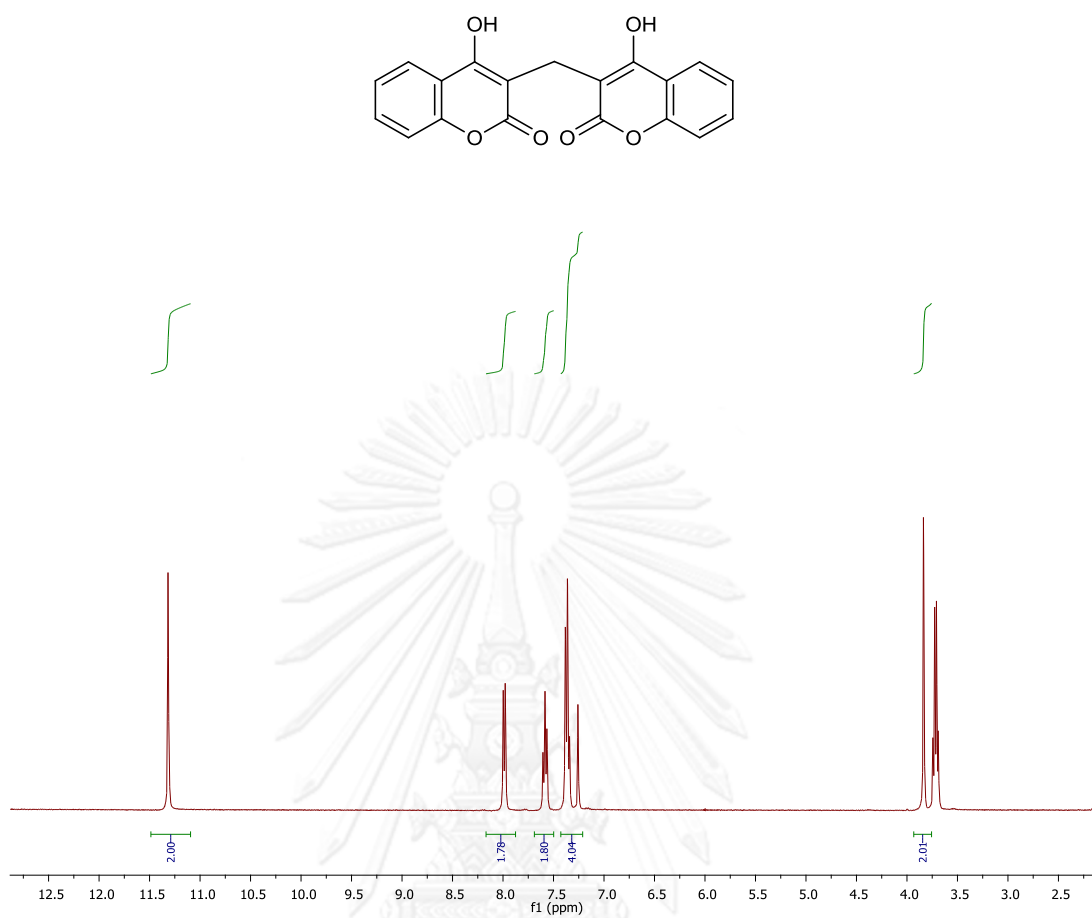


Figure A. 1 The ^1H NMR spectrum of 3,3'-methylene-bis-4-hydroxy-2H-chromen-2-one (1)

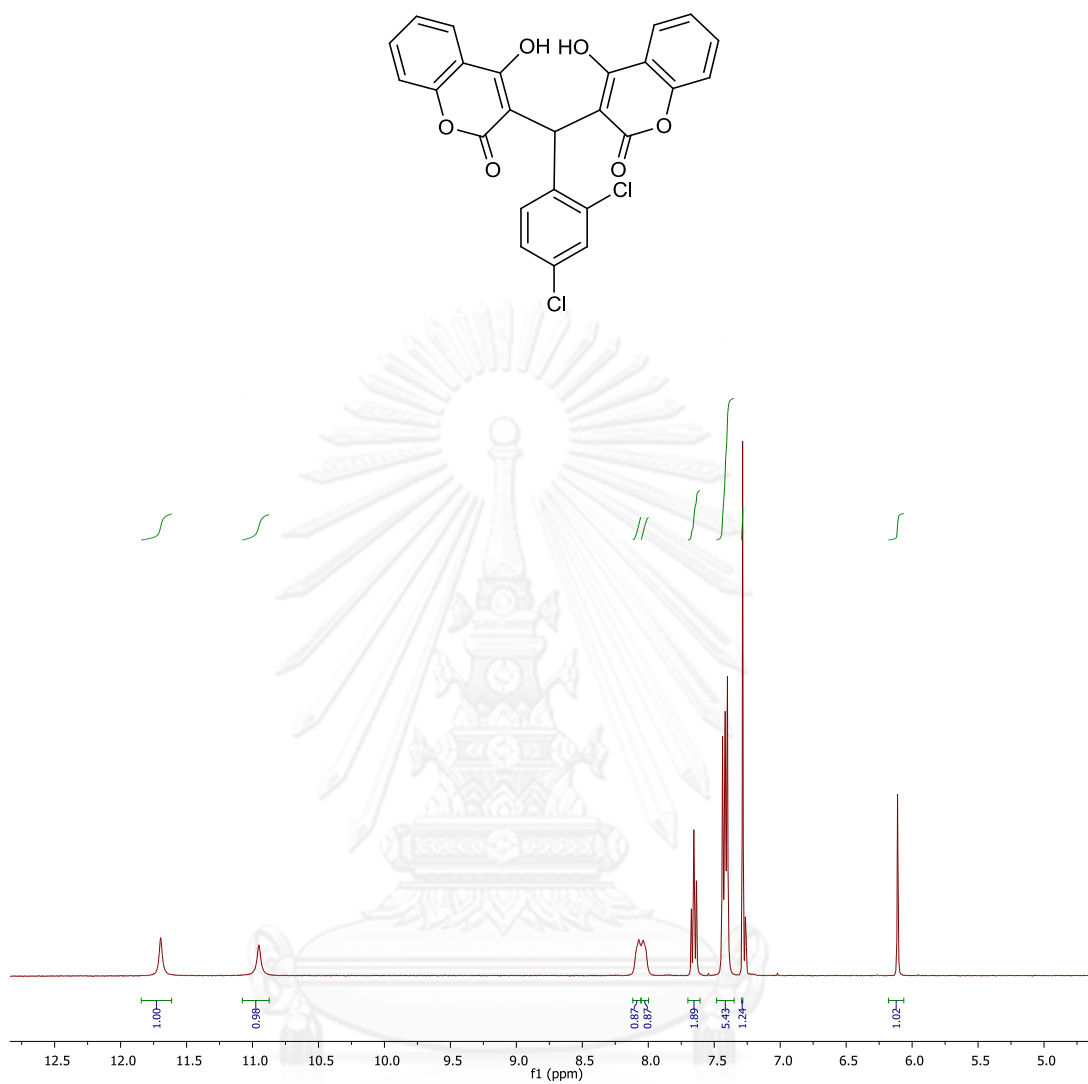


Figure A. 2 The ¹H NMR spectrum of 3,3'-(2,4-dichlorophenylmethylene)bis-(4-hydroxy-2H-chromen-2-one) (2)

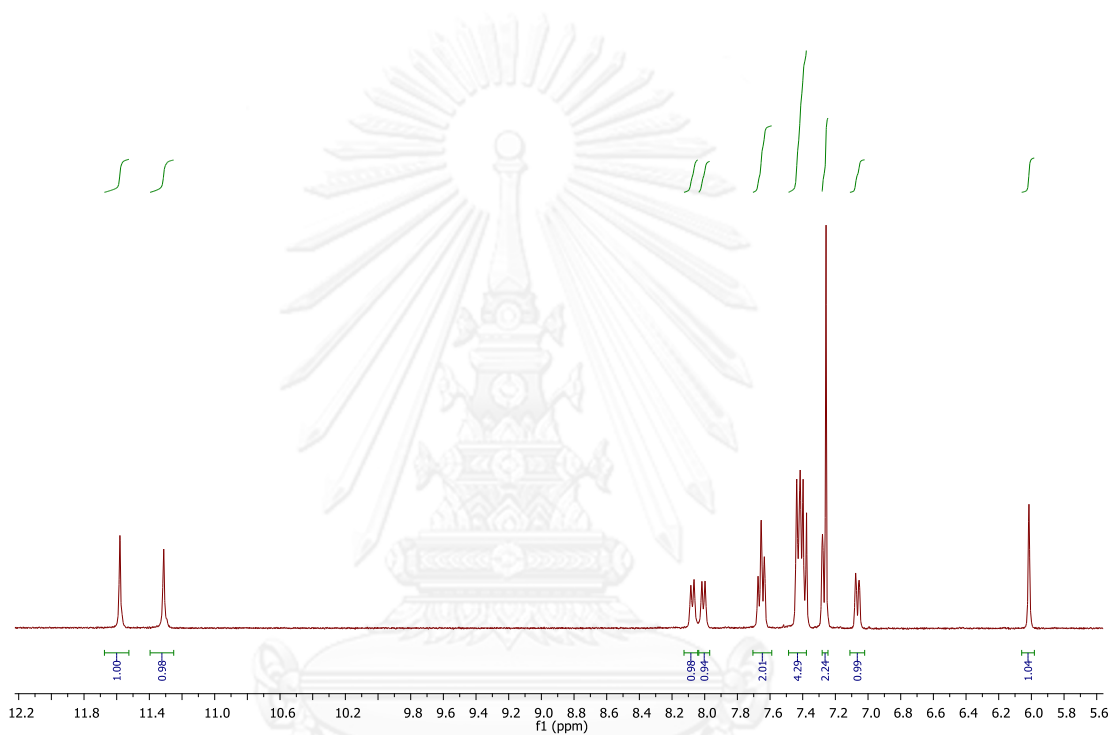
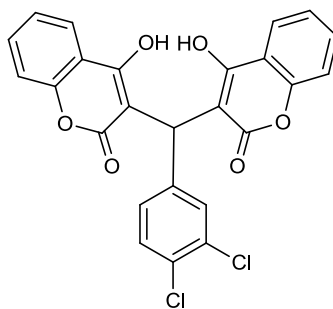


Figure A. 3 The ^1H NMR spectrum of **3,3'**-(3,4-dichlorophenylmethylene)bis-(4-hydroxy-2H-chromen-2-one) (**3**)

CHULALONGKORN UNIVERSITY

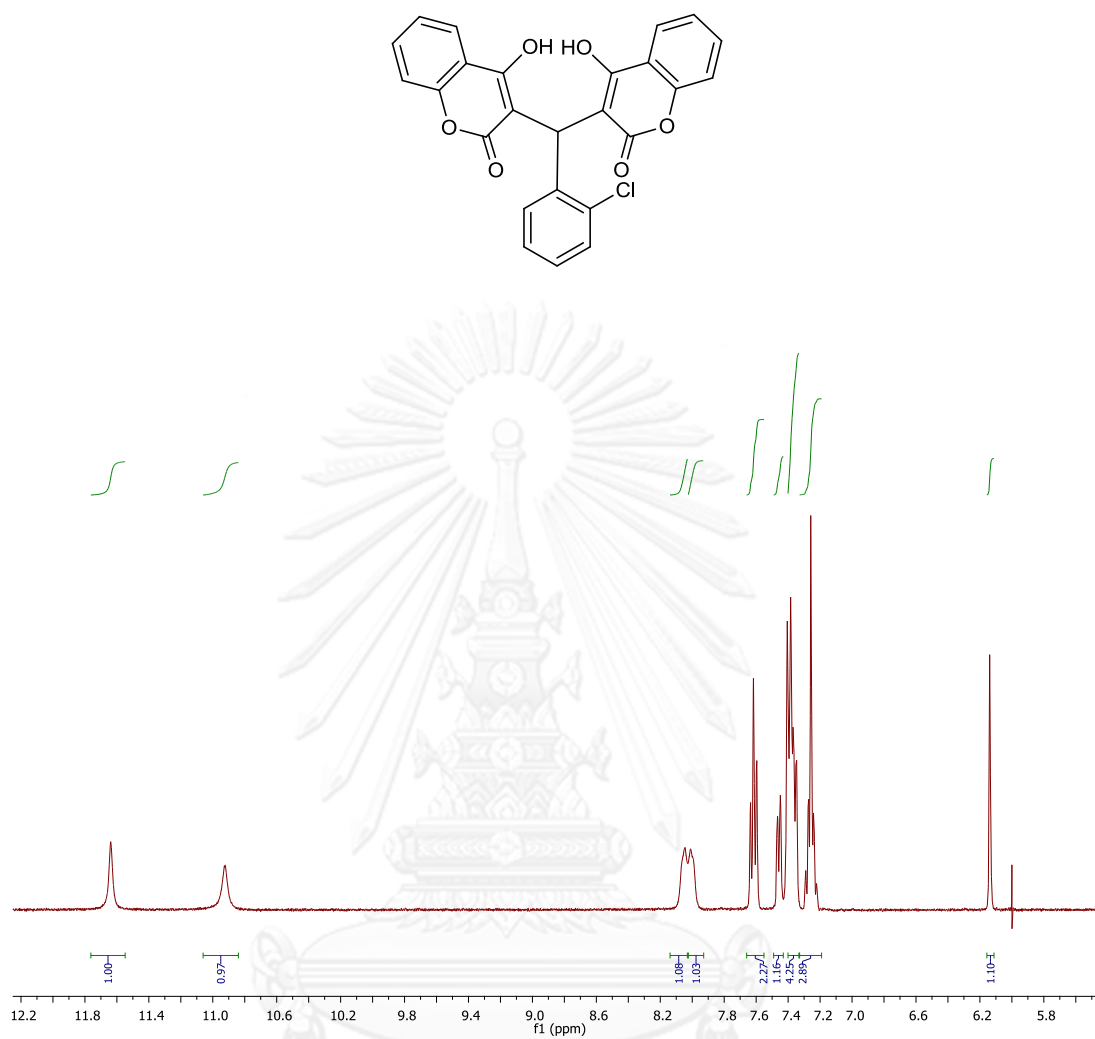


Figure A. 4 The ¹H NMR spectrum of 3,3'-(2-chlorophenylmethylene)bis-(4-hydroxy-2H-chromen-2-one) (4)

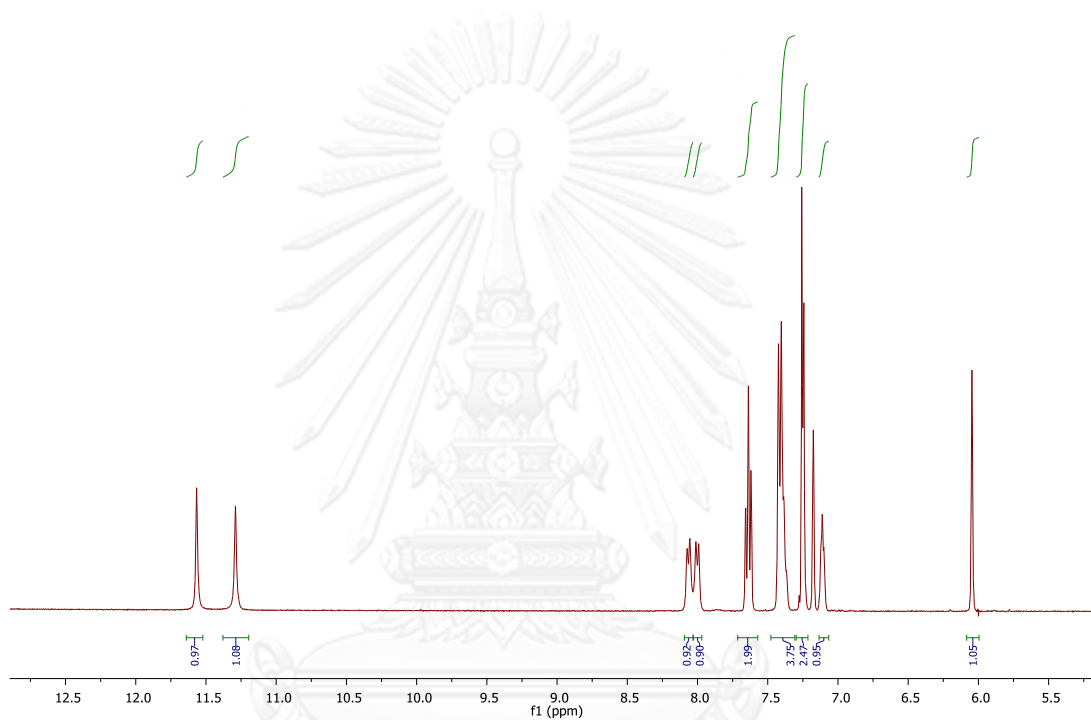
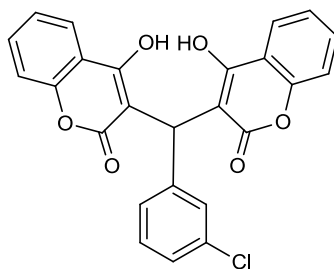


Figure A. 5 The ^1H NMR spectrum of 3,3'-(3-chlorophenylmethylene)bis(4-hydroxy-2H-chromen-2-one) (5)

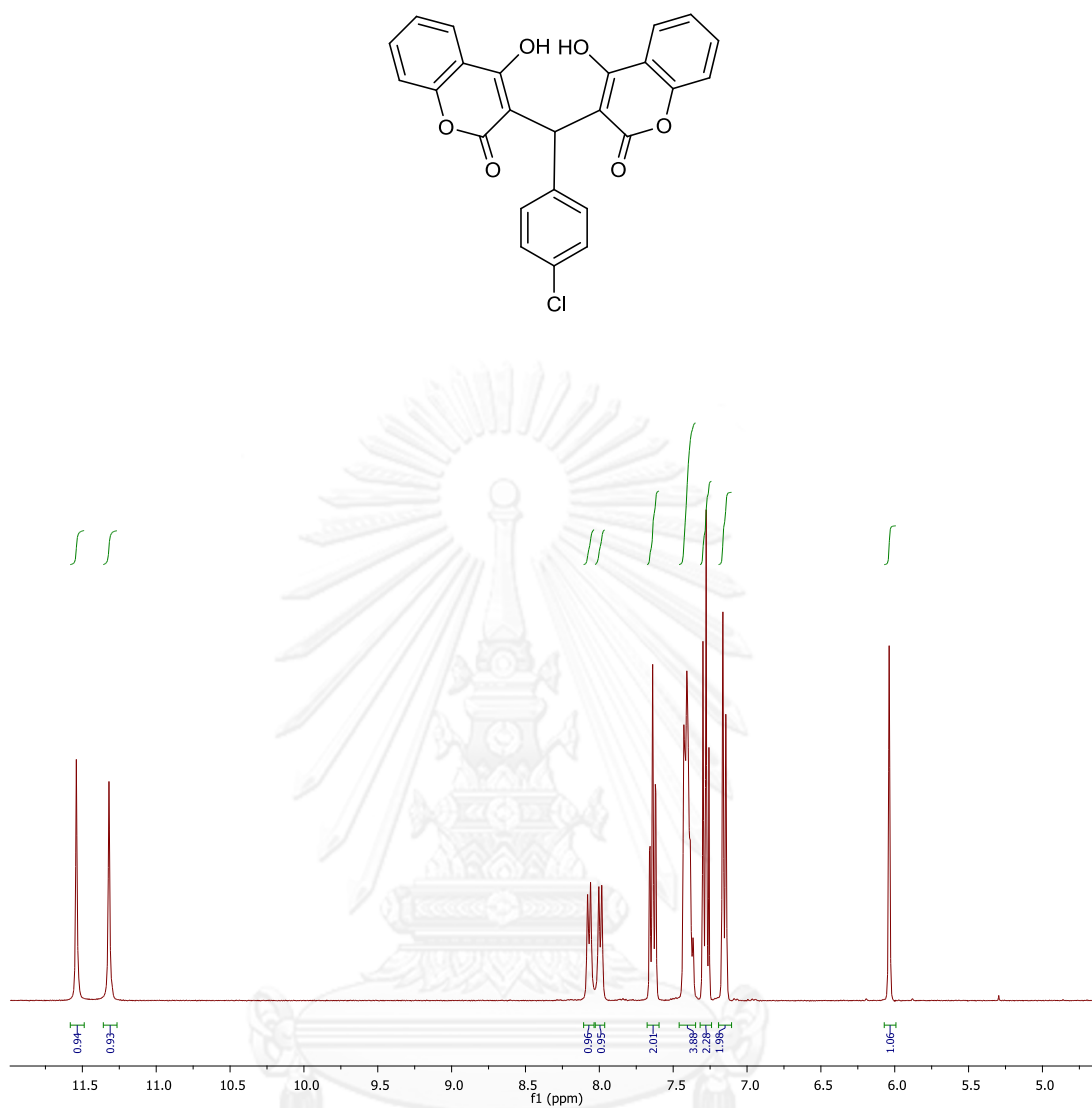


Figure A. 6 The ¹H NMR spectrum of 3,3'-(4-chlorophenylmethylene)bis-(4-hydroxy-2H-chromen-2-one) (6)

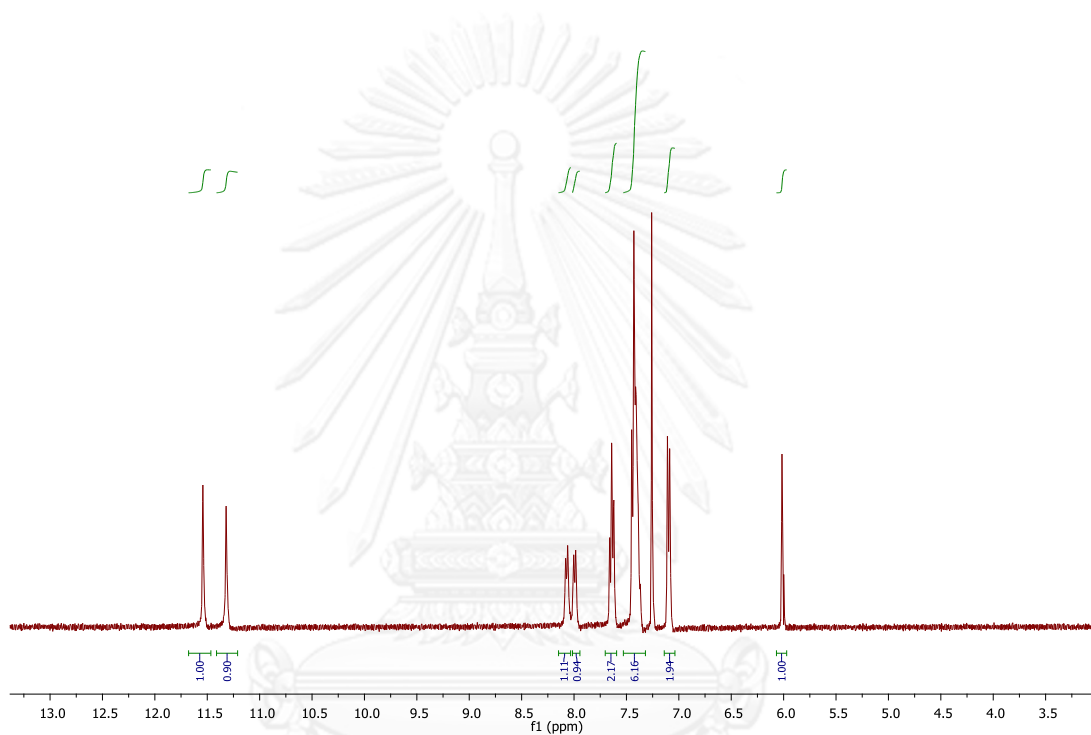
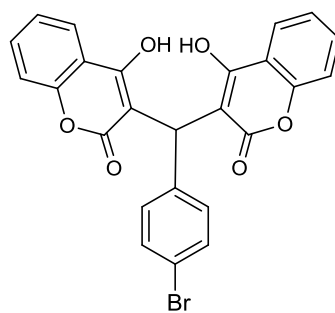


Figure A. 7 The ^1H NMR spectrum of 3,3'-(4-bromophenylmethylene)bis(4-hydroxy-2H-chromen-2-one) (7)

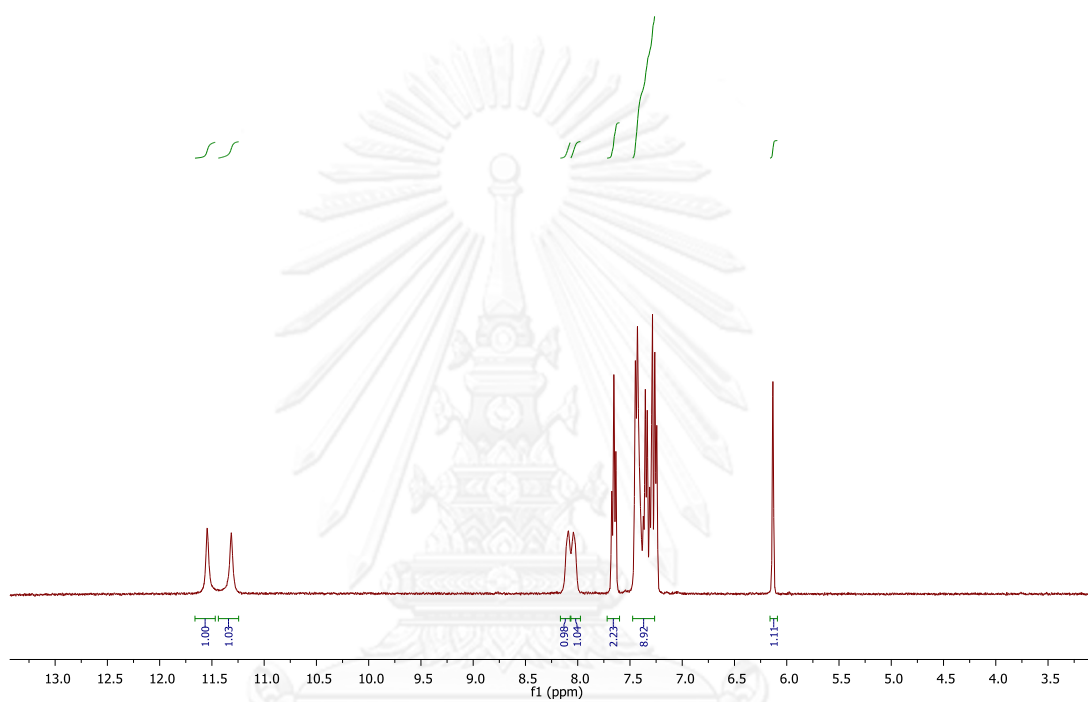
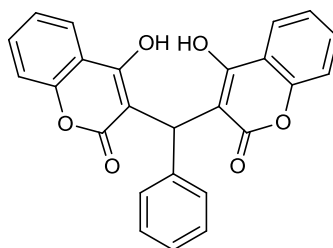


Figure A. 8 The ^1H NMR spectrum of 3,3'-(phenylmethylene)bis-(4-hydroxy-2H-chromen-2-one) (**8**)

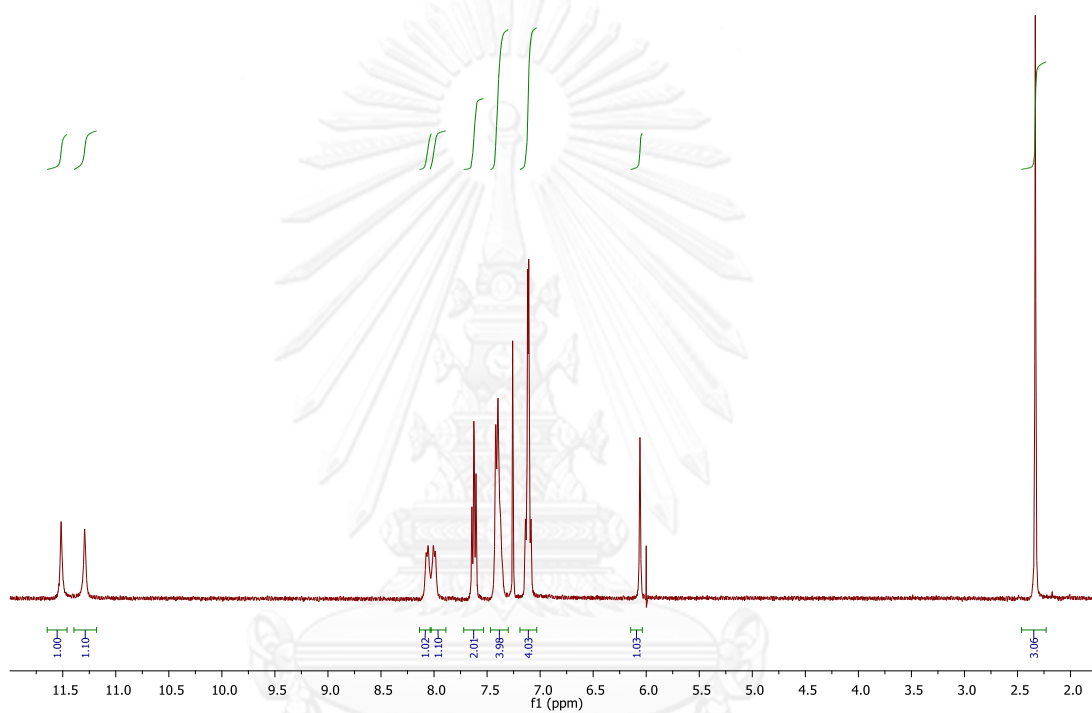
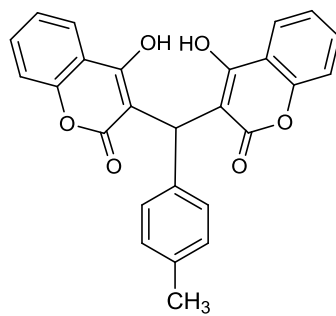


Figure A. 9 The ^1H NMR spectrum of 3,3'-(4-methylphenylmethylene)bis(4-hydroxy-2H-chromen-2-one) (9)

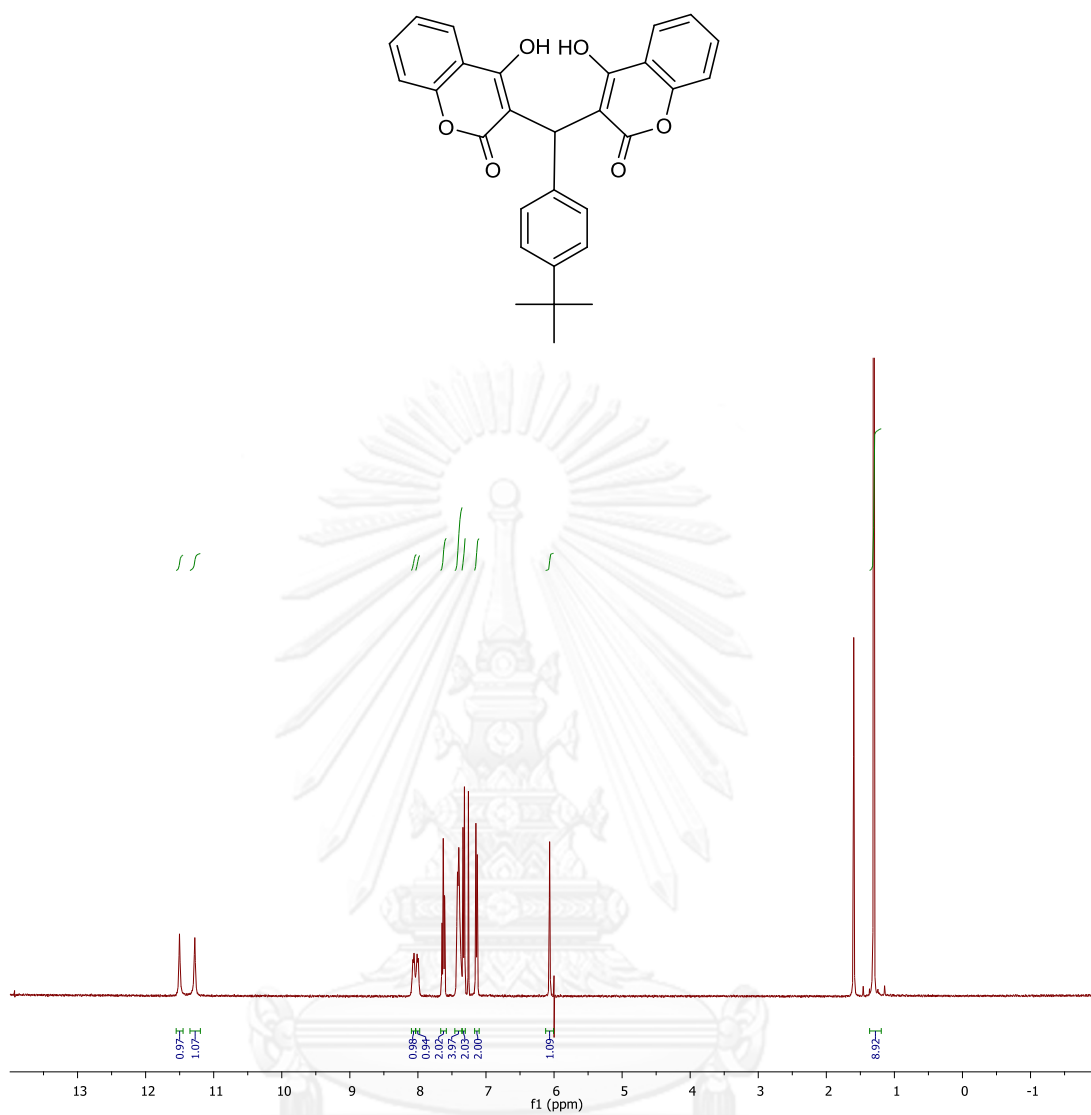


Figure A. 10 The ^1H NMR spectrum of 3,3'-(4-tertbutylphenylmethylene)bis-(4-hydroxy-2H-chromen-2-one) (10)

CHULALONGKORN UNIVERSITY

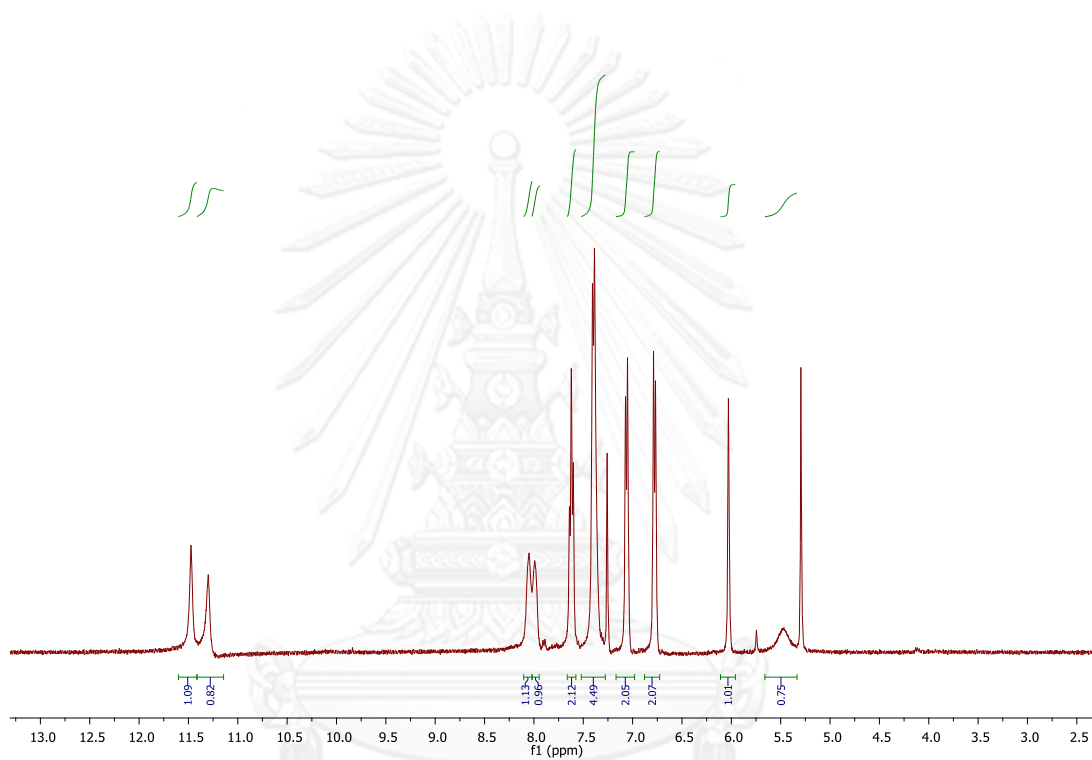
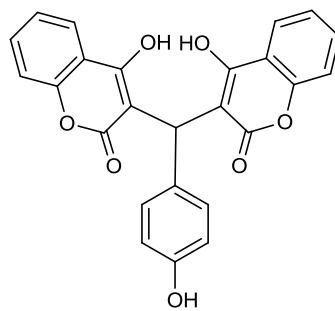


Figure A. 11 The ^1H NMR spectrum of 3,3'-(4-hydroxyphenylmethylene)bis-(4-hydroxy-2H-chromen-2-one) (**11**)

CHULALONGKORN UNIVERSITY

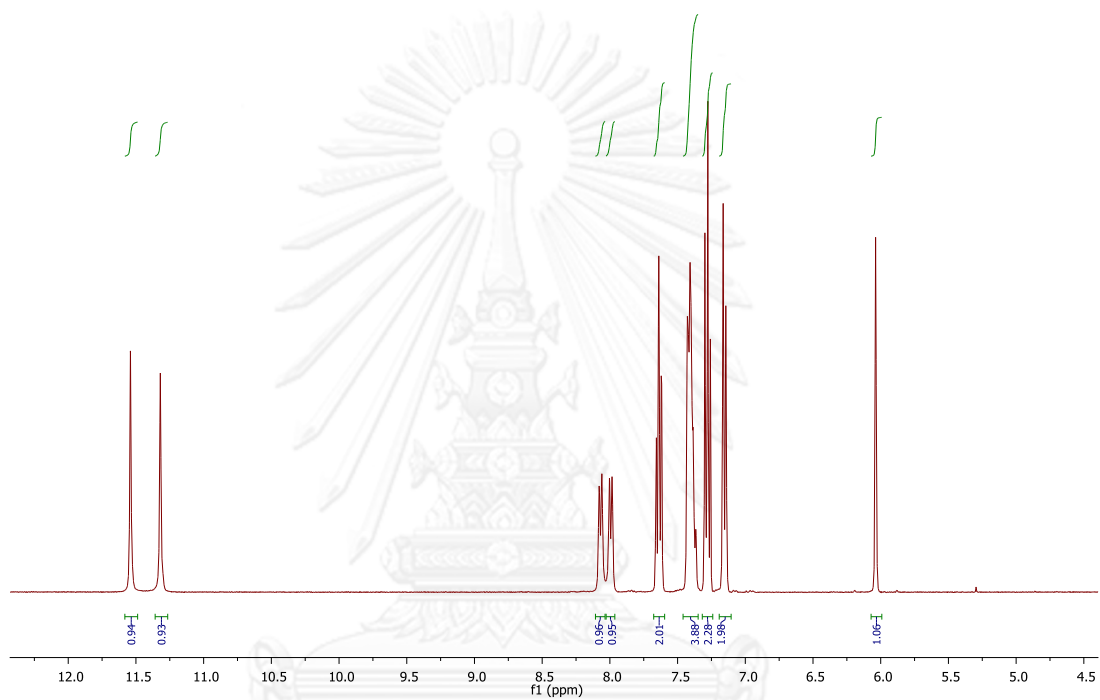
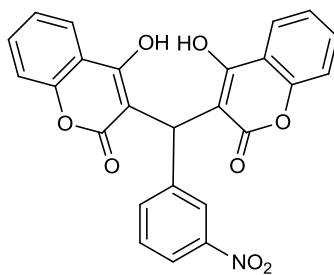


Figure A. 12 The ^1H NMR spectrum of 3,3'-(3-nitrophenylmethylene)bis(4-hydroxy-2H-chromen-2-one) (**12**)

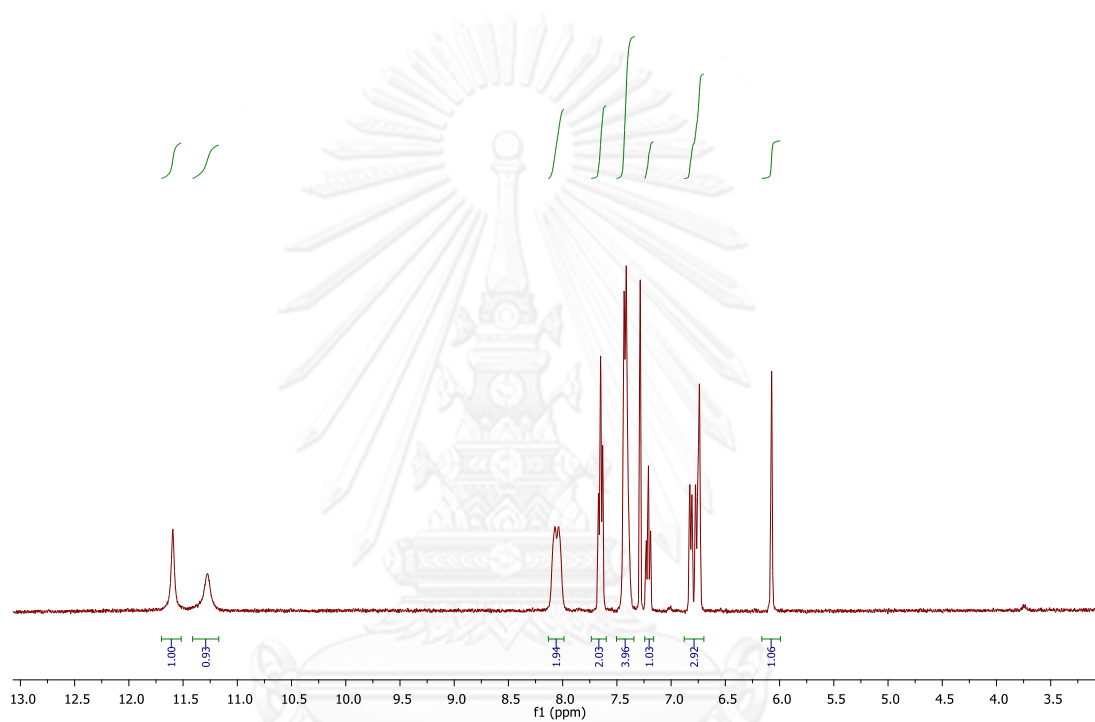
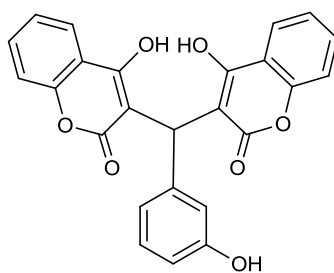


Figure A. 13 The ^1H NMR spectrum of 3,3'-(3-hydroxyphenylmethylene)bis-(4-hydroxy-2H-chromen-2-one) (**13**)

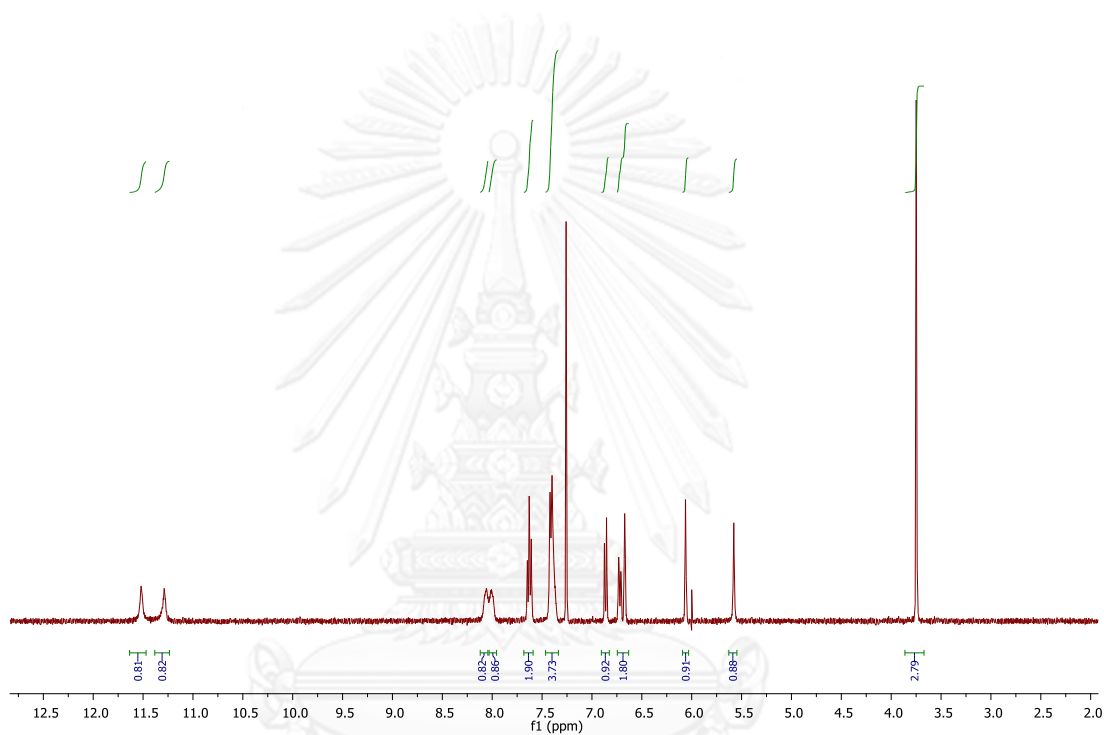
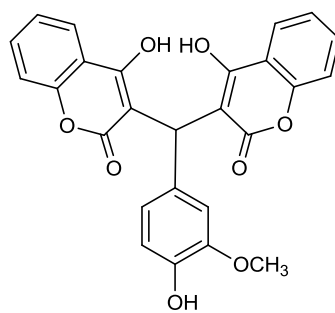


Figure A. 14 The ^1H NMR spectrum of 3,3'-(4-hydroxy-3-methoxyphenylmethylene)bis-(4-hydroxy-2H-chromen-2-one) (**14**)

CHULALONGKORN UNIVERSITY

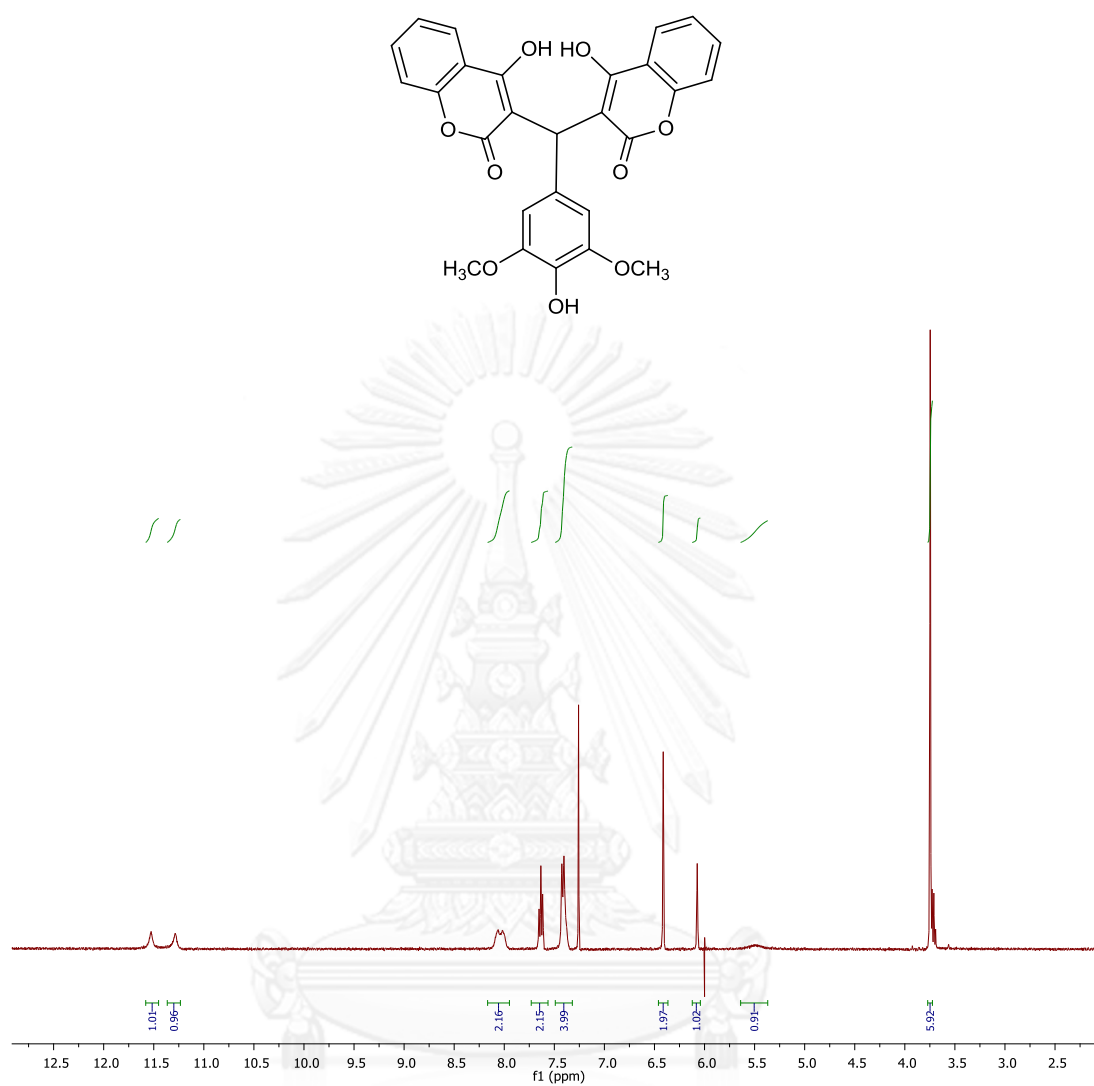


Figure A. 15 The ¹H NMR spectrum of 3,3'-(4-hydroxy-3,5-dimethoxyphenylmethylene)bis(4-hydroxy-2H-chromen-2-one) (15)

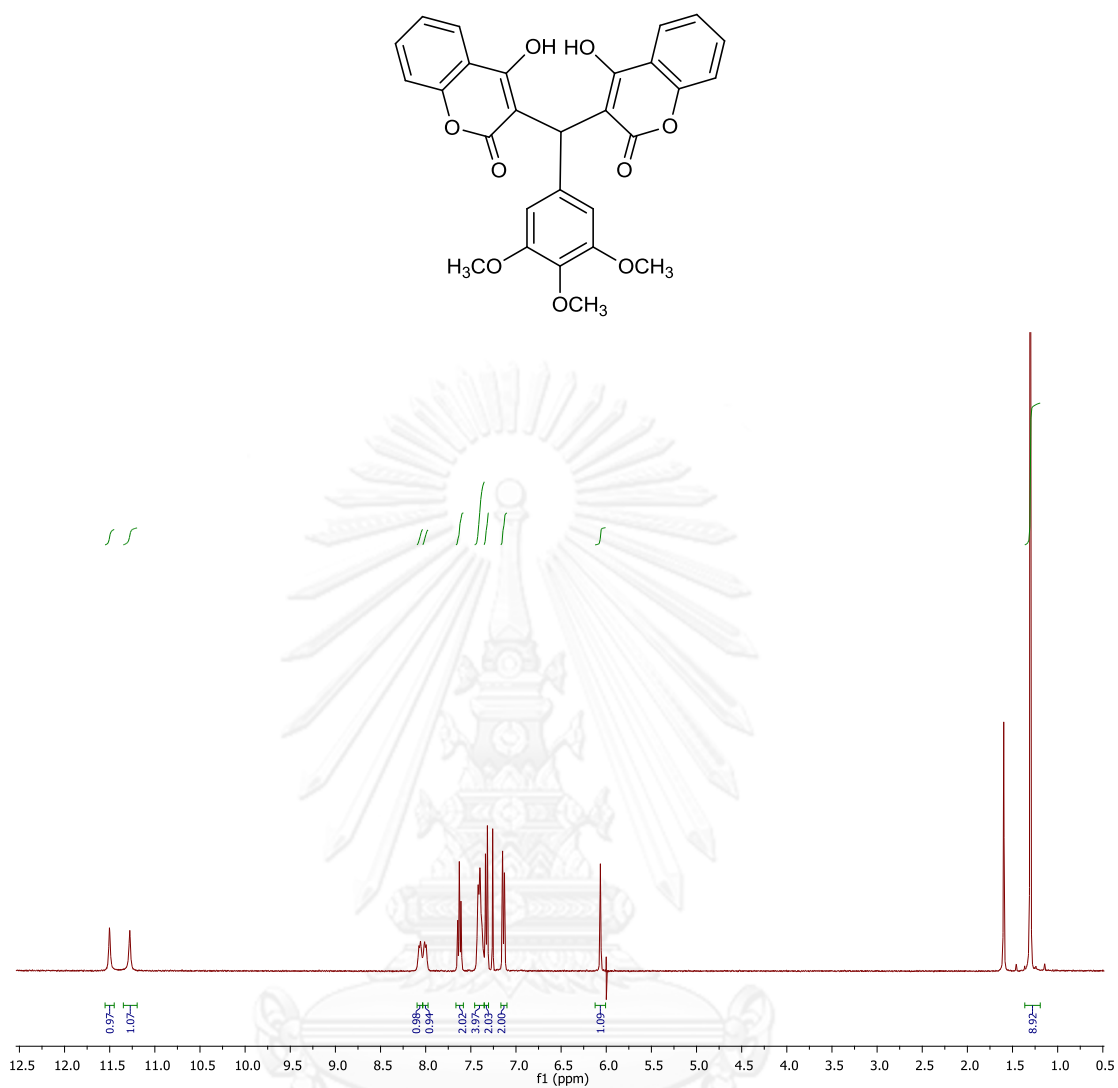


Figure A. 16 The ¹H NMR spectrum of 3,3'-(3,4,5-trimethoxyphenylmethylene)bis-(4-hydroxy-2H-chromen-2-one) (16)

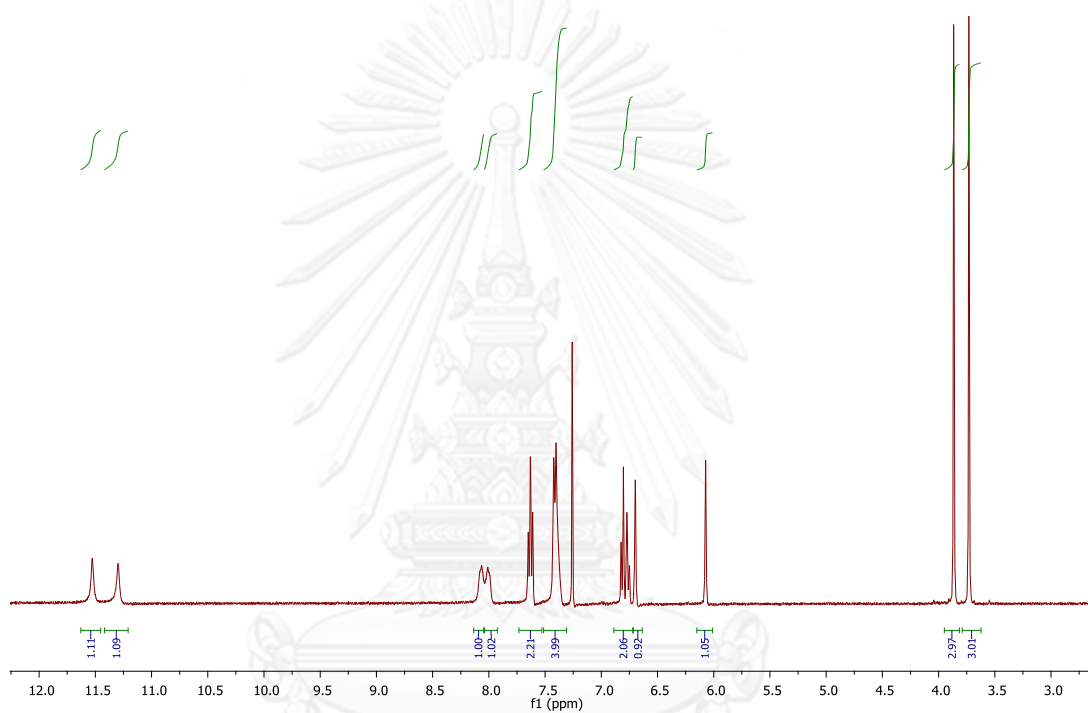
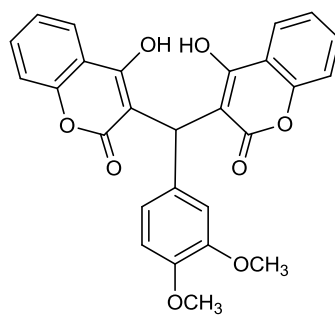


Figure A. 17 The ^1H NMR spectrum of 3,3'-(3,4-dimethoxyphenylmethylene)bis-(4-hydroxy-2H-chromen-2-one) (17)

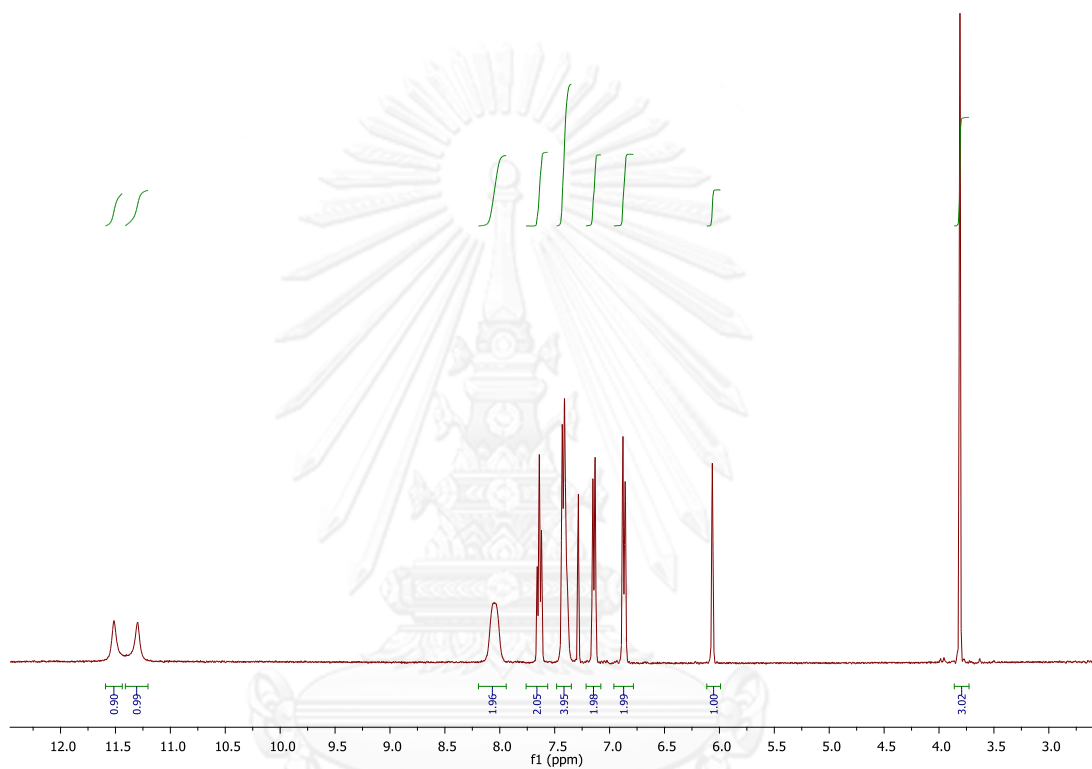
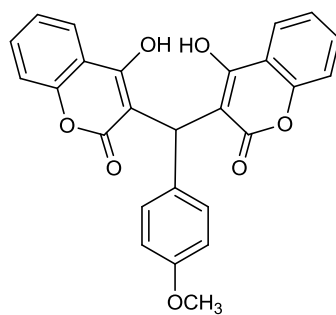


Figure A. 18 The ^1H NMR spectrum of 3,3'-(4-methoxyphenylmethylene)bis-(4-hydroxy-2H-chromen-2-one) (**18**)

CHULALONGKORN UNIVERSITY

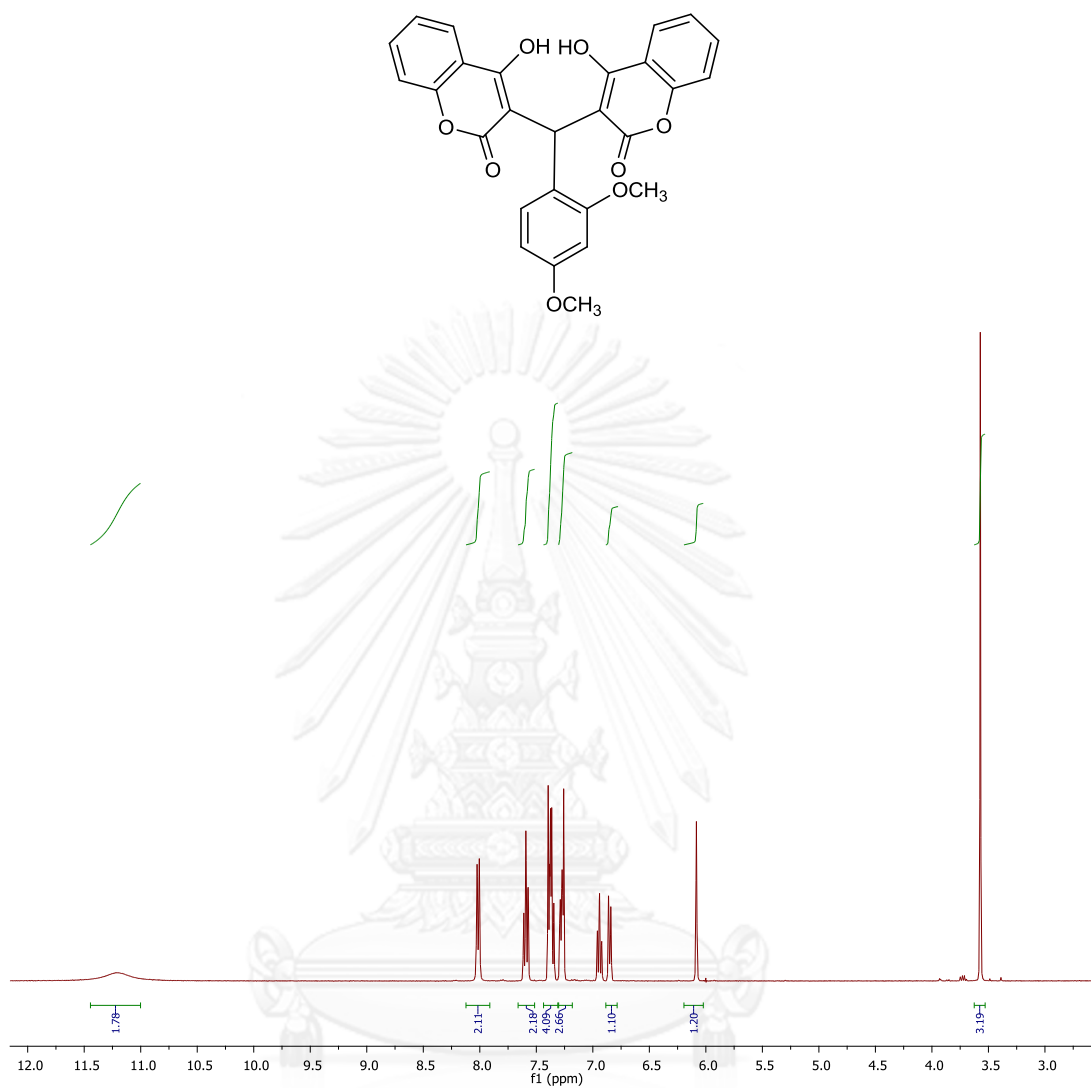


Figure A. 19 The ¹H NMR spectrum of 3,3'-(2-methoxyphenylmethylene)bis-(4-hydroxy-2H-chromen-2-one) (19)

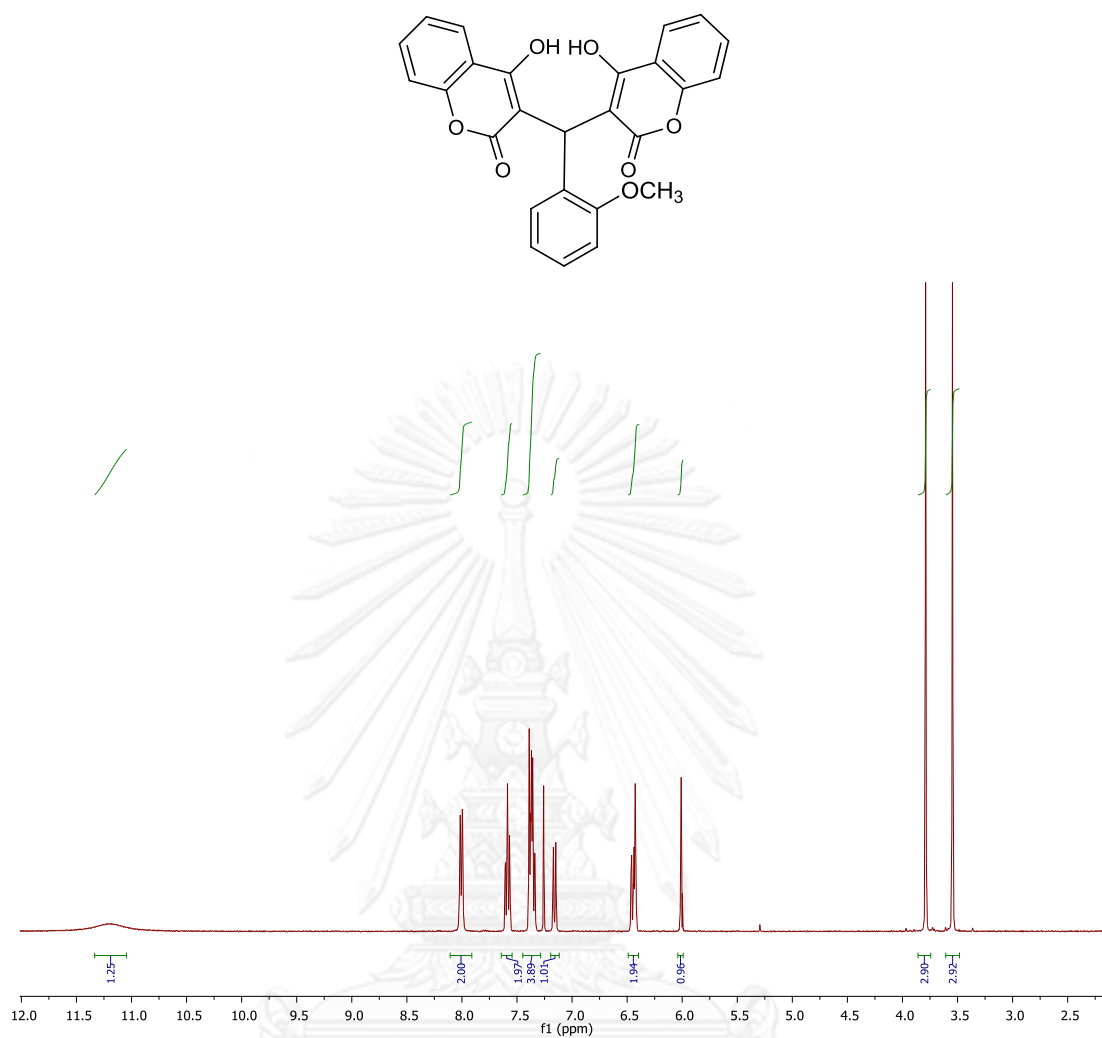


Figure A. 20 The ¹H NMR spectrum of 3,3'-(2,4-dimethoxyphenylmethylene)bis-(4-hydroxy-2H-chromen-2-one) (20)

VITA

Miss Kanokporn Petnapapun was born on April 10, 1989 in Chonburi, Thailand. She received a Bachelor Degree of Science in Chemistry at Chulalongkorn University in 2011. Since then, she has been a graduate student studying Organic Chemistry as her major course at Chulalongkorn University. During her studies towards the Master's degree, she was awarded the 90 th Anniversary of Chulalongkorn University Fund and Ratchadaphiseksomphot Endowment Fund and H.M. and the King's 72nd Birthday Scholarship, Chulalongkorn University. Her present address is 20/58 Moo 10, Naklua, Banglamung, Chonburi 20260.





จุฬาลงกรณ์มหาวิทยาลัย
CHULALONGKORN UNIVERSITY